MFI Zeolite Catalysts for Selective Production of para-Xylene and Light Olefins

VU VAN DUNG

September 2009

MFI Zeolite Catalysts for Selective Production of para-Xylene and Light Olefins

VU VAN DUNG

Department of Materials Engineering Science

Graduate School of Engineering Science

Osaka University, Japan

September 2009

Abstract

This doctoral thesis consists of seven main chapters dealing the development of new catalyst design through controlling active sites of H-ZSM-5 catalyst.

Chapter 1 covers a brief review of the properties of zeolite materials and recent advances of the use of zeolite layers in reactions. The modification techniques for zeolite were introduced. The objective of this study is to create new catalysts showing high selectivity by controlling active sites in zeolite catalysts by following two methods: (1) Control location of active sites by covering the external surface of zeolite catalyst with an inactive zeolite layer and (2) control acid strength distribution in a zeolite catalyst by a treatment with phosphoric acid. The background and the outline of this study will be described in this chapter.

Chapters 2 and 3 deal with the synthesis of H-ZSM-5 and silicalite/H-ZSM-5 composite catalysts with different Si/Al ratios and crystal sizes for the selective formation of *p*-xylene. The effects of reaction conditions over the prepared catalysts were investigated through the alkylation of toluene with methanol. To explain the high selective formation of *p*-xylene over the developed catalysts, the interlayer structure between ZSM-5 and silicalite layer was studied by FE-SEM and TEM observations.

A deposition of thick silicalite polycrystalline on the crystal surface was a problem. In **Chapter 4**, the morphology of the composite crystals was controlled to solve this problem. A synthesis method of a very thin layer without defect was developed. The zeolite composites with a new morphology were synthesized by controlling a nucleation density of silicalite.

Chapter 5 focuses on the application of the composite catalysts for the production of *p*-xylene in the toluene disproportionation reaction. The effect of Si/Al and the influence of the reaction conditions (temperature, *W/F*, etc) were investigated and suggested for practical production of *p*-xylene.

In **Chapter 6**, the synthesis of highly-active ZSM-5 nanocrystals through a special synthesis method was proposed. The structural and catalytic characterizations of the ZSM-5 nanocrystals were analyzed through the alkylation and isomerization reactions. In addition, the surface deactivation for the nanosized ZSM-5 by a silicalite layer was also studied.

In **Chapter 7**, control of acid strength distribution in a zeolite catalyst is shown. The zeolite catalyst has been treated with phosphoric acid and used for methanol-to-olefin (MTO) reactions. The effect of acid strength distribution to the selectivity to light olefin will be shown.

The summarization and suggestion for future work were described in **Chapter 8** of the dissertation.

Contents

Chapter 1

General Introduction 1

1.1 Reactions with Zeolite Layers 1

1.1.1 Zeolite Membrane Reactors 2

1.1.2 Particle Membrane Reactors 3

1.2 New Catalyst Design to Improve Product Selectivity 5

1.2.1 Problems in Zeolite Catalysts 5

1.2.2 The Modification of Crystal Surface of Zeolites 6

1.3 Control of Acidic Strength 8

1.4 Outline of this Thesis 9

References 10

Chapter 2

Core-Shell MFI Zeolite Composite: Selective Formation of *para*-Xylene over H-ZSM-5 Coated with Polycrystalline Silicalite Crystals

2.1 Introduction 14

2.2 Experimental Section 15

2.2.1 Synthesis of H-ZSM-5 15

2.2.2 Silicalite Coating 15

2.2.3 Alkylation 16

2.3 Results and Discussion 17

2.3.1 Morphology of the Silicalite-1/H-ZSM-5 Composites 17

2.3.2 Alkylation of Toluene 19

2.4 Conclusions 26

References 27

Chapter 3

Catalytic Activities and Structures of Silicalite-1/H-ZSM-5 Zeolite Composites

3.1 Introduction 30

3.2 Experimental 30

3.2.1 Preparation of HZSM-5 30

3.2.2 Preparation of Silicalite-1/HZSM-5 31

3.2.3 Characterizations 31

3.3 Results and Discussion 32

3.3.1 Morphology of H-ZSM-5 and Silicalite-1/H-ZSM-5 Composites 32

3.3.2 Influence of Crystal Sizes on Catalytic Activities 33

3.3.3 Crystalline Structure of Silicalite-1/H-ZSM-5 Composite 35

3.4 Conclusions 39

References 40

Chapter 4

Morphology Control of Silicalite/HZSM-5 Composite Catalysts for the Formation of *para*-Xylene

4.1 Introduction 42

4.2 Experimental 42

4.2.1 Catalyst Preparation and Characterization 42

4.2.2 Catalytic test 44

4.3 Results and Discussion 44

4.3.1 Morphology of Silicalite/H-ZSM-5 Composite 44

4.3.2 Catalytic Performances of HZSM-5 and Silicalite/HZSM-5 Catalyst 48

4.4 Conclusion 49

References 50

Chapter 5

Production of *para*-Xylene through Toluene Disproportionation over Silicalite-1/H-ZSM-5 Composite Catalysts

5.1 Introduction 52

5.2 Experimental 52

5.2.1 Catalyst Preparation 52

5.2.2 Catalytic Characterization 53

5.3 Results and Discussion 53

5.3.1 Morphology and Characterizations 53

5.3.2 Catalytic Activity 53

5.4 Conclusions 59

References 60

Chapter 6

Synthesis of Nanoscale H-ZSM-5 Crystals by Incorporating Al Species Dissolved from FAU Zeolite and αAl_2O_3

6.1 Introduction 62

6. 2 Experimental Section 62

6.2.1 Preparation of HZSM-5 62

6.2.2 Preparation of Silicalite-1/HZSM-5 63

6.2.3 Characterization 63

6.3 Results and Discussion 63

6.3.1 Morphology and Crystalline Characterizations 63

6.3.2 Catalytic Characterization 67

6.4 Conclusions 68

References 69

Chapter 7

Control of Acidic Strength of H-ZSM-5 Catalyst for Light Olefin Production: High Propylene Selectivity in the Methanol-to-Olefin Reaction over H-ZSM-5 Catalyst Treated with Phosphoric Acid

7.1 Introduction 72

7.2 Experimental 73

7.2.1 Catalyst Preparation and Characterization 73

7.2.2 Catalytic Test 73

7.3 Results and Discussion 74

7.3.1 Catalyst Characterizations 74

7.3.2 MTO Reaction over H-ZSM-5 and P-HZSM-5 76

7.4 Conclusions 82

References 83

Chapter 8

Summary and Suggestions for Future Work

8.1 Summarization 85

8.1.1 The production of *para*-Xylene over Silicalite-1/H-ZSM-5 Catalyst 85

8.1.2 Synthesis of Nanoscale H-ZSM-5 Crystals 87

8.1.3 Light Olefin Production 87

8.2 Suggestion for Future Work 87

References 89

List of Publications 91

Acknowledgments 93

Chapter 1

General Introduction

Chemical industry is mainly composed of reaction and separation processes. Selectivity to desired products in the reaction processes is not always high. A product stream from the reactors is separated to purify the desired products. The unreacted components are recycled as a reactant to improve overall conversions. For example, production of *p*-xylene is an important process because *p*-xylene is one of the most valuable aromatic compounds for the production of polymers. But, the fraction of *p*-xylene in xylene isomers, so-called *para*-selectivity, is only 23% at the thermodynamic equilibrium, which is much smaller than the market demand. *p*-Xylene in a product stream is separated from other xylene isomers (*o*-xylene and *m*-xylene) by adsorption processes. In addition, the separated *m*-xylene and *o*-xylene are then converted to *p*-xylene again by isomerization [1]. These separation and reaction processes are very large energy consuming. If the selectivity to *p*-xylene is improved up to 99.5%, the separation and isomerization processes are unnecessary anymore, reducing enormous energy consumption.

Development of new catalysts which show high selectivity is a key technology for the future chemical and petrochemical industry in terms of energy conservation. The objective of this study is to create new catalysts showing high selectivity by controlling active sites in zeolite catalysts by following two methods: (1) Control location of active site by covering the external surface of zeolite catalyst with an inactive zeolite layer and (2) control acid strength distribution in a zeolite catalyst by a treatment with phosphoric acid. The background and the outline of this study will be described in this chapter.

1.1 Reactions with Zeolite Layers

The zeolite layers have been used in reactions to improve product selectivity. The zeolite layers

have been combined with reactors and catalyst particles as shown in Fig. 1.1 (a) and (b) and will be described in the section 1.1.1 and 1.1.2, respectively. Then, the core/shell type zeolite composites which have been developed in this study (Fig. 1.1(c)) will be described in the next section 1.2.

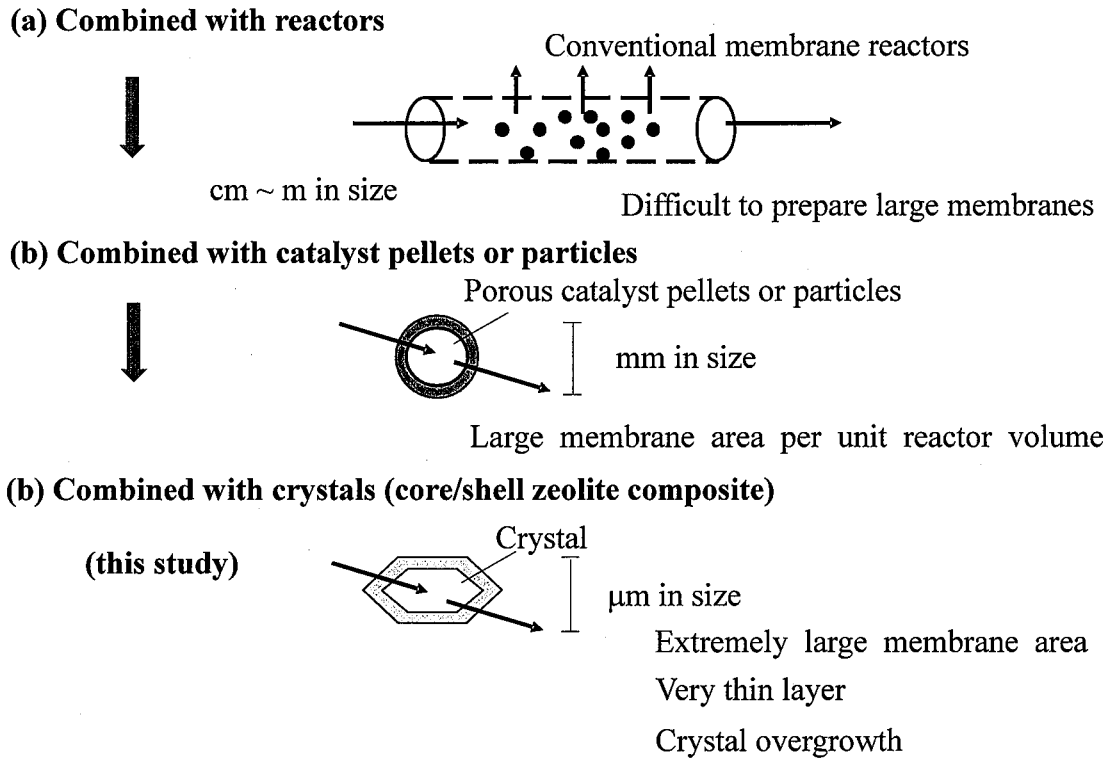

Fig. 1.1 The use of zeolite layers in reactions

1.1.1 Zeolite Membrane Reactors

The zeolite layers have been first used as a permselective membrane combined with reactors. A typical membrane reactor is composed of a catalytic packed-bed reactor surrounded by a permselective zeolite membrane as shown in Fig. 1.1(a). The products can be diffused out of the catalytic packed-bed reactor through the zeolite membrane. Improvement of product selectivity by a selective permeation thorough the zeolite membranes was demonstrated in oxidative dehydrogenation [2], and esterification [3,4].

Another type of zeolite membrane reactors is a catalytic membrane. In this case, the zeolite membranes have a catalytic activity themselves [5-7]. Reactions take place during the permeation through the zeolite layer. The residence time of reactants in the zeolite layer depends on the diffusivity in zeolite. The control of product selectivity in methanol-to-olefin (MTO) reaction [7]

and preferential oxidation of CO [2] have been demonstrated so far.

For the use of zeolite membranes in practical applications, the permeation flux through the zeolite membranes is too small due to their small pore size. A sufficiently large membrane area is required to attain compatible permeation fluxes and reaction rates. Although many interesting separation properties of the zeolite membranes synthesized in a laboratory-scale have been reported [8-20], it is still hard to prepare large-area membranes without any defects. Several different kinds of defects such as cracks, open grain boundaries and pinholes are believed to form during calcination at high temperature.

1.1.2 Particle Membrane Reactors

New type zeolite layers have been developed to solve the above problems. Nishiyama et al. have proposed catalyst particles covered with a permselective membrane [21] as shown in Fig. 1.1 (b). The core catalysts are porous catalyst pellets or particles with a few mm in size. This type composite catalyst has a larger membrane area per unit reactor volume compared to the conventional membrane reactors.

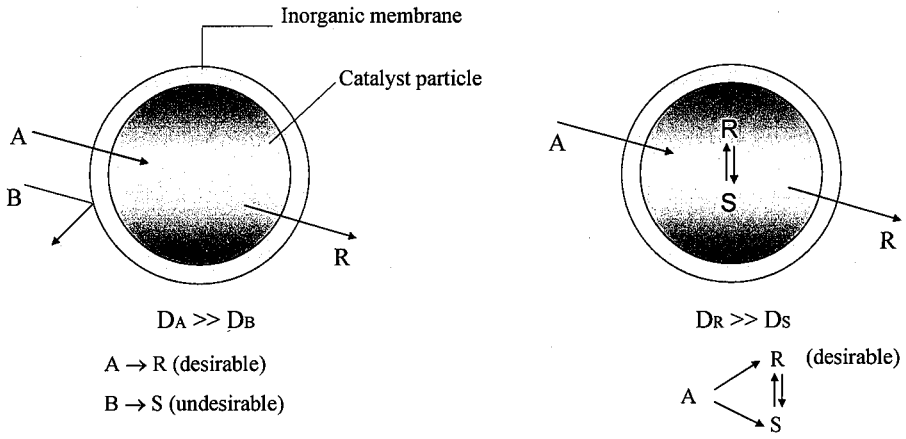

Fig 1.2 Principle of operation of a catalyst particle with a permselective membrane
(a): Selective addition of reactants; (b): Selective removal of products.

The basic concept of the composite catalysts is shown in Fig. 1.2: (1) selective addition of reactants to the reaction zone and (2) selective removal of products from the reaction zone. In the first case, if the diffusivity of one reactant (A) in the membrane is much large than that of the other components (B), the reactant (A) selectively diffuses into a catalyst particle through the membrane. Undesired reactions or the adsorption of poisons (B) on the catalyst can be prevented. In the second

case, the reaction has a limited yield or selectivity controlled by thermodynamics. The selective removal of desired product from the catalyst particle gives enhancement of selectivity when the diffusivity of one product (R) in the membrane is much greater than that of the other products (S). As an example of the selective removal of products, Foley at al. [22] anticipated a selective formation of dimethylamine over a catalyst coated with a carbon molecular sieve layer. Nishiyama et al. [21] demonstrated the concept of the selective removal of products. In their study, a porous silica-alumina catalyst with a diameter of 1.5 mm was covered with an inactive silicalite layer with a thickness of 20-30 μm. The composite catalyst was used for disproportionation and alkylation of toluene to produce *p*-xylene. The selectivity to *p*-xylene on the uncoated silica-alumina catalyst was only 22%, the value of thermodynamic equilibrium value. On the other hand, the selectivity to *p*-xylene over silicalite-coated catalyst (85%) was largely exceeded the equilibrium value. As shown in Fig. 1.3, a distribution of produced xylene isomers in macroporous silica-alumina is governed by the thermodynamic equilibrium because a diffusion of products in the macropores of silica/alumina is very fast (reaction control region). On the other hand, the overall reaction rates over the silicalite-coated catalyst were governed by diffusion of xylene isomers through the silicalite membrane. The high *para*-selectivity in the toluene disproportionation is caused by the selective removal of *p*-xylene from the silica-alumina particles through the silicalite layer leading to an apparent equilibrium shift between xylene isomers.

However, the toluene conversion is low because the silicalite layer on the silica-alumina catalyst was very thick (more than 20 μm). The increased resistance for diffusion of products resulted in a decrease of the toluene conversion. The permselective layer should be as thin as possible. A new structured catalyst is required for improving both selectivity and conversion.

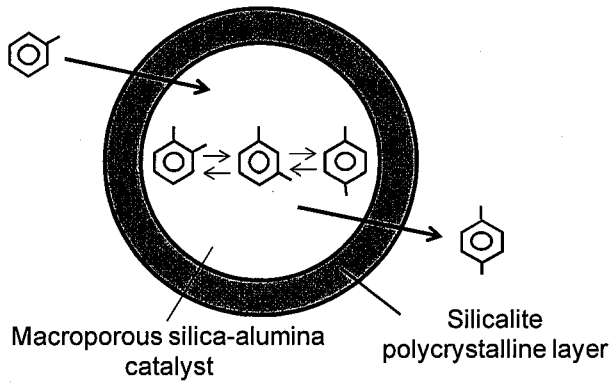

Fig. 1.3 Selective removal of *p*-xylene from silica-alumina particles.

1.2 New Catalyst Design to Improve Product Selectivity

In this study, a new technique of a zeolite coating on zeolite crystals has been developed as shown in Fig. 1.1(c). The size of zeolite crystals is from a few μm to 50 μm, which is much smaller than the particles shown in Fig. 1.1(b). The advantages of this method are that (1) a very thin zeolite layer can be synthesized and (2) the external (membrane) surface of the crystal is extremely large.

The core catalyst used in this study is proton-type ZSM-5, which possesses stronger acid sites than silica-alumina. In this study, the H-ZSM-5 catalysts were used for the *p*-xylene production and methanol-to-olefin reactions. In the next sections, the selectivity and activity of the zeolite catalysts will be described with respect to the effect of diffusion limitation.

1.2.1 Problems in Zeolite Catalysts

Zeolites are known to be shape selective catalysts. For example, in the reaction to produce *p*-xylene, the diffusion of *p*-xylene in the zeolite pores is much faster than that of *m*-xylene and *o*-xylene [23] when an overall reaction rate is governed by diffusion. In the diffusion control region, *p*-xylene can selectively diffuse out of the zeolite crystals. Instead, the overall reaction rate is limited by a diffusion resistance of xylene isomers.

The relation between *para*-selectivity and conversion of reactant is summarized in Fig. 1.4. From the above reason, *p*-xylene is selectively formed when the crystal size of zeolite is large because of the diffusion control. With decreasing the crystal size of zeolite, the diffusion resistance decreased, resulting in an increase of the conversion of reactant along the line (a) in Fig. 1.4. Instead of that, *para*-selectivity is decreased in the reaction control region.

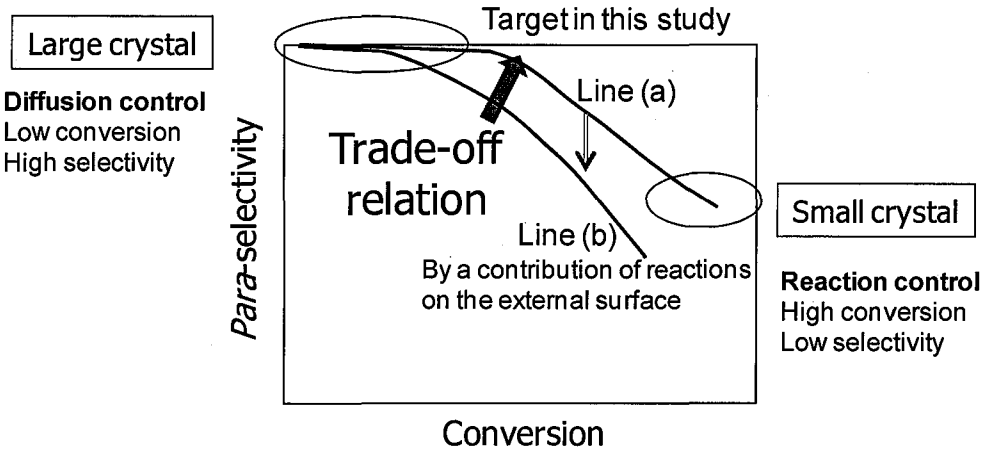

Fig. 1.4 Trade-off relation between *para*-selectivity and conversion of reactants

However, the shape selectivity has not been maximized even in the diffusion control region because acid sites present both inside and outside the crystals. Even though *p*-xylene diffuses out of the crystals, isomerization from *p*-xylene to *m*- and *o*-xylenes takes place on the external surface [24]. Selective reactions based on the microporous structure of zeolites do not occur in isomerization on the external surface of zeolite crystals. Consequently, the actual *para*-selectivity (line (b)) is lower than the values without the effect of reactions on the external surface (line (a)). The contribution of the reactions on the external surface is large especially for the catalysts with a small crystal size. Therefore, the trade-off relationship between the *para*-selectivity and conversion can be expressed as the line (b) in Fig. 1.4.

1.2.2 The Modification of Crystal Surface of Zeolites

The objective of this study is to overcome this trade-off line (Fig. 1.4, the line (b)) by a modification of the external surfaces with an inactive silicalite layer. In this section, modification techniques reported so far will be introduced. After that, the methods in this thesis will be described.

A post-synthesis modification by chemical vapor deposition (CVD) of silicon alkoxides, such as tetraethoxysilane (TEOS) and tetramethoxysilane (TMOS), is one of the most effective methods to enhance the shape selectivity of HZSM-5 zeolites [25]. The silylation mechanism by means of CVD has been well documented by Niwa et al. [26-28]. Because the minimum kinetic diameters of the silicon alkoxides are larger than the pore diameter of HZSM-5, only hydroxyl groups on the external surface and near the pore openings react with the silylating agents. The formed Si–O–Si or Si–O–Al bonds act as a passivation of these unselective acid sites. As a result, the pore openings are simultaneously narrowed or partially blocked.

Alternatively, chemical liquid deposition (CLD) can be used to modify the external surface of zeolites [29-32]. The main advantage of the reaction in liquid phase (CLD) compared to the reaction in gas-phase (CVD) is that the liquid reaction can be more easily applied to a large-scale industrial preparation. However, coke deposition on the external surface of H-ZSM-5 during reactions was a problem due to a pore mouth narrowing [33,34]. The same problem was also present in the CVD method.

Other than the above silica coating methods, the surface dealumination of zeolite catalytic particles is one of the effective ways to reduce the density and strength of the external acid sites. The poisoning adsorption of external acid sites have been studied over zeolites by pyridine [35],

4-methylquinoline [36] and 2,4-dimethylquinoline [37]. However, the catalytic activities were much decreased after the treatment due to the removal of number of strong acid sites [37,38].

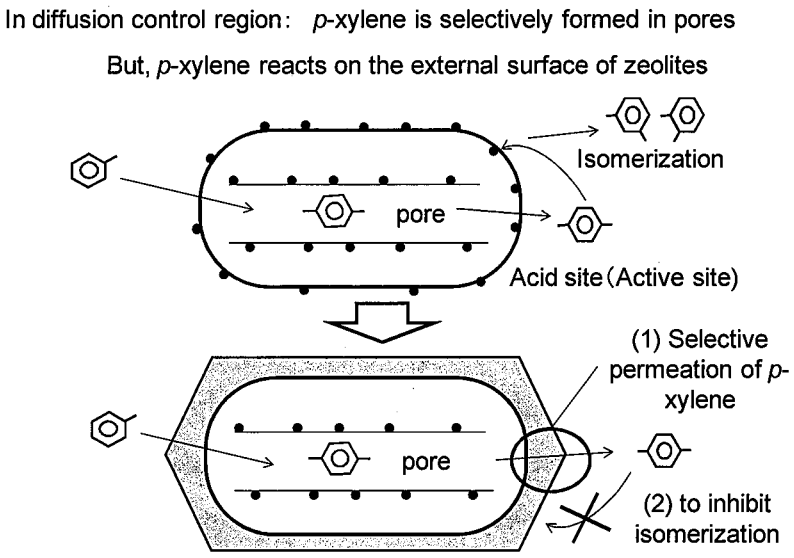

Fig. 1.5 Problems in zeolite catalysts and a concept of the composite catalyst in this study

Even by using the above methods such as CVD, CLD and dealumination, it is difficult to fully remove acid sites on the external surface. Recently, Miyamoto et al. [39] developed a new composite zeolite catalyst consisting of a zeolite crystal with an inactive silicalite layer. A schematic illustration for the silicalite coating on ZSM-5 catalyst is shown in Fig. 1.5. The acidity of zeolite is caused by the present of trivalent elements such as aluminum. Substitution with a trivalent element introduces a negative charge. The charge is to be balanced by cation exchanged with proton and/or alkaline earth metal cations. The proton-type ZSM-5 has strong acid sites both in the crystal and on the external surface. Silicalite is the zeolite whose framework structure is the same as ZSM-5 with a code name of MFI [40]. But, silicalite does not contain Al in the framework and shows no acidity. Two possible effects of the silicalite layer in this study are as follows: firstly, the selective permeation of *p*-xylene through the inactive silicalite layer can be expected. Secondly, the inactive silicalite layer inhibits the isomerization from *p*-xylene to other xylene isomers on the external surface. In the diffusion control region, *p*-xylene is mainly formed inside crystals. In this case, the second effect is more important to improve *para*-selectivity.

In my study, silicalite layers were grown on the surface of ZSM-5 catalysts by a crystal overgrowth under hydrothermal conditions. A crystal overgrowth technique seems to be more

feasible to cover the external surface of core catalysts compared to a coating on macroporous catalysts such as silica-alumina. Miyamoto et al. [39] showed a high *para*-xylene selectivity in alkylation of toluene by using the silicalite/H-ZSM-5 composite catalysts. However, a deposition of thick silicalite polycrystalline from the solution was not inevitable for a full coverage on the crystal surface, which causes a reduction of catalyst activity, mechanical strength, compactness of the silicalite layer. The morphology of the composite crystals should be controlled to solve these problems. Especially for a long-time use in practical applications, different-type zeolite composites would be required. The development of a synthesis method of a very thin layer without defect is a target in this study. In this study, the zeolite composites with a new morphology were developed by controlling a nucleation density of silicalite.

In addition, it is very important to know how diffusion and reaction rates affect on the selectivity. The reactions using different crystal sizes at different reaction conditions were carried out to demonstrate the effect of shape-selectivity in a diffusion control region.

1. 3 Control of Acidic Strength

Acid strength and the amount of acid sites are one of the most important properties when zeolites are used as catalysts. A control of acid strength distribution would be a very useful technique to enhance the product selectivity. To describe the acidity of zeolite, J. Weitkamp [41] clearly distinguished between the nature of acid sites (Brönsted vs. Lewis acidity), the density of these sites, the strength distribution and the precise location of the acid sites to study the fundamentals of zeolite materials. Many catalyst preparation techniques for enhancing a yield and product selectivity have been intensively studied through a control of the strength of active sites.

For light olefin production, several modification methods for ZSM-5 were suggested in order to improve the selectivity to light olefin in methanol-to-olefin (MTO) reactions, especially with respect to ion-exchange and impregnation methods: Cs^{+}; Ba^{2+} [42]; B-ZSM-5 [43-46], Mo [47], Mg modification [48,49]. The researches revealed that higher olefin selectivities could be obtained with modified catalysts.

In this thesis, a simple post-synthesis method for H-ZSM-5 was proposed for controlling acid strength distribution. A modification of H-ZSM-5 with phosphorous acid has been developed for improving the selectivity to propylene in the MTO reaction.

1.4 Outline of the Thesis

Zeolites have shown many advantages in practical applications especially in the field of separation and catalysis. In fact, many reactions using zeolite catalysts in the industry are limited by kinetics and thermodynamics which are not favorable for the target products. The objective of this study is to develop new high-selective catalysts for future energy-saving processes in chemical and petrochemical industry. The proposed methods in this thesis are (1) control location of active site by covering the external surface of zeolite catalyst with an inactive zeolite layer (Chapter 2-6) and (2) control acid strength distribution in a zeolite catalyst by a treatment with phosphoric acid (Chapter 7).

Chapters 2 and 3 deal with the synthesis of H-ZSM-5 and silicalite/H-ZSM-5 composite catalysts with different Si/Al ratios and crystal sizes for the selective formation of *p*-xylene. The effects of reaction conditions over the catalysts were investigated through the alkylation of toluene with methanol. To explain the high selective formation of *p*-xylene over the developed catalysts, the interlayer structure between ZSM-5 and silicalite layer was studied by FE-SEM and TEM observations.

A deposition of thick silicalite polycrystalline on the crystal surface was a problem in the previous study. In **Chapter 4**, the morphology of the composite crystals was controlled to solve this problem. A synthesis method of a very thin layer without defects was developed. The zeolite composites with a new morphology were synthesized by controlling a nucleation density of silicalite.

Chapter 5 focuses on the application of the composite catalysts for the production of *p*-xylene in the toluene disproportionation reaction. The effect of Si/Al and the influence of the reaction conditions (temperature, *W/F*, etc) were investigated and suggested for practical production of *p*-xylene.

In **Chapter 6**, the synthesis of highly-active ZSM-5 nanocrystals through a special synthesis method was proposed. The structural and catalytic characterizations of the ZSM-5 nanocrystals were analyzed through the alkylation and isomerization reactions. In addition, the surface deactivation for the nanosized ZSM-5 by a silicalite layer was also studied.

In **Chapter 7**, control of acid strength distribution in a zeolite catalyst is shown. The zeolite catalyst has been treated with phosphoric acid and used for methanol-to-olefin (MTO) reactions. The effect of acid strength distribution to the selectivity to light olefin will be shown.

References

[1] http://www.exxonmobilchemical.com/Public_Products/TechLicensing/Worldwide/Technologies/Tech_Technologies_Aro_PxMax.asp

[2] A. Pantazidis, J.-A. Dalmon and C. Mirodatos, Catal. Today 25 (1995) 403

[3] K. Tanaka, R. Yoshikawa, C. Ying, H. Kita and K. Okamoto, Catal. Today 15 (2001) 121

[4] M.P. Bernal, J. Coronas, M. Menéndez and J. Santamaría, Chem. Eng. Sci. 57 (2002) 1557

[5] Y. Hasegawa, K. Kusakabe and S. Morooka, J. Membr. Sci. 190 (2001) 1

[6] T. Masuda, T. Asanuma, M. Shouji, S.R. Mukai, M. Kawase and K. Hashimoto, Chem. Eng. Sci. 58 (2003) 649

[7] R.J. Wang, T. Fujimoto, T. Shido, M. Ichikawa, J. Chem. Soc., Chem. Commun. (1992) 962

[8] H. Kita, K. Horii, Y. Ohtoshi, K. Tanaka, K. Okamoto, J. Mater. Sci. Lett. 14 (1995) 206

[9] M. Kondo, M. Komori, H. Kita and K. Okamoto, J. Membr. Sci. 133 (1997) 133

[10] X. Xu, W. Yang, J. Liu and L. Lin, Adv. Mater. 12 (2000) 195

[11] K. Kusakabe, T. Kuroda and S. Morooka, J. Membr. Sci. 148 (1998) 13

[12] M. Lassinantti, J. Hedlund and J. Sterte, Micropor. Mesopor. Mesopor. Mater. 38 (2000) 25

[13] N. Nishiyama, K. Ueyama and M. Matsukata, Micropor. Mesopor. Mater. 7 (1996) 299

[14] X. Lin, E. Kikuchi and M. Matsukata, Chem. Commun. (2000) 957

[15] N. Nishiyama, T. Matsufuji, K. Ueyama and M. Matsukata, Micropor. Mesopor. Mater. 12 (1997) 293

[16] J.C. Poshusta, V.A. Tuan, J.L. Falconer and R.D. Noble, Ind. Eng. Chem. Res. 37 (1998) 3924

[17] S. Li, J.L. Falconer and R.D. Noble, J. Membr. Sci. 241 (2004) 121

[18] V.A. Tuan, S. Li, J.L. Falconer and R.D. Noble, Chem. Mater. 14 (2002) 489

[19] M.L. Maloncy, A.W.C. van den Berg, L. Gora and J.C. Jensen, Micropor. Mesopor. Mater. 85 (2005) 96

[20] Y.T. Munoz Jr. and K.J. Balkus Jr., J. Am. Chem. Soc. 121 (1999) 139

[21] N. Nishiyama, M. Miyamoto, Y. Egashira, K. Ueyama, Chem. Commun. (2001) 1746

[22] H.C. Foley, D.S. Lafyatis, R.K. Mariwala, G.D. Sonnichsen, L.D. Brake, Chem. Eng. Sci. 49 (1994) 4771

[23] G. Mirth, J. Cejka, J.A. Lercher, J. Catal. 139 (1993) 24.

[24] F. Bauer, W-H. Chen, Q. Zhao, A. Freyer, S-B. Liu, Micropor. Mesopor. Mater. 47 (2001) 67

[25] S. Zheng, H.R. Heydenrych, A. Jentys, J.A. Lercher, J. Phys. Chem. B 106 (2002) 9552

[26] M. Niwa, N. Katada, T. Murakami, J. Phys. Chem. 94 (1990) 6441

[27] M. Niwa, N. Kanada, Y. Murakami, J. Catal. 134 (1992) 340

[28] M. Niwa, S. Kato, T. Hattori, Y. Murakami, J. Chem. Soc., Faraday Trans. 1 80 (1984) 3135

[29] Y.H. Yue, Y. Tang, Y. Liu, Z. Gao, Ind. Eng. Chem. Res. 35 (1996) 430

[30] C. Gründling, G. Eder-Mirth, J.A. Lercher, J. Catal. 160 (1996) 299

[31] R.W. Weber, K.P. Möller, M. Unger, C.T. OConner, Micropor. Mesopor. Mater. 23 (1998) 179

[32] R.W. Weber, K.P. Möller, C.T. OConner, Micropor. Mesopor. Mater. 35 (2000) 533

[33] J. Cejka, N. Zilkova, B. Wichterlova, Zeolites 17 (1996) 265

[34] S. Al-Khattaf, Chemical Engineering and Processing 46 (2007) 964

[35] V.S. Nayak, V.R. Choudhary, Appl. Catal 9 (1984) 251

[36] J.R. Anderson, K. Foger, T. Mole, R.A. Rajadhyakshs, J.V. Sanders, J. Catal. 58 (1979) 105

[37] P. Wu, T. Komatsu, T. Yashima, Micropor. Mesopor. Mater. 22 (1998) 343

[38] C. Ding, X. Wang, X. Guo, S. Zhang, Catal. Commun 9 (2007) 487

[39] M. Miyamoto, T. Kamei, N. Nishiyama, Y. Egashira, K. Ueyama, Adv. Mater. 17 (2005) 1985

[40] http://izasc.ethz.ch/fmi/xsl/IZA-SC/ft.xsl

[41] J. Weitkamp, Solid State Ionics 131 (2000) 175

[42] H. Shoji, Japanese Patent Application 59 219 134, 1984.

[43] M.R. Klotz, US Patent 4 292 458, 1981

[44] C.T.-W. Chu, G.H. Kuehl, R.M. Lago, C.D. Chang, J. Catal. 93 (1985) 451

[45] G. Coudurier, A. Auroux, J.C. Vedrine, R.D. Farlee, L. Abrams, R.D. Shannon, J. Catal. 108 (1987) 1

[46] M.B. Sayed, A. Auroux, J.C. Vedrine, J. Catal. 116 (1989) 1

[47] I. Balkrishnan, B.S. Rao, S.G. Hegde, A.N. Kotasthane, S.B. Kulkarni, P. Ratnaswamy, J. Mol. Catal. 17 (1982) 261

[48] J. Liang, G. Chen, S. Zhao, Q. Wang, H. Li, G. Cai, Chem. Express. 1 (1986) 729

[49] G. Cai, G. Chen, Q. Wang, Q. Xin, X. Wang, X. Li, J. Liang, Zeolites (1985) 319.

Chapter 2

Core-shell MFI Zeolite Composite: Selective Formation of *para*-Xylene over H-ZSM-5 Coated with Polycrystalline Silicalite Crystals

H-ZSM-5 catalysts with different Si to Al ratios of 30, 50 and 70 were synthesized and coated with polycrystalline silicalite-1 layers by a repeated hydrothermal synthesis. The formed silicalite-1 layers were affected by the morphology of the substrate H-ZSM-5. The catalysts were used for the alkylation of toluene with methanol reaction. The silicalite-1/HZSM-5 composites expressed very high *para*-selectivity up to 99.9 % under all reaction conditions. The silicalite coating on the H-ZSM-5 catalysts not only improved *para*-selectivity but also prevented deactivation of the catalysts. The enhanced *para*-selectivity may originate from diffusion resistance through the inactive silicalite layer on the H-ZSM-5, resulting in an increased diffusion length. In addition to that, the high selectivity to *p*-xylene and high stability can be explained by the removal of acid sites on the external surface of H-ZSM-5.

2. 1. Introduction

The processes of the formation of dialkyl-benzene from monoalkyl-benzene such as disproportionation and alkylation are one of the most important processes in chemical industry. The selective formation of *p*-xylene is a challenging process because *p*-xylene is one of the most valuable aromatic compounds required for the raw material of terephthalate and polyester. The selective formation of *p*-xylene in the disproportionation of toluene as well as the alkylation of toluene with methanol and transalkylation of methylbenzenes has been studied over acidic zeolites such as ZSM-5 [1-6], Mordenite [7], zeolite Beta [8,9], zeolite X [10], zeolite Y [11-13] and MCM-22 [14,15] and mesoporous aluminum silicate Al-MCM-41 [16]. ZSM-5, in particular, is very interesting because its pore size is suitable to separate *p*-xylene from a mixture of xylene isomers. Over the last few decades, there have been many reports concerning pore modification of ZSM-5 to enhance *para*-selectivity [1,2,12-26] and techniques impregnation of phosphorous, MgO or boron [1,2], deposition of inert silica on the pore mouth by chemical vapor deposition (CVD) [19,20,22,25] or chemical liquid deposition (CLD) [6,17,18,20] and so on. However, further improvement of *para*-selectivity with high toluene conversion is still a challenging target because a decrease in toluene conversion is inevitable after the pore modification.

Recently, Nishiyama et al. have developed a porous catalyst covered with a permselective microporous membrane [27-29]. Silica-alumina catalyst particles coated with silicalite-1 membranes [27] showed higher *para*-selectivity (about 90%) than the thermodynamic equilibrium value (23%), because of a selective removal of the produced *p*-xylene through the silicalite-1 membrane. However, the reaction rate largely decreased due to the diffusion resistance of reactants and products through the thick silicalite-1 layer. Consequently, in this study, a novel composite catalyst consisting of a zeolite crystal of H-ZSM-5 with an inactive thin silicalite-1 layer has been developed in the hope of solving this problem.

A number of cases of zeolite overgrowth on different framework structures had been reported so far, such as FAU on LTA [31], MCM-41 on FAU [32] and FAU on EMT zeolite [33]. On the other hand, silicalite-1 has the same structure as the substrate H-ZSM-5, resulting in an oriented crystal over growth [30].

However, as several researchers have reported, in the silicalite-1 layer grown on the ZSM-5, the so-called zoned MFI [34-36], the structure and thickness of silicalite layer depend on the Si/Al ratio, crystal size and shape of the substrate H-ZSM-5. In this study, silicalite overgrowth on H-ZSM-5 with different Si/Al ratios was studied. In addition, the catalytic activity of H-ZSM-5 depends on the Si/Al ratio, which might affect the overall activity and deactivation behavior on silicalite-coated H-ZSM-5. The thickness, structure and quality of the silicalite layer as well as catalytic performance will be discussed here.

2. 2. Experimental Section

2.2.1. Synthesis of H-ZSM-5

ZSM-5 crystals with different Si to Al ratios were prepared by hydrothermal synthesis at 453 K for 24 h. The synthesis solution consisted of tetraethyl orthosilicate (TEOS), aluminum nitrate ($Al(NO_3)_3 \cdot 9H_2O$), sodium hydroxide (NaOH), tetrapropylammonium bromide (TPABr). The molar composition was 1.5-3.5 SiO_2: 0.025 Al_2O_3: 0.5 TPABr: 0.25 Na_2O: 120 H_2O. The synthesis solution was mixed for 30 min at 303 K. This solution was poured into a Teflon lined stainless steel vessel to carry out the hydrothermal treatment. The resulting ZSM-5 powders were calcined at 773 K for 5 h. A proton-exchange process was carried out by using an ammonium chloride (NH_4Cl, 1 N) aqueous solution after the hydrothermal synthesis. The ZSM-5 crystals were mixed with the NH_4Cl aqueous solution for 12 h at room temperature. The crystals were then calcined again at 773 K. The H-ZSM-5 samples synthesized using precursor solutions with the molar Si/Al ratios of 30, 50 and 70. Hereafter, the samples would be named as order of H-ZSM-5(30), H-ZSM-5(50) and H-ZSM-5(70), respectively.

2.2.2 Silicalite Coating

The process of silicalite coating on H-ZSM-5 crystals was as follows. A starting sol for synthesis of silicalite-1 coatings consisted of TEOS as silica source, tetrapropylammonium hydroxide (TPAOH) as structure-directing agent (SDA), ethanol (EtOH) and deionized water. The H-ZSM-5 crystals were immersed in the precursor solution with a molar ratio of 2.0 SiO_2: 0.5 TPAOH: 8 EtOH: 120 H_2O. The crystallization was carried out at 453 K for 24 h in a stainless steel vessel by hydrothermal synthesis with agitating condition. The coating process was repeated twice. The products were rinsed repeatedly

with deionized water and dried at 363 K overnight and then calcined in air at 773 K for 6 h with a heating rate of 1 K/min. The products were characterized by scanning electron microscopy (SEM, Hitachi S-2250) and X-ray diffraction (XRD) recorded on Rigaku MiniFlex using Cu-Kα radiation.

2.2.3 Alkylation

Catalytic activity of silicalite/H-ZSM-5 was investigated on alkylation of toluene with methanol. The reaction was performed using a fixed bed reactor. The products were directly characterized by a Shimadzu GC-14B FID gas chromatograph with a Bentone34+DNP 5% column (Shimadzu GLC Ltd.). The scheme of the experiment was described in Fig. 2.1.

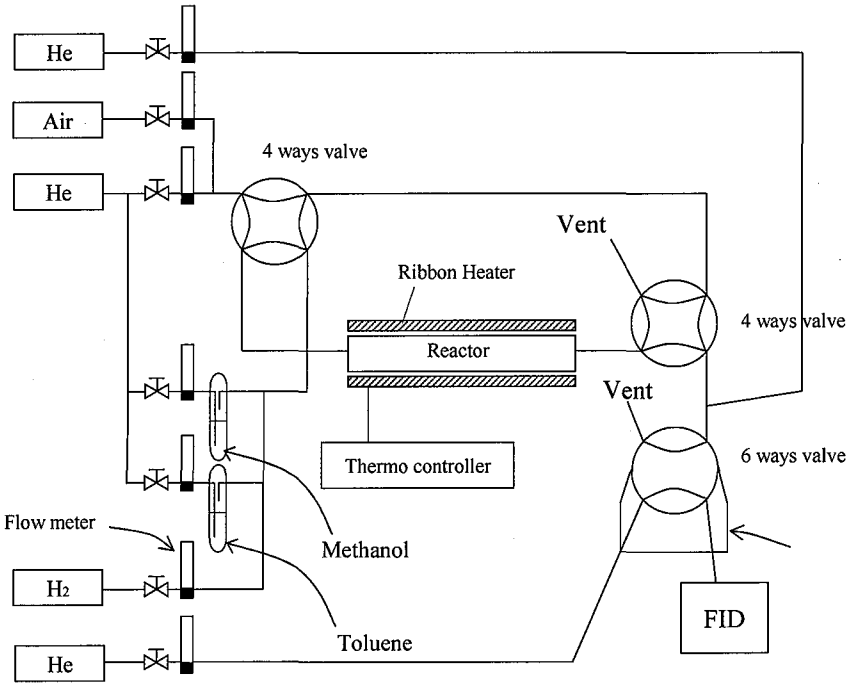

Fig. 2.1 Schematic diagram of the experimental apparatus for catalytic tests.

2.3 Results and Discussion

2.3.1 Morphology of the Silicalite-1/H-ZSM-5 Composites

Fig. 2.2 shows XRD patterns of the uncoated and coated samples. After the coating, the XRD patterns did not include reflection peaks for amorphous silica and impurities other than an MFI structure, suggesting that the products are silicalite/ZSM-5 composites. The SEM images of synthesized H-ZSM-5 and silicalite/H-ZSM-5 with different Si to Al ratios were shown in Fig. 2.3. H-ZSM-5(70) crystals were hexagonal cylinder in shape and with the crystal size was approximately 12 μm. After the first silicalite coating, small silicalite-1 crystals were formed on the H-ZSM-5 crystal. A silicalte-1 layer was grown along the external surface of the H-ZSM-5 crystal. Miyamoto et al. [28] have reported that the silicalite-1 crystals were oriented in the same direction as the substrate ZSM-5 crystals and the silicalite-1 crystals grew on the ZSM-5 crystal surfaces perpendicular to the a and b axes. The silicalite/H-ZSM-5 was as a single crystal-like structure [28]. For observation, in this work, the formed silicalite-1 layer consisted of oriented polycrystals. Finally, large amount of silicalite-1 crystals (less than 2 μm) were formed on the first silicalite-1 layer.

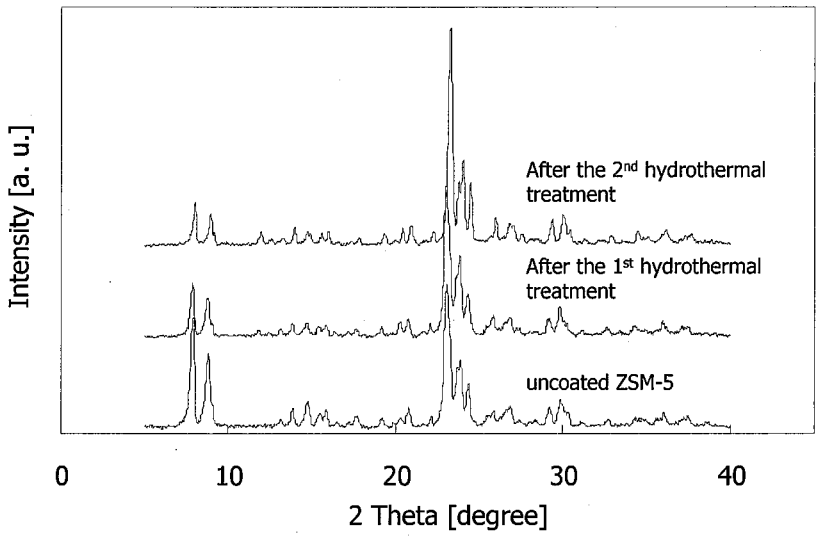

Fig. 2.2 XRD patterns of uncoated and coated H-ZSM-5(70) crystals.

The different morphology of the silicalite layer must be due to the different Si to Al ratios of the substrate H-ZSM-5. The presence of Al in the H-ZSM-5 must have affected the formation of the

polycrystalline layer. H-ZSM-5(50) and H-ZSM-5(30) crystals were close to spherical in shape and the crystal size was approximately 7 μm and 10 μm, respectively. The morphology of these two silicalite/H-ZSM-5 crystals was very similar regardless of the Si to Al ratio of the substrate H-ZSM-5. The morphologies of the silicalite layers on H-ZSM-5(30) and H-ZSM-5(50) were also very similar. This result indicates that the morphology of formed silicalite-1 layer is affected by the shape of the substrate H-ZSM-5 crystals.

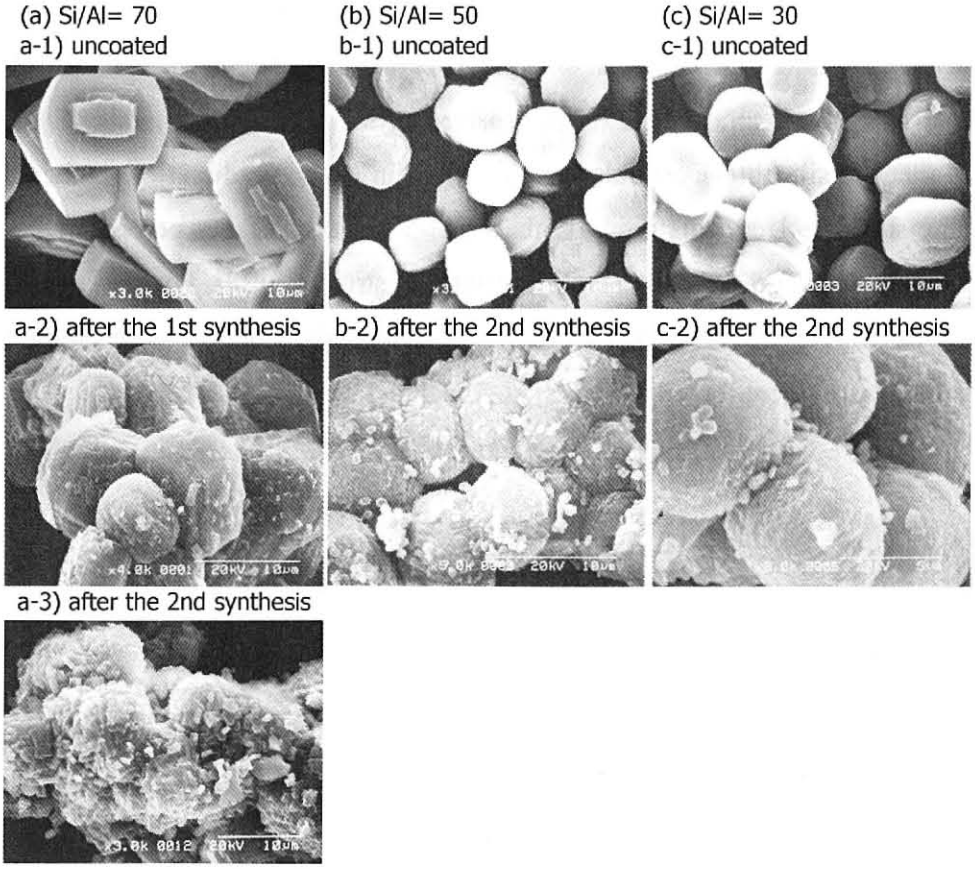

Fig. 2.3 SEM images of H-ZSM-5 and silicalite/H-ZSM-5 crystals.

The silicalite layer on H-ZSM-5(50) seems to consist of a closely-packed layer of 1 μm silicalite crystals with hexagonal cylindrical shape. In addition to that, the silicalite layers grew in the same direction of H-ZSM-5 crystals as in the case of the silicalite/H-ZSM-5(70) after the first hydrothermal synthesis. The deposited polycrystals after the second synthesis are randomly oriented and are not densely packed. However, the silicalite layer in the vicinity of the external surface of H-ZSM-5 seems

to be oriented and compact. A study on the epitaxial growth of silicalite layer at the silicalite/ZSM-5 interface using TEM measurements will be reported in the next chapter.

2.3.2 Alkylation of Toluene

Alkylation of toluene with methanol was carried out over uncoated H-ZSM-5 and silicalite/H-ZSM-5 catalysts. The molar fraction of produced *p*-xylene in all the produced xylene isomers is defined as the *para*-selectivity. Table 2.1 lists the toluene conversion, the aromatic product distribution and the fraction of xylene isomers before and after silicalite coating of H-ZSM-5(70).

Table 2.1 Alkylation of toluene with methanol over H-ZSM-5(70) and silicalite/H-ZSM-5(70).

	Silicalite/H-ZSM-5(70)	H-ZSM-5(70)
Conversion of toluene [%]	49.9	53.7
Product composition [%]		
Benzene	*D.L.*	0.2
p-Xylene	46.1	23.9
m-Xylene	*D.L.*	16.3
o-Xylene	*D.L.*	7.5
Ethyl toluenes	3.7	0.6
Trimethyl benzenes	0.1	4.1
Fraction of xylenes [%]		
p-Xylene	99.9	50.1
m-Xylene	<0.05	34.2
o-Xylene	<0.05	15.7

Reaction temperature: 673 K; Time on stream (TOS) = 60 min; W/F= 0.20 [kg-catalyst h mol^{-1}]; *D.L.*: below detection limit.

The toluene conversion and *para*-selectivity over H-ZSM-5 and silicalite/H-ZSM-5 with different Si to Al ratios were shown in Table 2.2. The *para*-selectivity increased significantly after silicalite coating in all the samples. The toluene conversion over silicalite/H-ZSM-5 was high even after the silicalite coating. The fraction of trimethyl benzene decreased from 4.1 to 0.1 % after silicalite coating. On the other hand, the yield of ethyl toluenes increased after silicalite-1 coating. The silicalite coating

did not only decrease the production of *o*-, *m*-ethyl toluenes and trimethyl benzenes, but also increased the fraction of *p*-ethyl toluene [28]. Since the molecular sizes of *o*- and *m*-ethyl toluenes are larger than the pore size of silicalite-1, the produced ethyl toluenes over silicalite/H-ZSM-5 must be *p*-ethyl toluene.

Table 2.2 Alkylation of toluene with methanol over H-ZSM-5 and silicalite/H-ZSM-5.

	Silicalite/H-ZSM-5(30)		Silicalite/H-ZSM-5(50)		Silicalite/H-ZSM-5(70)	
	toluene conversion [%]	*para*-selectivity [%]	toluene conversion [%]	*para*-selectivity [%]	toluene conversion [%]	*para*-selectivity [%]
Uncoated H-ZSM-5*	63	40	65	38	65	49
Silicalite/H-ZSM-5**	42	>99.9	52	>99.9	55	>99.9

Reaction temperature: 673 K, TOS = 60 min, * W/F= 0.09 [kg-catalyst h mol^{-1}], ** W/F= 0.15 [kg-catalyst h mol^{-1}]

Mirth et al. [4,5] studied toluene alkylation and isomerization on a H-ZSM-5 catalyst. They suggested that the high *para*-selectivity is obtained above 573 K because the rate of reaction is governed by a diffusion limitation at high temperature. Above 573 K, the rate of isomerization is higher than that of methylation, resulting in the accumulation of *m*-xylene and *o*-xylene in the pores. The ratios of diffusivities of three xylene isomers were determined to be *p*: *m*: *o* = 1000: 1: 10 [4]. At the reaction conditions, the *para*-selectivity is higher than that of the thermodynamic equilibrium value (23%) even for the uncoated catalyst. Thus, the rate of reaction must be controlled by a diffusion limitation for both the uncoated and coated catalysts. The effectiveness of the catalyst is low even for the uncoated catalyst. Even though *p*-xylene selectively forms in H-ZSM-5 in the diffusion control region, the isomerization on acid sites on the external surface reduces the *para*-selectivity for the uncoated catalyst. But, the silicalite layer could remove the acid sites on the external surface of H-ZSM-5 and inhibit isomerization of *p*-xylene. The enhancement of *para*-selectivity by a pore mouth modification using CVD [19,20,22,25] and CLD [6,17,18,26] methods has been reported by several research groups. But all the acid sites on the external surface have been difficult to remove by surface

modifications such as silylation. The silicalite coating is an excellent technique to cover the ZSM-5 crystals with an inactive layer. Further, in this method, the size of pore opening does not reduce after coating. This is the reason why the toluene conversion over silicalite/H-ZSM-5 was also high even after the silicalite coating.

The toluene conversion over silicalite/H-ZSM-5(30) was much lower than those over the other two silicalite/H-ZSM-5 catalysts. The silicalite-1 layer on H-ZSM-5(30) must be thicker than that of the other two H-ZSM-5 crystals, since toluene conversion and selectivity could significantly be affected by the quality and thickness of the silicalite-1 layer [27].

Changes of toluene conversion and *para*-selectivity over the uncoated H-ZSM-5(70) catalysts and silicalite/H-ZSM-5(70) with reaction time are shown in Fig. 2.4. Reaction temperature was 673 K and the space time (*W/F*) was 0.12 kg-catalyst h mol^{-1}.

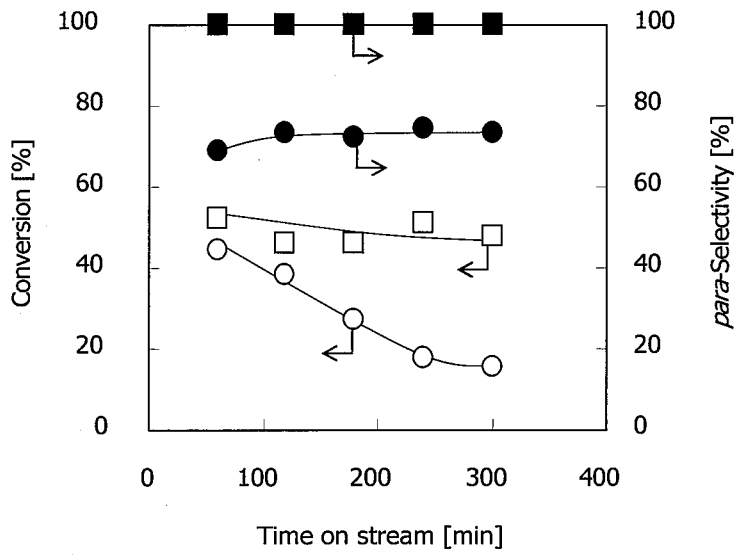

Fig. 2.4 Alkylation of toluene with methanol over the uncoated H-ZSM-5(70) and silicalite/H-ZSM-5(70) catalysts at 673 K. *W/F*= 0.12 kg-catalyst h mol^{-1}, methanol/toluene= 1.0. Open symbol; toluene conversion, filled symbol; *para*-selectivity. H-ZSM-5(70); Circle, silicalite/H-ZSM-5(70); square.

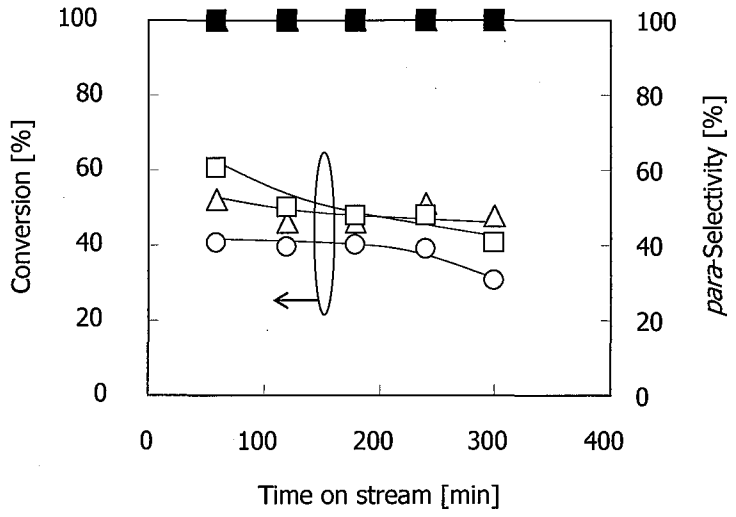

Fig. 2.5 Activity of the alkylation of toluene with methanol over silicalite/H-ZSM-5(70) with different methanol/toluene feed ratios at 673 K. *W/F*= 0.12 kg-catalyst h mol^{-1}. Open symbol; toluene conversion, filled symbol; *para*-selectivity. Methanol/toluene = 0.5; circle, 1.0; triangle, 2.0; square.

Toluene conversion and *para*-selectivity at the early period over the uncoated H-ZSM-5(70) catalyst were more than 40% and 65%, respectively. The toluene conversion rapidly decreased to less than 20 % after 240 min but the *para*-selectivity increased slightly with reaction time and reached about 70 % after 300 min. Compared to the uncoated H-ZSM-5, silicalite/H-ZSM-5(70) showed excellent *para*-selectivity (>99.9 %). The toluene conversion was more than 40 % which was larger than that of the uncoated H-ZSM-5(70) because the toluene conversion was constant during the reaction. This result indicates that the silicalite coating inhibited a coke formation caused by the reaction. The coke formation has been one of the biggest issues in the solid acid catalysts. The silicalite coating could not only enhance *para*-selectivity but also prevent deactivation of the catalysts. This result indicates that the coke formation occurs near the external surface of the H-ZSM-5 crystals. Because of diffusion resistance, the reaction mainly takes place near the surface of H-ZSM-5. Thus, coke formation largely affected on the reaction rate for the uncoated catalyst. The high stability of the coated catalyst under reaction can be explained by the removal of acid sites on the external surface of H-ZSM-5.

The activity of the alkylation of toluene with methanol over silicalite/H-ZSM-5(70) at different methanol to toluene ratios was shown in Fig. 2.5. The silicalite/H-ZSM-5 catalysts retained excellent *para*-selectivity, higher than 99.9 %, for 300 min under all reaction conditions. At the methanol/toluene molar ratio of 0.5, the maximum toluene conversion was theoretically 50 %. Since the toluene conversion was approximately 40 %, 80 % of methanol could be used for alkylation of toluene. In other words, the relative toluene conversion is 80 %. At the methanol/toluene molar ratio of 1.0, the toluene conversion was approximately 55 %. This result shows that methanol could be consumed for alkylation more efficiently at the lower molar ratio of methanol/toluene.

The toluene conversion and *para*-selectivity over the silicalite/H-ZSM-5(70) and uncoated H-ZSM-5(70) catalyst at different reaction temperatures were shown in Fig. 2.6 (a,b) respectively.

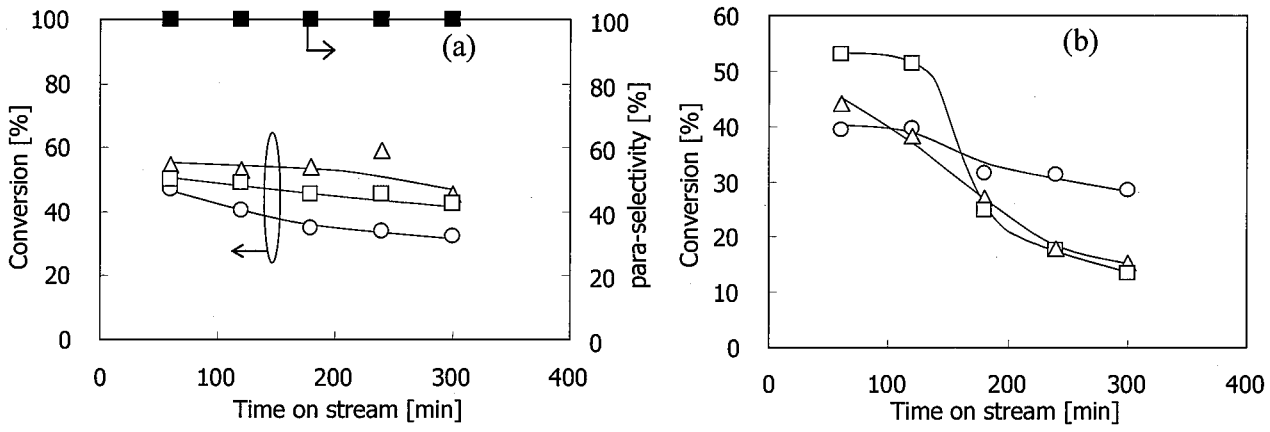

Fig. 2.6 Activity of the alkylation of toluene with methanol over (a) silicalite/H-ZSM-5(70) and (b) uncoated H-ZSM-5(70) at different reaction temperature. W/F= 0.15 [kg-catalyst h mol^{-1}] methanol/toluene= 1.0. Open symbol; toluene conversion, filled symbol; *para*-selectivity. 623 K; circle, 673 K; triangle, 773 K; square.

The *para*-selectivity was higher than 99.9% at all the temperatures and stable during the reaction for 300 min. The toluene conversion at 673 K was higher than that at 623 K, but the toluene conversion at 773 K was lower than that at 673 K. Both the diffusion rate and reaction rate of toluene are expected to increase as the reaction temperature increases. Hence, deactivation of catalysts might occur at the

earlier stage of the reaction at 773 K. The toluene conversion over the uncoated H-ZSM-5 significantly decreased at high temperatures, indicating that the deactivation of the uncoated H-ZSM-5 rapidly occurred at high temperatures. The deactivation rate was still low over the silicalite-coated catalyst at high temperatures.

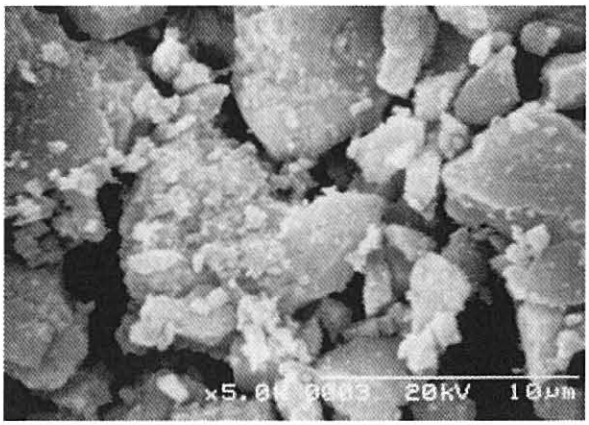

Fig. 2.7 SEM image of crushed silicalite/H-ZSM-5 crystals(70).

Fig. 2.7 shows an SEM image of the crushed silicalite/ZSM-5. The silicalite coating layer must have been broken completely by grinding. The activity and selectivity on the alkylation of toluene over the crushed silicalite/ZSM-5 were summarized in Table 2.3. The *para*-selectivity over the crushed silicalite/ZSM-5 was decreased to the same level of the uncoated ZSM-5. This result strongly suggests that a compact silicalite layer play an important role in enhancing the *para*-selectivity.

In Fig. 2.8, the toluene conversion and *para*-selectivity over the silicalite/H-ZSM-5 catalyst in this study were compared to those over various reported H-ZSM-5 catalysts modified by silylation and impregnation. Normally, the *para*-selectivity has a trade-off relationship with the conversion. However, the silicalite/H-ZSM-5 catalyst shows high *para*-selectivity even when the toluene conversion is high, indicating that the silicalite coating on the external surface of ZSM-5 crystals is one of the most effective techniques to inhibit the isomerization from *p*-xylene to the other xylene isomers near the external surface of ZSM-5.

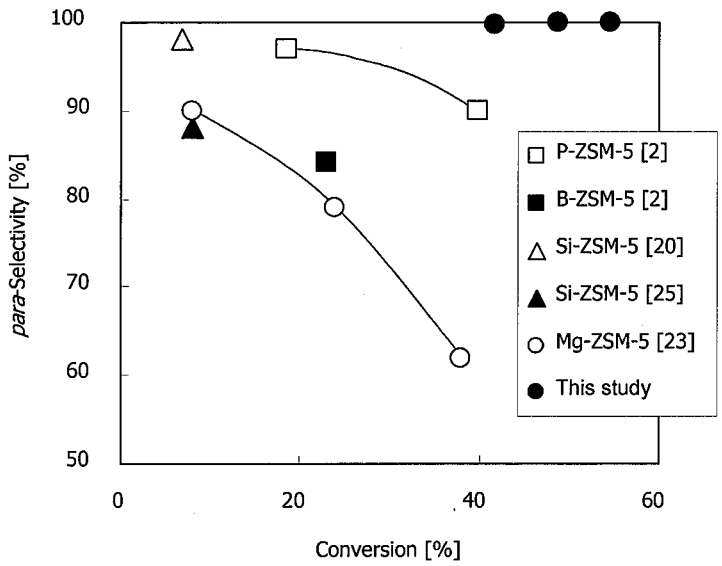

Fig. 2.8 The alkylation of toluene with methanol over various modified H-ZSM-5 catalysts and silicalite/H-ZSM-5(70).

Table 2.3 Alkylation of toluene with methanol over crushed silicalite/H-ZSM-5(70).

	Crushed silicalite/H-ZSM-5(70)
Conversion of toluene [%]	64.3
Fraction of xylenes [%]	
p-Xylene	48.0
m-Xylene	39.9
o-Xylene	12.0

Reaction temperature: 673 K, TOS = 60 min, W/F= 0.20 [kg-catalyst h mol^{-1}]

The enhanced *para*-selectivity may originate from diffusion resistance through the inactive silicalite layer on the H-ZSM-5 resulting in an increased diffusion length. This mechanism is similar to those reported for the surface-modified zeolites by silylation. [6,17,19] The excellent *para*-selectivity higher than the reported values suggests that silicalite coating under hydrothermal conditions is an effective way to remove acid sites from the external surface of zeolite.

2. 4 Conclusions

H-ZSM-5 crystals with different Si/Al molar ratios were coated with silicalite-1 layers by hydrothermal synthesis. The silicalite layers formed consisted of oriented polycrystallites of a few μm thicknesses which grew on the surface of the substrate H-ZSM-5 in the early stage of synthesis. The presence of Al in the H-ZSM-5 must have affected the formation of the polycrystalline layer.

When applied in the alkylation of toluene with methanol, the silicalite/H-ZSM-5 catalysts showed excellent *para*-selectivity, >99.9 %, under all the reaction conditions. The toluene conversion over the silicalite/H-ZSM-5 catalyst was almost constant, indicating that the silicalite coating inhibited coke formation on the external surface of H-ZSM-5. The high selectivity to *p*-xylene and high stability can be explained by the removal of acid sites on the external surface of H-ZSM-5.

References

[1] N.Y. Chen, W.W. Kaeding, F.G. Dwyer, J. Am. Chem. Soc. 101 (1979) 6783

[2] W.W. Kaeding, C. Chu, L.B. Young, B. Weinstein, S.A. Butter, J. Catal. 67 (1981) 159

[3] M.A. Uguina, J.L. Sotelo, D.P. Serrano, Appl. Catal. A 76 (1991) 183

[4] G. Mirth, J. Cejka, J.A. Lercher, J. Catal. 139 (1993) 24

[5] G. Mirth, J.A. Lercher, J. Catal. 147 (1994) 199

[6] J. Cejka, N. Zilkova, B. wichterlova, G. Elder-Mirth, J.A. Lercher, Zeolites 17 (1996) 265

[7] R. Mantha, S. Bhatia, M.S. Rao, Ind. Eng. Chem. Res. 30 (1991) 281

[8] T. Yashima, H. Ahmad, K. Yamazaki, M. Katsuta, N. Hara, J. Catal. 16 (1970) 273

[9] T. Yashima, K. Sato, T. Hayasaka, N. Hara, J. Catal. 26 (1972) 303

[10] A.E. Palomares, G. Elder-Mirth, J. A. Lercher, J. Catal. 168 (1997) 442

[11] E. Dumitriu, V. Hulea, S. Kaliaguine, M.M. Huang, Appl. Catal. A 135 (1996) 57

[12] P. Ratnasarmy, R.N. Bhat, S.K. Pokhriyal, J. Catal. 119 (1989) 65

[13] J. Das, Y.S. Bhat, A.B. Halgeri, Catal. Lett. 23 (1994) 161

[14] P. Wu, T. Komatsu, T. Yashima, Micropor. Mesopor. Mater. 22 (1998) 343

[15] P. Prokesova, N. Zilkova, S. Mintova, T. Bein, J. Cejka, Appl. Catal. A 281 (2005) 85

[16] S. Zheng, H.R. Heydenrych, A. Jentys, J. A. Lercher, J. Phys. Chem. B 106 (2002) 9552

[17] S. Zheng, H. Tanaka, A. Jentys, J. A. Lercher, J. Phys. Chem. B 108 (2004) 1337

[18] S. Laforge, D. Martin, J.L. Paillaud, M. Guisnet, J. Catal. 220 (2003) 92

[19] M. Niwa, M. Kato, T. Hattori, Y. Murakami, J. Phys. Chem. 90 (1986) 6233

[20] T. Hibino, M. Niwa, Y. Murakami, J. Catal. 128 (1991) 551

[21] M.A. Uguina, D.P. Serrano, Van R. Grieken, S. Vènes, Appl. Catal. A 99 (1993) 97

[22] J.-H. Kim, A. Ishida, M. Okajima, M. Niwa, J. Catal. 161 (1996) 387

[23] Y.-G. Li, W.-H. Xie, S. Yong, Appl. Catal. A 150 (1997) 231

[24] L.-Y. Fang, S.-B. Liu, I. Wang, J. Catal. 185 (1999) 33

[25] A.B. Halgeri, J. Das, Catal. Today 73 (2002) 65

[26] S. Zheng, H.R. Heydenrych, H.P. Röger, A. Jentys, J.A. Lercher, Topics in Catal. 22 (2003) 101

[27] N. Nishiyama, M. Miyamoto, Y. Egashira, K. Ueyama, Chem. Commun. (2001) 1746

[28] N. Nishiyama, K. Ichioka, D.-H. Park, Y. Egashira, K. Ueyama, L. Gora, W. Zhu, F. Kapteijn, J.A. Moulijn, Ind. Eng. Chem. Res. 43, (2004) 1211

[29] N. Nishiyama, K. Ichioka, M. Miyamoto, Y. Egashira, K. Ueyama, L. Gora, W. Zhu, F. Kapteijn, J.A. Moulijn. Micropor. Mesopor. Mater. 83 (2005) 244

[30] M. Miyamoto, T. Kamei, N. Nishiyama, Y. Egashira, K. Ueyama, Adv. Mater. 17 (2005) 1985

[31] E.D. Burchart, J.C. Jansen, H. van Bekkum, Zeolites 9 (1989) 432

[32] K.R. Kloetstra, H.W. Zandbergen, J.C. Jansen, van H. Bekkum, Micropor. Mesopor. Mater. 6 (1996) 287

[33] A.L. Yonkeu, V. Buschmann, G. Miehe, H. Fuess, A.M. Goosses, J.A. Martens, Crystal Engineering 4 (2001) 253

[34] C. S. Lee, T. J. Park, W. Y. Lee, Appl. Catal. A 96 (1993) 151

[35] Q. Li, J. Hedlund, J. Sterte, D. Creaser, A.-J. Bons, Micropor. Mesopor. Mater. 56 (2002) 291

[36] Q. Li, Z. Wang, J. Hedlund, D. Creaser, H. Zhang, X. Zou, A.-J. Bons, Micropor. Mesopor. Mater. 78 (2005) 1.

Chapter 3

Catalytic Activities and Structures of Silicalite-1/H-ZSM-5 Zeolite Composites

Polycrystalline silicalite layers were formed on H-ZSM-5 with different crystal sizes of 5 – 30 μm. The silicalite-1/H-ZSM-5 composite with a crystal size of 5 μm showed high catalytic activity and excellent of *para*-xylene selectivity. But, *para*-selectivity slightly decreased with increasing the crystal size, indicating that the surface of the large H-ZSM-5 crystals was not fully covered by the silicalite-1 layer. The toluene conversion over the catalyst with a small crystal size (5 μm) was very stable with reaction time, while the catalysts with large crystal sizes were rapidly deactivated. The crystalline structure of the interface between silicalite-1 and H-ZSM-5 crystals was studied by FE-SEM and TEM observations. The silicalite-1 crystals were epitaxially grown on the surface of the H-ZSM-5 crystals and their pores must be directly connected to the pores of H-ZSM-5.

3.1 Introduction

Medium pore size MFI zeolites have found to be suitable for the production of *para*-dialkyl aromatics because their pore size is similar to the molecular dimensions of these aromatics. To enhance *para*-selectivity, a number of modification techniques have been reported [1-6]. Although these modification techniques could increase *para*-selectivity, the conversion was decreased significantly because a diffusion resistance of products increased by narrowing of the pore-opening size.

On the other hand, both high *para*-xylene selectivity and high toluene conversion were provided over silicalite/ZSM-5 composite catalysts as shown in Chapter 2. The silicalite-1 coating significantly increased the *para*-selectivity to nearly 100%. In this chapter, the crystalline structure of the interface between silicalite-1 and H-ZSM-5 was observed carefully. The reasons for the high *para*-selectivity and high toluene conversion will be discussed from the viewpoint of the structure of the composite. High catalytic activity and selectivity of silicalite-1/H-ZSM-5 composites might be caused by the direct connection between H-ZSM-5 and silicalite-1 and an oriented crystal growth of the silicalite-1 crystals along the surface of the H-ZSM-5 crystals [7].

According to the reports on silicalite-1 layers grown on ZSM-5 [8-10], the structure and thickness of the silicalite layer depend on the Si/Al ratio, crystal size and shape of the substrate H-ZSM-5. In this chapter, silicalite layers were formed on H-ZSM-5 catalysts with different crystal sizes. In addition, the influence of the crystal size on the catalytic activity and deactivation behavior for the alkylation of toluene was investigated.

3.2 Experimental

3.2.1 Preparation of HZSM-5

ZSM-5 zeolites were synthesized under hydrothermal conditions with a Si/Al ratio of 70. The reactant materials used for the synthesis were tetraethylorthosilicate (TEOS; $(C_2H_5O)_4Si$; Wako Pure Chemical Industries Co., Ltd.) and colloidal silica (CS; Nissan Chemical Co., Ltd.) as silica sources, aluminum nitrate ($Al(NO_3)_3 \cdot 9H_2O$; Wako Pure Chemical Industries Co., Ltd.) as an alumina source, tetraprophylammonium bromide (TPABr; Wako Pure Chemical Industries Co., Ltd.), deionized water (H_2O), and sodium hydroxide (NaOH). The molar composition was 2.5 SiO_2 (TEOS): 1.0 SiO_2 (CS): 0.025 Al_2O_3: 0.5 TPABr: 0.25 Na_2O: 120 H_2O.

The synthesis solution was mixed for 30 min at 303 K. The crystallization was carried out in closed Teflon-lined stainless steel vessels under autogenous pressure at 453 K for 24 h. To stir the

solution during the hydrothermal synthesis, the vessel was rotated in an oven. The crystalline size of ZSM-5 zeolites was controlled by changing a rotating speed and a volume of the closed vessel. The products were then calcined at 873K for 5 h to remove TPA cations remaining in their structures. A proton-exchange process was carried out by using an ammonium chloride (NH_4Cl, 1 N) aqueous solution. The ZSM-5 crystals were mixed with the NH_4Cl aqueous solution for 12 h at ambient temperature. The crystals were then calcined again at 873 K.

3.2.2 Preparation of Silicalite-1/HZSM-5

H-ZSM-5 with different crystal sizes was used as a core zeolite for the silicalite coatings. The precursor solution consisted of TEOS, tetraprophylammonium hydroxide (TPAOH), ethanol (EtOH) and deionized water with the molar ratios of 0.5TPAOH: $120H_2O$: 8EtOH: $2SiO_2$. The H-ZSM-5 crystals were immersed in the precursor solution at the mass ratio of 0.06. The crystallization was carried out at 453 K for 24 h in a stainless steel vessel by hydrothermal synthesis with agitation condition. The coating was repeated twice. The products were rinsed repeatedly by deionized water and dried at 363K overnight, then calcined in air at 873K for 5 h with a heating rate of 1K min^{-1}. The products were gathered by using filtration. Here, the mass changes after coating were measured after both the first and second coating.

3.2.3. Characterizations

The products were characterized by X-ray diffraction (XRD) recorded on a Rigaku Miniflex using Cu-Kα radiation and scanning electron microscope (SEM) on a Hitachi S-2250N. The crystalline structure of the silicalite-1/H-ZSM-5 composite was observed by the field emission scanning electron microscopy (FE-SEM) on a Hitachi S-5000L microscope at an acceleration voltage of 21 kV and the transmission electron microscope (TEM) on FEI Tecnai 20 at 120 kV and 200 kV.

Alkylation of toluene with methanol over the ZSM-5 and silicalite/ZSM-5 catalysts with different crystal sizes was performed using a fixed bed reactor at 673K. The space time *W/F* is 0.14 [kg-catalyst h mol^{-1}] and the molar ratio of methanol/toluene was 1.0. The products of alkylation were analyzed by a gas chromatograph GC-2014 (Shimadzu Co.) equipped with a flame ionization detector (FID) using a Xylene Master column PRC 7791 (50 m, 0.32 mm).

3.3. Results and Discussion

3.3.1 Morphology of H-ZSM-5 and Silicalite-1/H-ZSM-5 Composites

Fig. 3.1 shows the SEM images of H-ZSM-5 crystals with different crystal sizes. The samples are labeled as S1-S4. The crystal sizes of the S1-S4 HZSM-5 crystals are 5, 10, 20 and 30 μm, respectively. The XRD analysis of the uncoated and coated samples did not include reflection peaks for amorphous silica and impurities other than an MFI structure (data not shown). The crystal sizes changed at different rotating speeds of the vessels. The stirring conditions seem to influence a nucleation rate of H-ZSM-5.

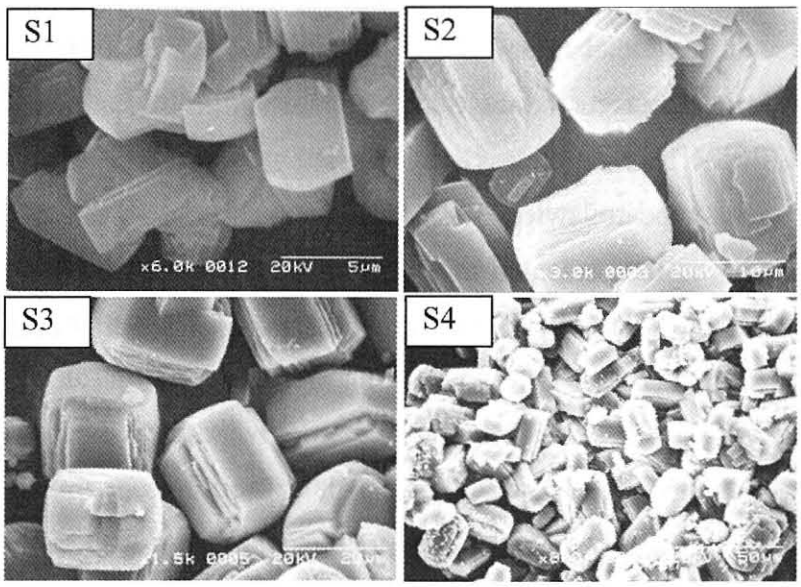

Fig. 3.1 SEM images of H-ZSM-5 with different crystal sizes.

The SEM images of the S1-S4 HZSM-5 after the silicalite coating are shown in Fig. 3.2. An overgrowth of a silicalite-1 layer on the H-ZSM-5 crystals (S1) was observed clearly. The coatings were composed of silicalite-1 polycrystals with a size of 1 μm. The crystal size did not increase so much even after the second coating. The thickness of the silicalite-1 layer must be less than a few μm.

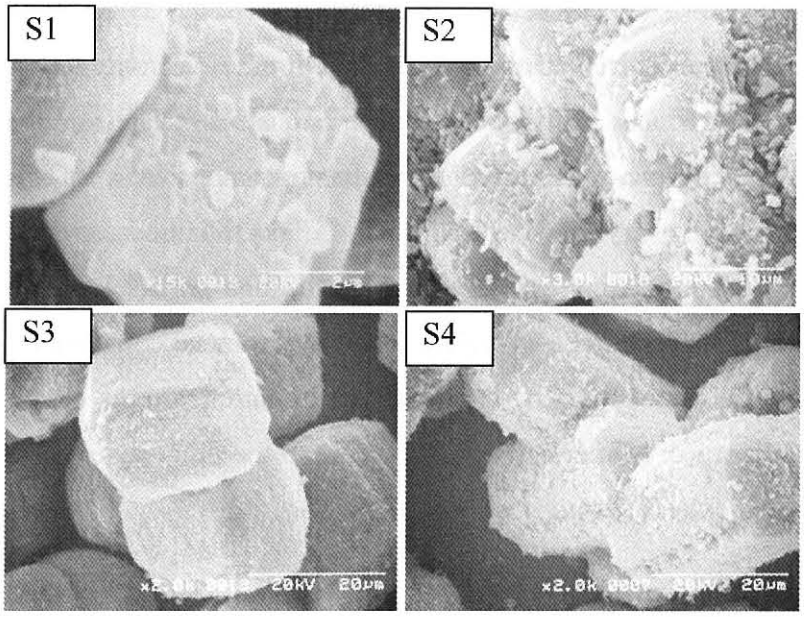

Fig. 3.2 SEM images of silicalite-1/H-ZSM-5 zeolite composites.

The mass gain was slightly increased with decreasing crystal size because of an increase in an external surface area of H-ZSM-5. The mass gain after the silicalite-1 coating was too large for all the samples, considering that the silicalite-1 layer formed on the H-ZSM-5 surface was very thin. This result indicated that a large amount of silicalite-1 crystals was formed through a homogeneous nucleation in the solution. These crystals do not contribute to the external surface modification of the H-ZSM-5 crystals. Revised synthesis conditions to inhibit homogeneous nucleation will be reported in the next chapter.

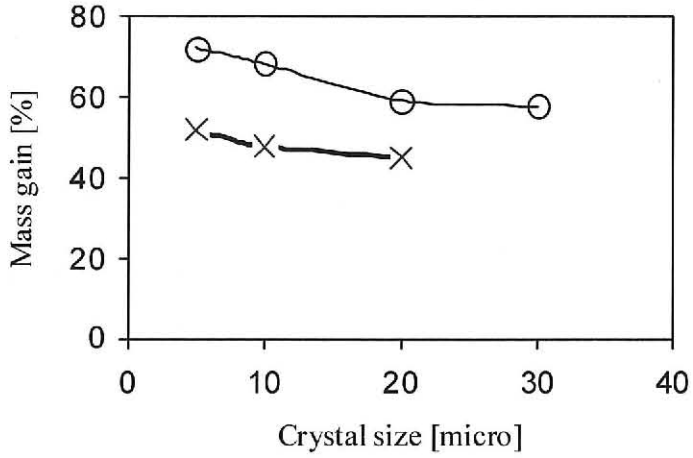

Fig. 3.3 Mass gain after silicalite-1 coating after. ×: the 1st synthesis; o: the 2nd synthesis.

3.3.2 Influence of Crystal Sizes on Catalytic Activities

Alkylation of toluene with methanol was carried out over the uncoated H-ZSM-5 and silicalite/H-ZSM-5 catalysts. The molar fraction of produced *p*-xylene in all the produced xylene isomers is defined as the *para*-selectivity. The toluene conversion and *para*-selectivities were plotted as a function of the crystal size in Fig. 3.4. The toluene conversion on the uncoated H-ZSM-5 decreased with increasing crystal size. Instead, high *para*-selectivity was obtained over the large H-ZSM-5 crystals. The trade-off relation between toluene conversion and *para*-selectivity indicates that the reaction is governed by the diffusion limitation. On the other hand, small crystals have a large external surface. Isomerization of *p*-xylene to the other xylene isomers takes place on the external surface, which reduces *para*-selectivity.

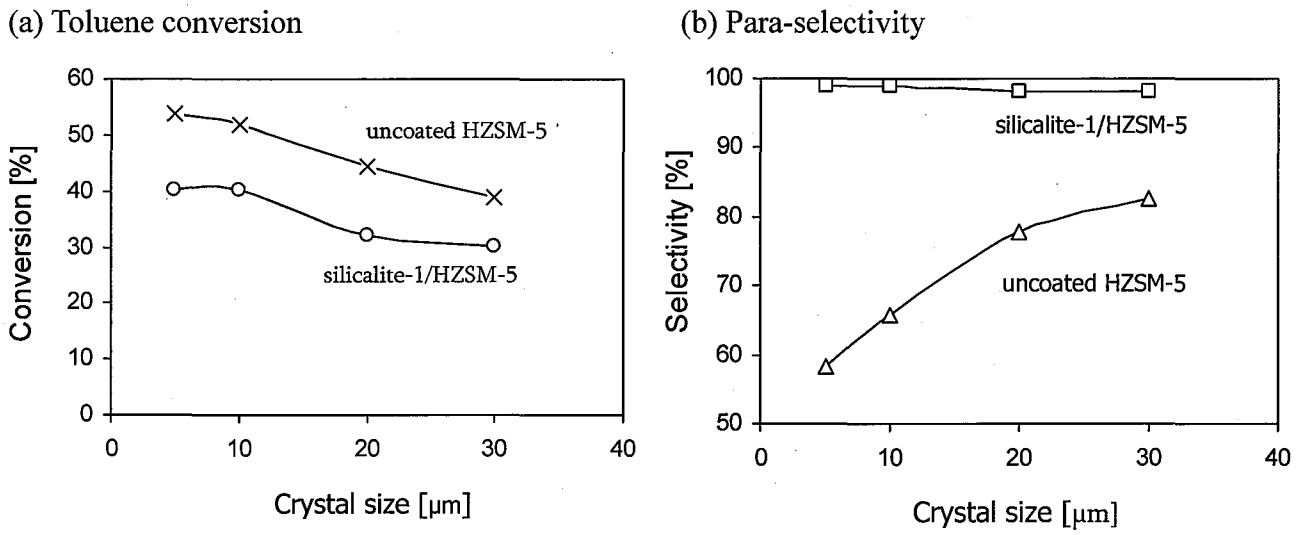

Fig. 3.4 Toluene conversion and *p*-xylene selectivity in toluene alkylation as a function of crystal size of the zeolite catalysts. T = 673K, W/F = 0.14 [kg-cat h mol^{-1}], [MeOH]/ [toluene] = 1.0. TOS = 60 min.

The toluene conversion over the silicalite-1/H-ZSM-5 composites was less than that over the uncoated ones, which would be caused by an increase in diffusion length for the reaction products through the inactive silicalite membrane. Instead, the *para*-selectively largely increased after the silicalite-1 coating for all the samples. The silicalite/H-ZSM-5 composite of the smallest crystal size (5 μm) showed extremely high *p*-xylene selectivity (nearly 100%). The high *para*-selectivity can be explained by the removal of acid sites on the external surface of H-ZSM-5. But, *para*-selectivity slightly decreased with increasing crystal size, indicating that the large crystals could not be fully

covered with a silicalite layer. The silicalite coating not only enhanced *para*-selectivity, but also prevented catalyst deactivation. This result indicates that coke formation occurred near the external surface of H-ZSM-5 crystals. Because of diffusion resistance, the reaction occurred mainly near the surface of H-ZSM-5. Thus, coke formation significantly affected on the reaction rate for uncoated catalyst that was also discussed in Chapter 2.

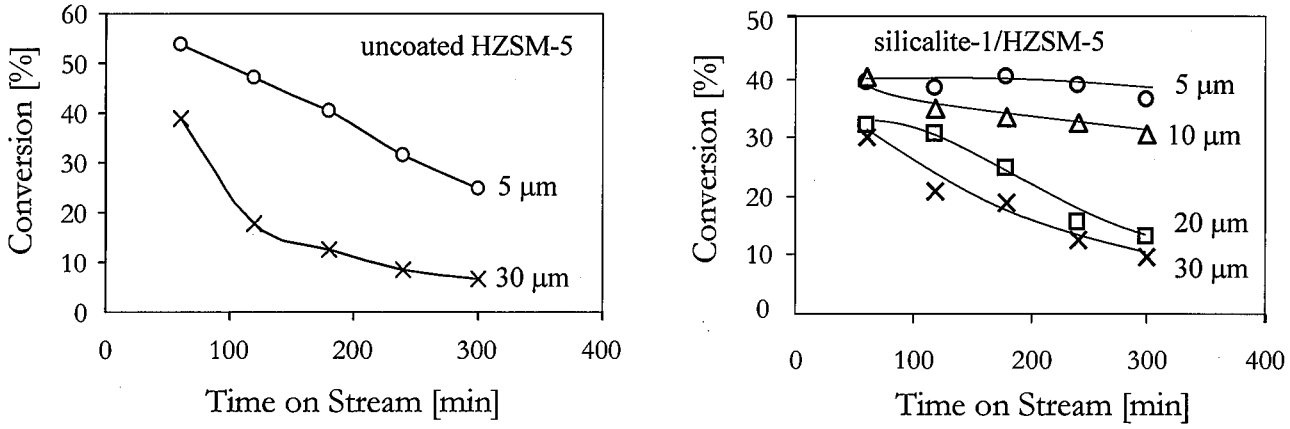

Fig. 3.5 Time course of the toluene conversion over uncoated H-ZSM-5 and silicalite/H-ZSM-5 composites. T = 673K. W/F = 0.14 [kg-cat h mol^{-1}], [MeOH]/[toluene] = 1.0. ○: 5 μm; Δ: 10 μm; □: 20 μm; ×: 30 μm.

Time course of the toluene conversion on the silicalite-1/H-ZSM-5 composites with different crystal sizes is shown in Fig. 3.5.

The toluene conversion on the silicalite/H-ZSM-5 composite with a crystal size of 5 μm was high and almost constant with the reaction time. The toluene conversion decreased with increasing crystal size due to an increase in the length of intracrystalline diffusion pathway as described above. Furthermore, the catalysts with large crystal sizes of 20 μm and 30 μm were rapidly deactivated. Coking on the acid sites which remain on the external surface of the large H-ZSM-5 crystals must contribute to the deactivation. This result indicates that it is hard to fully cover large H-ZSM-5 crystals with silicalite layers. In conclusion, small H-ZSM-5 crystals coated by a thin silicalite layer with a high surface coverage are required to attain both high activity and high selectivity. The silicalite coating must have inhibited coke formation near the surface of H-ZSM-5.

3.3.3 Crystalline Structure of Silicalite-1/H-ZSM-5 Composite

The crystalline structure of silicalite-1/H-ZSM-5 composites was observed by FE-SEM and TEM measurements. For the TEM measurements, very small H-ZSM-5 crystals were synthesized. The small H-ZSM-5 crystals were coated by silicalite. The preparation procedure for small ZSM-5 and coating process were described in Chapter 6. The FE-SEM images of the silicalite-1/ZSM-5 composite were shown in Fig. 3.6.

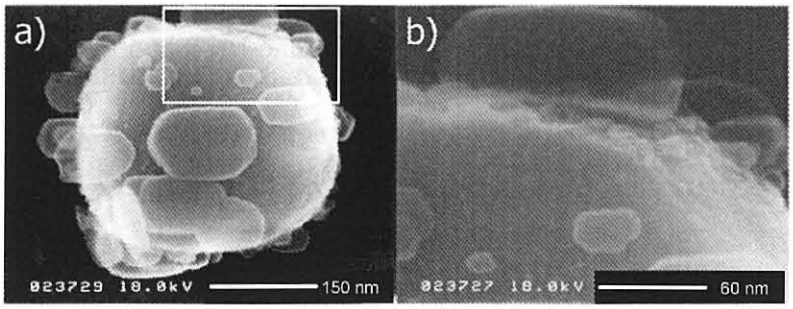

Fig. 3.6 FE-SEM images of a silicalite-1/H-ZSM-5 composite. Acceleration voltage of 21 kV.

A number of small silicalite-1 crystals were formed on the H-ZSM-5 crystal. The H-ZSM-5 and silicalite-1 crystals were estimated approximately 300 nm and 10-150 nm in size, respectively. The ZSM-5 crystal was a disk in shape. All silicalite-1 crystals were longer in the [001] direction compared to in the [100] and [010] directions.

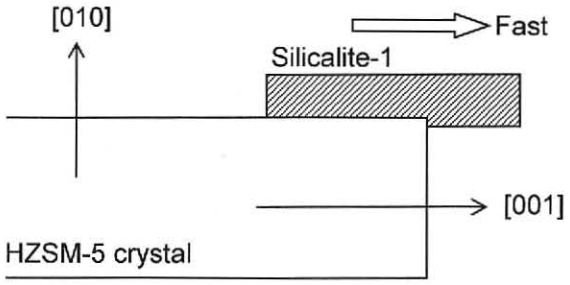

Fig. 3.7 Schematic diagram of silicalite-1 growth on the (010) surface of the H-ZSM-5 crystal.

The crystalline growth rate of silicalite-1 to the direction of c axis must be larger than the other directions. A preferential nucleation of silicalite-1 on the (100) and (010) surfaces of the ZSM-5 crystal was observed. Especially, the crystal nucleus formed on the (010) surface protruded to the direction of c axis from the edge of ZSM-5 as displayed in Fig. 3.7. The silicalite-1 crystals were grown on the (010) surface of ZSM-5 in the direction of a and c axes.

Fig. 3.8a shows a low magnification image of the silicalite-1/H-ZSM-5 composite. Fig. 3.9b was a high-resolution electron microscopy (HREM) image of the composite observed at the

location pointed in Fig. 3.7. The incident beam direction was [010]. The [101] lattice fringes of the silicalite-1 layers formed at different positions on the ZSM-5 surface were parallel.

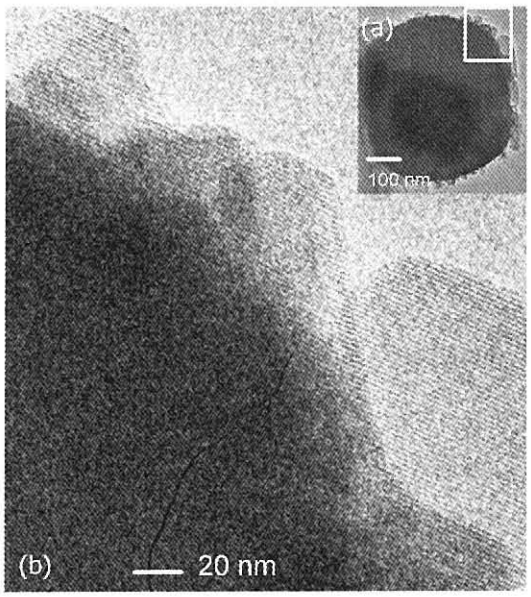

Fig. 3.8 TEM images of a silicalite-1/H-ZSM-5 composite at 200 kV. The incident beam direction is [010].

Then, the TEM images in Fig. 3.9 show a crystalline structure of the interface between the H-ZSM-5 substrate and silicalite-1 crystals. These silicalite-1 crystals were grown on the surface of ZSM-5 perpendicular to the a axis, estimated by the morphology of the ZSM-5 crystal. The silicalite-1 crystals must have grown fast to the direction of c axis because the aspect ratio of the crystals was high in this direction. The HREM image in Fig. 3.9b provides the lattice fringe of the ZSM-5 crystal and the silicalite-1 crystals in the [101] direction. No discontinuity of the lattice fringe was observed between the ZSM-5 and silicalite-1 crystals. Silicalite-1 crystals have the same MFI crystalline structure as ZSM-5 crystals although the lattice constants between these crystals are slightly different (less than 1 %). The interface between the ZSM-5 and the silicalite-1 was continuous without any misfits. In other words, the silicalite-1 crystals can be grown epitaxially on the ZSM-5 crystal in the early stage of the silicalite-1 growth, and the interface between silicalite-1 and ZSM-5 is coherent. Therefore, the silicalite-1 channels must be connected continuously to the ZSM-5 pores. Similar epitaxial intergrowth of silicalite on ZSM-5 was reported by Hedlund's group [10].

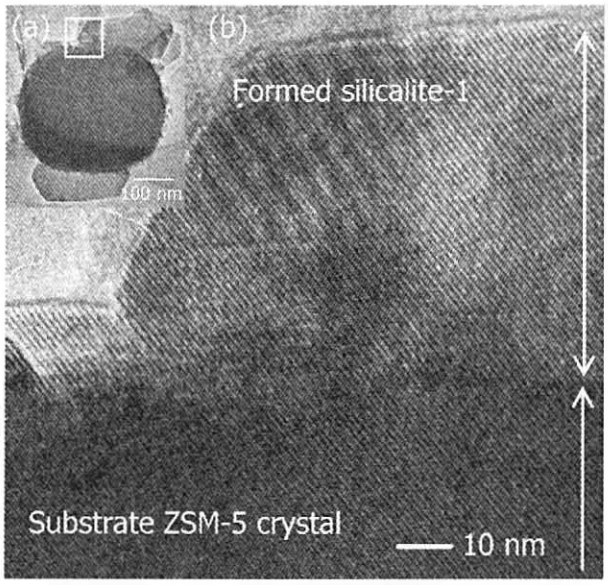

Fig. 3.9 TEM image of the composite crystal (a) and the HREM image at the interface between silicalite-1 and H-ZSM-5 (b) at 120 kV.

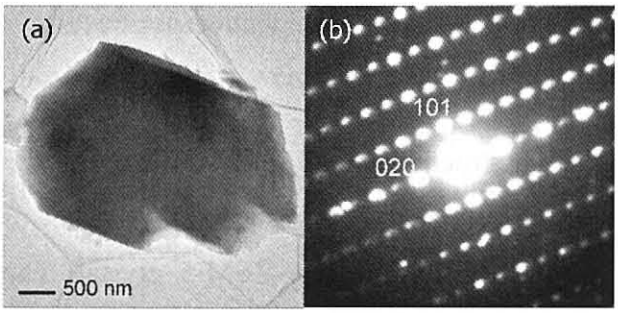

Fig. 3.10 TEM image of silicalite-1/H-ZSM-5 large crystal with a low magnification (a) and the electron diffraction pattern of the composite taken along [101] (b) at 200 kV.

Next, a silicalte-1/ZSM-5 composite with a crystal size of ca. 3 μm was used for the TEM observation. Fig. 3.10 shows the TEM image and electron diffraction pattern of the silicalite/ZSM-5 composite. The incident beam direction was [101]. The crystal boundaries between ZSM-5 and silicalite-1 can not be observed clearly in Fig. 3.10a.

The diffraction pattern (Fig. 3.10b) was indexed to be a single phase. These results indicate that the silicalite-1 monolayer could cover a whole ZSM-5 crystal with the same orientation as the core crystal. Therefore, the pores in the silicalite-1 monolayer might be connected to the ZSM-5 pores at the early stage of synthesis.

The silicalite-1 layer could extend the diffusion path length for xylenes. Therefore, the excellent *para*-selectivity was achieved by an increase in diffusion resistance for *o*- and *m*-xylene

because their molecular sizes are larger than the pore size of silicalite-1. On the other hand, the diffusivity of *p*-xylene did not decrease so much because of smaller molecular size of *p*-xylene. These effects might have contributed to the high toluene conversion on the alkylation of toluene. Further, acid sites on the external surface of H-ZSM-5 can be removed by the full coverage of the H-ZSM-5 surface with epitaxially grown silicalite-1 layers. This coating layer must effectively inhibit coking near the surface of the H-ZSM-5 catalysts.

3. 4 Conclusions

Polycrystalline silicalite layers were formed on H-ZSM-5 with different crystal sizes of 5 – 30 μm. The silicalite/HZSM-5 composite with a crystal size of 5 μm showed high *para*-xylene selectivity (nearly 100%). The toluene conversion over the silicalite/HZSM-5 composite (5 μm) was high and stable with reaction time. The silicalite coating must have inhibited coke formation near the surface of H-ZSM-5.

Para-selectivity slightly decreased with increasing crystal size and the catalyst with a large crystal size rapidly deactivated, indicating that the large crystals could not be fully covered with a silicalite layer. The acid site on the external surface for the large crystal must contribute to the deactivation. Small H-ZSM-5 silicalite core-shell composites are expected for industrial applications.

High catalytic activity and selectivity of silicalite-1/H-ZSM-5 composites must be caused by the direct pore-to-pore connection between H-ZSM-5 and silicalite-1. An oriented crystal growth of the silicalite-1 crystals along the surface of the H-ZSM-5 crystals was found at the early stage of the hydrothermal synthesis.

References

[1] T. Hibino, M. Niwa, Y. Murakami, J. Catal. 128 (1991) 551

[2] J.-H. Kim, A. Ishida, M. Okajima, M. Niwa, J. Catal. 161 (1996) 387

[3] J. Cejka, N. Zilkova, B. Wichterlova, G. Elder-Mirth, J.A. Lercher, Zeolites 17 (1996) 265

[4] S. Zheng, H. Tanaka, A. Jentys, J.A. Lercher, J. Phys. Chem. B. 108 (2004) 1337

[5] N.Y. Chen, W.W. Kaeding, F.G. Dwyer, J. Am. Chem. Soc. 101 (1979) 6783

[6] W.W Kaeding, C. Chu, L.B. Young, B. Weinstein, S.A. Butter, J. Catal. 67 (1981) 159

[7] M. Miyamoto, T. Kamei, N. Nishiyama, Y. Egashira, K. Ueyama, Adv. Mater. 17 (2005) 1985

[8] W. Li, J. Hedlund, J. Sterte, D. Creaser, A.-J. Bons, Micropor. Mesopor. Mater. 56 (2002) 291

[9] Q. Li, J. Hedlund, D. Creaser, J. Sterte, J. Chem. Commun. (2001) 527

[10] Z. Wang, J. Hedlund, H. Zhang, X. Zou, Micropor. Mesopor. Mater. 95 (2006) 89.

Chapter 4

Morphology Control of Silicalite/HZSM-5 Composite Catalysts for the Formation of *para*-Xylene

Single- and poly-crystalline silicalite/HZSM-5 core-shell composite catalysts were synthesized by optimizing the silicalite coating conditions. At low molar ratios of SiO_2 (fumed silica) and tetraprophylammonium hydroxide (TPAOH) in the coating solutions, a crystal growth of silicalite layer on the HZSM-5 surface was dominant instead of a homogeneous nucleation in the solution. The mass gain after the coating was also inhibited at low molar ratios of silica source and TPAOH. High *para*-selectivities of silicalite/HZSM-5 composites in the toluene alkylation with methanol were obtained over the single crystal-like silicalite/H-ZSM-5 composite catalyst prepared by one coating process.

4.1 Introduction

In previous chapters, novel silicalite-1/HZSM-5 composite catalysts have been developed. The composites showed excellent *para*-selectivities and high conversions in the alkylation reaction of toluene with methanol compared to those of other proposed catalysts [1-9]. The effects of Si/Al ratios and crystal sizes as well as reaction conditions on the catalytic activity of catalysts were investigated in previous chapters. The high toluene conversions over the composite catalysts could be explained by the interlayer between silicalite and HZSM-5, those were directly connected together. However, the top layer was composed of deposited polycrystals, which were randomly oriented and were not densely packed. Thus, repeated coating processes were required for obtaining highly selective catalysts. These polycrystalline layers seem to have a low mechanical strength and will become a problem in severe conditions such as in fluidized bed reactors. Another problem is a homogeneous nucleation of silicalite crystals in the solution. Namely, the silicalite crystals formed not only on the ZSM-5 surface but also in the solution. It is not easy to separate the silicalite crystals formed in the solution from the silicalite/ZSM-5 composites. Thus, the mass gain of the products after the coating was very large in the previous reports. Considering the thin silicalite layer on the surface of HZSM-5 crystals, the mass gain was mainly due to the homogeneous nucleation of silicalite in the liquid phase. The presence of silicalite crystals without catalytic activity would reduce the efficiency of catalysts. Furthermore, the repeated silicalite coating synthesis seems to be complicated from the viewpoint of large scale application.

In this chapter, morphology of the silicalite/HZSM-5 composite crystals was studied by changing the molar ratios of silica source and structure directing agent (SDA) in the coating solutions. The alkylation of toluene with methanol was performed using the composite catalysts with different morphologies.

4.2 Experimental

4.2.1. Catalyst Preparation and Characterization

HZSM-5 crystals were used as a core for the silicalite coatings. The preparation of HZSM-5 was described in Chapter 2. HZSM-5 catalyst with a Si/Al ratio of 100 was prepared by hydrothermal synthesis at 453 K for 24 h. The synthesis solution consisted of tetraethoxysilane (TEOS), aluminum nitrate [$Al(NO_3)_3 \cdot 9H_2O$], sodium hydroxide (NaOH), and tetrapropylammonium bromide (TPABr). The molar ratio was: 2.0 SiO_2: 0.01 Al_2O_3: 0.5 TPABr: 0.25 Na_2O: 120 H_2O.

The precursor solution for the silicalite coatings consisted of fumed silica (Aerosil 200; Wako Pure Chemical Industries Co., Ltd.) and TEOS as silica sources, tetraprophylammonium hydroxide (TPAOH; Wako Pure Chemical Industries Co., Ltd.), TPABr, deionized water (H_2O), and ethanol (EtOH). The molar ratios of the coating solutions were shown on the Table. 1. Here, approximately 0.3 g of HZSM-5 crystals was immersed in 15 g of the precursor solution. The crystallization was carried out in a closed Teflon-lined stainless steel vessel under autogenous pressure at 453 K for 24 h. To stir the solution during the hydrothermal synthesis, the vessel was rotated in an oven. The products were then calcined at 873K for 5 h to remove TPA cations remaining in their structures. The final products were characterized by X-ray diffraction (XRD) recorded on a Rigaku Miniflex using Cu-Kα radiation and scanning electron microscope (SEM) on a Hitachi S-2250N.

Table 4.1 Molar ratios of the coating solutions and the mass gain of the products

Silica source	Sample	Molar ratios x SiO_2: y TPAOH: z TPABr: 8 EtOH: 120 H_2O	PH	Coating time	Mass gain [%]
Aerosil	A1	$x = 2.0, y = 0.12, z = 0$	10.4	1	+167
	A2	$x = 2.0, y = 0.12, z = 0.12$	-	1	+194
	A3	$x = 2.0, y = 0.06, z = 0.06$	11.39	1	+88
	A4	$x = 2.0, y = 0.03, z = 0.09$	10.04	1	+56
	A5	$x = 1.0, y = 0.12, z = 0$	-	1	+127
	A6	$x = 0.5, y = 0.12, z = 0$	11.12	1	+40
	A7-1	$x = 0.5, y = 0.06, z = 0$	11.05	1	+51
	A7-2	$x = 0.5, y = 0.06, z = 0$	-	2	-
	A8	$x = 0.5, y = 0.03, z = 0$	10.56	1	+36
TEOS	T1	$x = 2.0, y = 0.5, z = 0$	11.5	1	+180
	T2	$x = 1.5, y = 0.5, z = 0$	12.05	1	+151
	T3	$x = 1.0, y = 0.12, z = 0$	10.7	1	+120
	T4	$x = 1.0, y = 0.06, z = 0$	-	1	+71
	T5	$x = 0.5, y = 0.12, z = 0$	10.82	1	+65
	T6	$x = 0.5, y = 0.06, z = 0$	9.98	1	+44
	T7	$x = 0.5, y = 0.03, z = 0$	9.65	1	+35

4.2.2 Catalytic Test

Alkylation of toluene with methanol over the HZSM-5 and silicalite/H-ZSM-5 catalysts was performed using a fixed bed reactor at 673K. The space time *W/F* is fixed at 0.11 [kg-catalyst h mol^{-1}] with the molar ratio of methanol/toluene was 1.0. The products of alkylation were analyzed by a gas chromatograph GC-2014 (Shimadzu Co.) equipped with a flame ionization detector (FID) using a Xylene Master column PRC 7791 (50 m, 0.32 mm).

4.3 Results and Discussion

4.3.1. Morphology of Silicalite/H-ZSM-5 Composite

Table 4.1 lists the effects of molar ratios of the coating solutions on the mass gain of the products after coating. XRD patterns of all the coated samples (data not shown) did not contain reflection peaks for amorphous silica and impurities other than an MFI structure, indicating that the mass gain is due to the formation of silicalite crystals.

Here, two different silica sources (fumed silica and TEOS) were used for the silicalite coating. The samples are labeled as A1-A8 (fumed silica) and T1-T7 (TEOS). The mass gain (%) of the products was calculated as the mass increase after the coating divided by the mass of HZSM-5 core zeolites. The mass gain was too large at high molar ratio of TPAOH/silica sources (A1&A2; T1&T2) due to the formation of silicalite crystals through a homogeneous nucleation in the coating solution.

Figures 4.1 and 4.2 show the SEM images of uncoated and coated catalysts. A number of undesired silicalite crystals were formed in the liquid phase and randomly deposited on the silicalite/H-ZSM-5 composites at high silica and TPAOH concentrations. The morphology of the A1 sample was considerably different from that of uncoated HZSM-5. The silicalite-coated HZSM-5 crystals were intergrown each other substantially, which might cause grain boundaries between crystals.

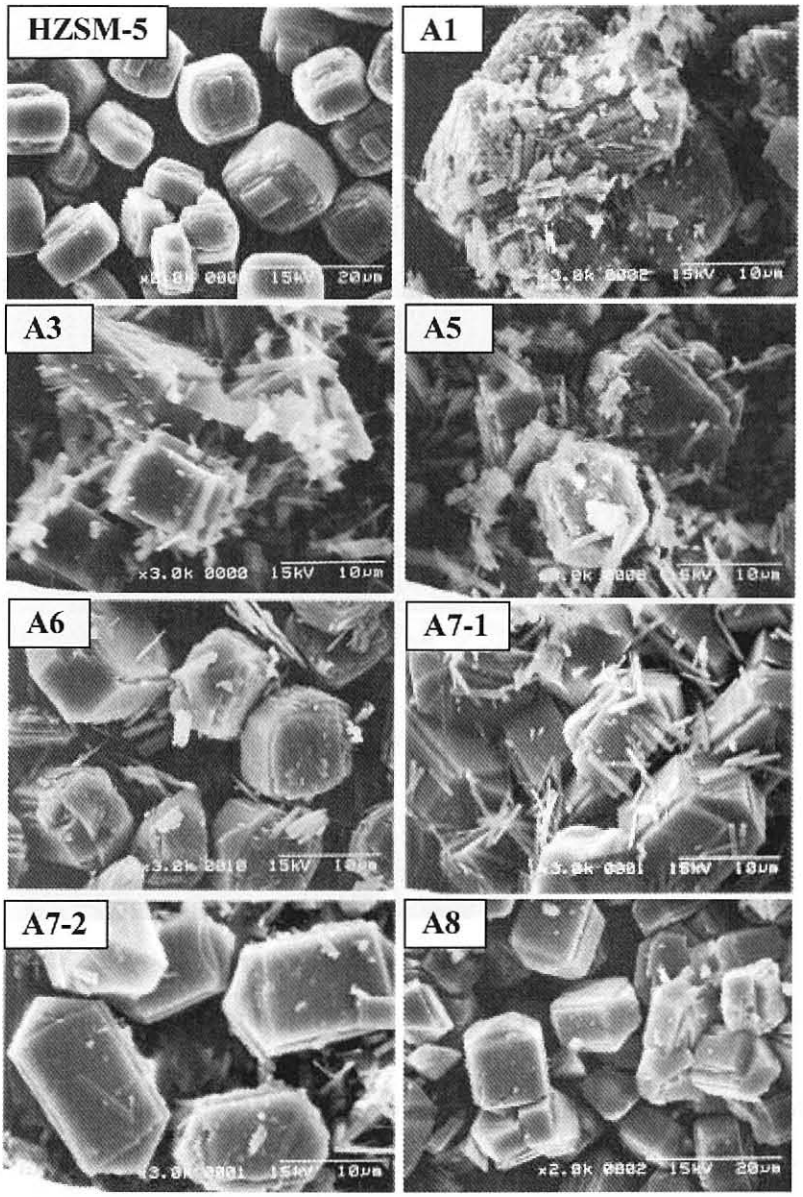

Fig. 4.1 Selected SEM images of HZSM-5 and silicalite/HZSM-5 composites prepared using fumed silica.

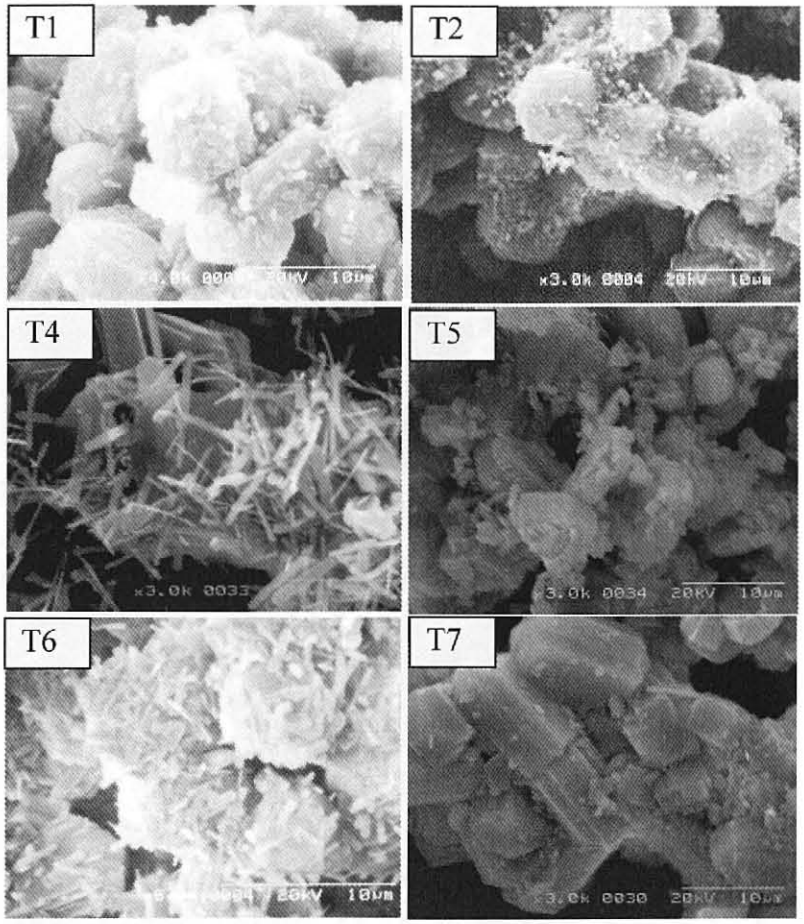

Fig. 4.2 Selected SEM images of silicalite/HZSM-5 composites coated using TEOS.

From the SEM observation, the products were classified into polyclystals (p) and single crystals (s) by their morphology. The composites with a large amount of undesired and randomly deposited silicalite crystals were composed of polycrystals (p). On the other hand, composite crystals with a thin silicalite layer grown on the HZSM-5 surface look like single crystals (s). Figure 4.3 shows the effect of SiO_2 and TPAOH molar ratios in the coating solutions on the morphology of the composite crystals. Single crystals-like silicalite/HZSM-5 composites were obtained at low molar ratios of SiO_2 (fumed silica) and TPAOH. At high molar ratios of silica source and TPAOH, a homogeneous nucleation in the solution was apparently dominant instead of a crystal growth of silicalite layer on the HZSM-5 surface. The mass gain was also very large at high molar ratios of SiO_2 and TPAOH.

On the other hand, single crystal-like composites could not be obtained by using TEOS as a silica source, which can be explained by high nucleation rate caused by high solubility of TEOS. A

decrease of the molar ratio of silica sources and TPA ions would prevent the intergrowth and the formation of undesired silicalite crystals resulting in a decrease of a mass gain after the coating. The presence of TPA ions accelerates the nucleation and crystal growth of silicalite in the liquid phase. To completely prevent the formation of undesired silicalite crystals, TPA ions-free coating conditions should be suggested for future study.

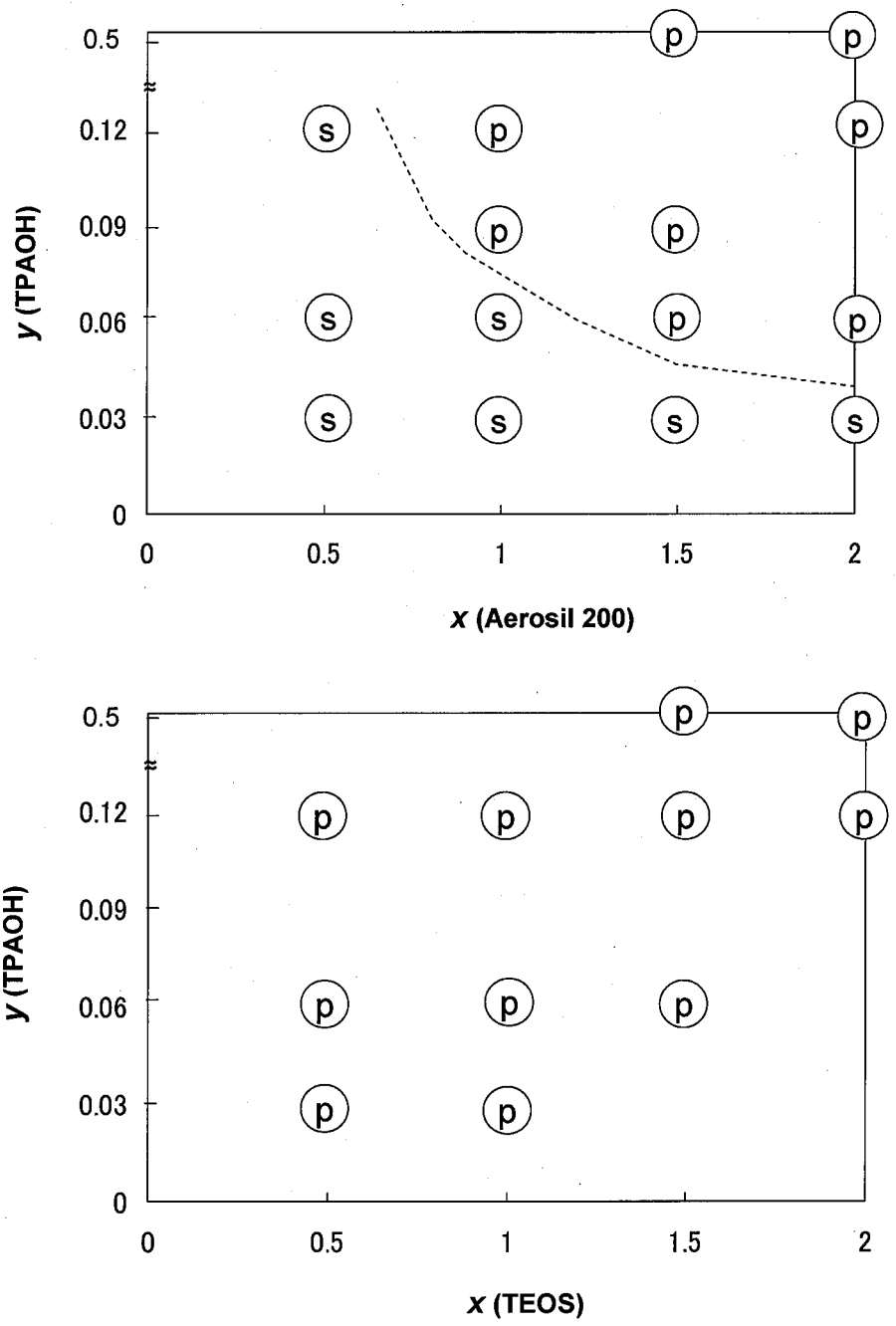

Fig. 4.3 Effect of molar ratios of the coating solutions on the morphology of the products. The symbols (s and p) represent single crystals (s) and polycrystals (p), respectively. The molar ratios of the solutions are x SiO_2: y TPAOH: z TPABr: 8 EtOH: 120 H_2O.

4.3.2. Catalytic Performances of HZSM-5 and Silicalite/HZSM-5 Catalysts.

Alkylation of toluene with methanol was carried out over the uncoated HZSM-5 and silicalite/HZSM-5 catalysts. The molar fraction of produced *para*-xylene in all the produced xylene isomers is defined as the *para*-selectivity. The reaction results were shown in Table 4.2. Regardless of the difference in the synthesis conditions, the coated catalysts provided higher *para*-selectivities compared to that of uncoated one.

For the catalysts prepared using TEOS as a silica source, the order of *para*-selectivity was T5 > T1 > T4, T6 > T7. The *para*-selectivity was significantly affected by the TEOS/TPAOH molar ratios. The medium TPAOH and TEOS concentration (T5) resulted in higher selectivity than that of the other samples. The formation of randomly deposited silicalite crystals on the surface of HZSM-5 crystals was clearly observed on T4 and T6. The result indicates that the formation of silicalite layer and alkalinity of coating solution, as mentioned above, affected on the *para*-selectivity of those silicalite/H-ZSM-5 catalysts.

The toluene conversions for the composite catalysts were increased at higher molar ratios of silica sources. High silica concentration resulted in a formation of a densely-packed silicalite layer on the HZSM-5 zeolite. But, toluene conversion decreased due to the diffusion limitation. In addition, decrease in toluene conversion was also caused by the presence of undesired silicalite crystals that were hard to be separated from the silicalite/HZSM-5 composites.

Table 4.2 Alkylation results of uncoated HZSM-5 and silicalite/H-ZSM-5 catalysts (TOS = 60 min).

	Uncoated	A1	A6	A7-1	A7-2	A8	T1	T4	T5	T6	T7
Toluene conversion [%]	46.7	35.3	36.5	39.4	33.3	38.6	34.5	38.0	43.9	46.6	41.7
Selectivity of xylenes [%]											
p-xylene	75.6	97.5	98.3	98.7	99.1	99.6	97.3	94.3	98.7	94.2	85.6
m-xylene	15.1	1.5	1.1	0.7	0.4	<0.1	1.86	4.01	0.7	3.4	12.29
o-xylene	9.3	1.0	0.6	0.6	0.5	0.3	0.86	1.72	0.6	2.6	5.12
Product composition [%]											
benzene	-	-	-	-	-	-	-	-	-	-	-
ethylbenzene	0.18	0.16	0.22	0.17	0.13	0.15	0.12	0.36	0.21	0.12	0.16
p-xylene	31.74	30.17	29.66	34.26	28.99	31.38	25.04	29.94	37.33	40.18	28.87
m-xylene	6.33	0.47	0.32	0.27	0.11	-	0.48	1.27	0.94	1.45	4.29
o-xylene	3.93	0.31	0.19	0.20	0.14	0.08	0.22	0.55	0.67	1.00	1.79
p-ethyltoluene	4.05	3.31	5.28	3.29	2.95	5.73	3.96	4.41	2.41	2.11	3.01
m-ethyltoluene	1.61	0.09	0.10	0.06	0.04	0.03	0.22	0.28	1.34	1.29	0.37
o-ethyltoluene	0.01	0.02	0.02	-	-	-	2.92	0.67	0.18	0.27	1.99
trimethylbenzene	5.31	0.78	0.72	1.10	0.91	1.02	0.20	0.24	0.71	-	0.27

For the catalysts prepared using fumed silica, the order of selectivity of was A8 > A7-1 > A6 > A1, in which the *para*-selectivity of A8 reached to 99.6% after one coating. The A8 sample is classified into the single crystals. These results indicate that single crystal-like catalysts prepared at lower concentration of SiO_2 (fumed silica) and TPAOH in the solutions show higher *para*-selectivity. As mentioned above, high concentrations of silica source and TPAOH accelerate a nucleation and crystal growth and then, polycrystalline silicalite layers are formed.

The effect of the coating time was also investigated. The reaction results for A7-1 and A7-2 were shown in Table 4.2. With repeated coatings, the *para*-selectivity was enhanced and reached to 99.1% (A7-2). Similarly to the chapters 2&3, repeated coating processes need to obtain *para*-selectivity higher than 99% for the polycrystal-type composite catalysts. In the present study, however, we could control the morphology of the silicalite/HZSM-5 composite and prepare highly *para*-selective composite catalyst by only one coating process.

Another reason for the low *para*-selectivities of silicalite/HZSM-5 composites prepared at high TPAOH concentrations might be high alkalinity of the solutions. In high alkaline coating solutions, aluminum species of the core HZSM-5 would be dissolved into the coating solution. Then, these aluminum ions would be incorporated into the external surface of the composite catalysts.

The single-crystal catalysts show higher *para*-selectivity over the polycrystals catalysts. The single-crystal like zeolite composites are thought to have high mechanical strength compared to the polycrystals. In addition, a homogeneous nucleation was inhibited in the synthesis conditions for single crystals. The high selectivity was achieved by only one coating. The improved coating method in this study gives a strong advantage from the viewpoint of industrial application.

4.4 Conclusion

The *para*-selectivity of the composite catalysts was significantly affected by the synthesis conditions. The catalysts prepared at lower concentration of SiO_2 (fumed silica) and TPA ions in the coating solutions showed higher *para*-selectivity. Excellent *para*-selectivity of 99.6% could be obtained over the single crystal-like composite crystals prepared by only one coating process. Revised synthesis conditions inhibited a homogeneous nucleation of silicalite in the solution. The mass gain of the single crystals was much reduced, and very thin silicalite layer was formed on the HZSM-5 surface.

References

[1] M. Niwa, M. Kato, T. Hattori, Y. Murakami, J. Phys. Chem. 90 (1986) 6233

[2] J.-H. Kim, A. Ishida, M. Okajima, M. Niwa, J. Catal. 161 (1996) 387

[3] A.B. Halgeri, J. Das, Catal. Today 73 (2002) 65

[4] J. P. Breen, R. Burch, P. J. Collier, S. E. Golunski, J. Am. Chem. Soc. 127 (2005) 5020

[5] J. P. Breen, R. Burch, M. Kulkarni, D. McLaughlin, P. J. Collier, S. E. Golunski, Appl. Catal. A: General 316 (2007) 53

[6] M. Ghiaci, A. Abbaspur, M. Arshadi, B. Aghabarari, Appl. Catal. A: General 316 (2007) 32

[7] J. Cejka, B. Wichterlova, Catal. Rev. Sci. Eng. 44 (2002) 375

[8] Y. Suji, Y. Kubota, K. Komura, N. Sugiyama, M. Hayashi, J.-H. Kim, G. Seo, Appl. Catal. A: General 299 (2006) 157

[9] N. Nishiyama, M. Miyamoto, T. Kamei, Y. Egashira, K. Ueyama Stud. Surf. Sci. Catal. 162 (2006) 275.

Chapter 5

Production of *para*-Xylene through Toluene Disproportionation over Silicalite-1/HZSM-5 Composite Catalysts

The toluene disproportionation over silicalite-1/H-ZSM-5 composite catalysts with different Si/Al ratios was performed under different reaction conditions. The catalytic activities and the selective formation of *p*-xylene could be controlled by reaction conditions. The yield of *para*-xylene was enhanced at high temperatures (873 K) and at high *W/F* conditions. The obtained *para*-selectivity (85%) and yield of *para*-xylene (9%) were much higher than the reported values in the toluene disproportionation. But, the *para*-selectivity decreased from 98% to 85% when temperature rose from 663 to 873K over the composite catalyst. This result can be explained by an increase of diffusivity of xylene isomers especially *m*–xylene and *o*-xylene at high temperature. The findings in this study would make suggestions for the practical applications.

5.1 Introduction

In previous chapters, a silicalite-1/H-ZSM-5 composite catalyst was developed for the alkylation of toluene with methanol to produce *para*-xylene. The *para*-selectivities (the molar fraction of produced *para*-xylene in all the produced xylene isomers) were excellent (>99.8%). However, the selectivity to *para*-xylene in the total products was not so high as expected because by-products were formed by series of side reactions of methanol to olefins (MTO) [1,12]. The MTO reactions occur over H-ZSM-5 catalysts even at low temperature [3]. Deposition of coke in zeolite pores may be another problem. This is caused by the formation of aromatic compounds through the MTO reactions.

To solve this problem, toluene disproportionation over ZSM-5 zeolite catalysts is one of candidates for reducing the formation of by-products. However, the catalytic activity of the H-ZSM-5 catalyst in the disproportionation of toluene is very low compared to the toluene alkylation with methanol. Therefore, catalytic performance on severe reaction conditions such as high temperature and large *W/F* should be examined. Diffusivity of xylene isomers must be affected by temperature.

In this chapter, silicalite-1/H-ZSM-5 composites with various Si/Al ratios were synthesized and used for the toluene disproportionation. The effect of reaction conditions on the selectivity to *para*-xylene and yield was studied.

5.2 Experimental

5.2.1 Catalyst Preparation

HZSM-5 crystals with various Si/Al ratios of 50, 70 and 100 were synthesized under hydrothermal synthesis at 453 K for 24 h. The synthesis solutions were consisted of tetraethyl orthsilicate (TEOS), aluminum nitrate ($Al(NO_3)_3 \cdot 9H_2O$), sodium hydroxide (NaOH), tetrapropylammonium bromide (TPABr). The molar composition was 1.5-5.0 SiO_2: 0.025 Al_2O_3: 0.5 TPABr: 0.25 Na_2O: 120 H_2O. The crystallization under hydrothermal conditions was described in the Chapter 2. Hereafter, the H-ZSM-5 samples synthesized using precursor solutions with Si/Al ratios of 50, 70, and 100 are designed as H-ZSM-5(50), H-ZSM-5(70) and H-ZSM-5(100), respectively.

HZSM-5 particles were immersed in the precursor solution of the same initial coating solution consisted of fumed silica (Aerosil 200), tetraprophylammonium hydroxide (TPAOH), deionized water, and ethanol (EtOH). The molar ratio of the coating solution was 0.5 SiO_2: 0.03 TPAOH: 120

H_2O. All of chemicals were purchased from Wako Pure Chemical Industries Co., Ltd. The coating process and product characterizations were shown and discussed in Chapter 4.

5.2.2 Catalytic Characterization

The disproportionation of toluene over the HZSM-5 and silicalite-1/H-ZSM-5 catalysts was performed using a fixed bed reactor at different temperatures of 673, 773 and 873K and different space time *W/F* (mass of the catalyst [kg] divided by the feed rate of toluene [mol/h]). In addition, the toluene alkylation with methanol and the MTH reactions over the catalysts were also studied for comparison. The products of reactions were analyzed by a gas chromatograph GC-2014 (Shimadzu Co.) equipped with a flame ionization detector (FID) using a Xylene Master column PRC 7791 (50 m, 0.32 mm).

5.3 Results and Discussion

5.3.1 Morphology and Characterizations

XRD patterns of the products (data not shown) did not contain reflection peaks for amorphous silica and impurities other than MFI structure. The crystal size of catalytic particles is about 10 μm. The morphologies of uncoated HZSM-5 and coated silicalite-1/HZSM-5 were similar. The SEM images of the zeolite composites were shown in the Chapter 4. Single-crystal like zeolite composites were obtained after the silicalite coating.

5.3.2 Catalytic Activity

Table 5.1 shows the reaction data of H-ZSM-5(70) and silicalite-1/H-ZSM-5(70) catalysts at 673 K. The molar fraction of produced *p*-xylene in all of the xylene isomers is defined as the "*para*-selectivity". The yield of *p*-xylene was calculated based on the reactant (toluene) in the feed, which is called "*para*-yield" in this chapter. The *para*-selectivity was reached nearly 98% at 673 K in the toluene disproportionation after coating by silicalite layer on H-ZSM-5, which would be caused by the inhibition of isomerization of xylenes on the external surface of HZSM-5 by an inactive silicalite layer. The decrease of toluene conversion after silicalite coating can be explained by an increase of diffusion resistance for the reactants and products [4]. When the feed of reactant was only methanol without toluene, both H-ZSM-5(70) and silicalite-1/H-ZSM-5(70) showed 100% methanol conversion to hydrocarbons, suggesting that H-ZSM-5 is highly active for the reaction of methanol itself. Consequently, the toluene conversion can not reach 100% when the molar ratio of

toluene/MeOH in the feed is 1. The catalytic activity of HZSM-5 in this reaction condition is in the order MTH > toluene alkylation with methanol > toluene disproportionation.

Table 5.1. Reaction data over H-ZSM-5(70) and silicalite-1/H-ZSM-5(70).

	Feed of reactant	W/F[a]	Conv. (%)	*para*-Selectivity (%)	*para*-Yield (%)	Fraction of C_1-C_5[e] (%)	Fraction of aromatics[e] (%)
H-ZSM-5(70)	Methanol	0.065	100	24.95	0.098[c]	89.7	10.39
	Toluene with methanol[b]	0.11	41.9	42.03	7.86[d]	55.9	44.1
	Toluene disproportination	0.11	3	49.6	0.63	D.L.	100
Silicalite-1/ H-ZSM-5(70)	Methanol	0.065	100	97	0.77[c]	95.31	4.69
	Toluene with methanol[b]	0.11	22.7	99.3	8.91[d]	73.5	26.5
	Toluene disproportination	0.11	0.88	98.35	0.44[d]	D.L.	100

At 673 K; TOS = 30 min; [a]: [kg-catalyst h mol^{-1}]; [b]: toluene/methanol=1/1; [c] yield calculated based on methanol in the feed; [d] yield calculated based on toluene in the feed; [e]: excluded unreacted toluene. D.L.: below detection limit;

For the alkylation of toluene with methanol, a large fraction of C_1-C_5 hydrocarbons as by-products was produced due to MTH reaction, which reduced *para*-yield in the final product and complicated separation processes in the practical production. In addition, the presence of water as a product of MTH reaction may cause side-effects on the devices used in the production lines.

The product distribution of toluene disproportionation over the composite catalyst produced a small amount of by-products. The *para*-selectivity and *para*-yield was 98.4% and 50%, respectively. However, very low toluene conversion was obtained. Similar correlations between high *para*-selectivity at low toluene conversion for H-ZSM-5 catalysts was reported so far [5-7].

To increase the toluene conversion, reaction tests were performed at higher temperature and higher *W/F* conditions. Table 5.2 shows results of disproportionation of toluene over H-ZSM-5(70) and silicalite-1/H-ZSM-5(70) at 873 K and *W/F* of 0.44 [kg h mol^{-1}]. The toluene conversions were much improved over both the coated and uncoated catalysts. The *para*-selectivity was increased and reached 84.6% after coating by a silicalite layer. The obtained *para*-selectivity (85%) and yield of *para*-xylene (9%) were much higher than the reported values in the toluene disproportionation. But, it was hard to improve the selectivity further at these reaction conditions, which would be caused by an increase of diffusivity of other xylene isomers (*o*- and *m*-xylenes) through the ZSM-5 zeolite channels at high temperature.

Table 5.2 The disproportionation of toluene over H-ZSM-5(70) and silicalite-1/H-ZSM-5(70).

	Silicalite-1/H-ZSM-5(70)	H-ZSM-5(70)
Conversion of toluene [%]	25.86	33.42
Product composition [%]		
Benzene	15.02	17.37
p-Xylene (*para*-yield)	8.80	6.32
m-Xylene	1.29	2.77
o-Xylene	0.35	0.79
Ethyl toluenes	0.19	0.74
Trimethyl benzenes	0.24	5.44
Selectivity of xylenes [%]		
p-Xylene	84.64	63.99
m-Xylene	11.71	28.05
o-Xylene	3.65	7.96
Fraction of C_1-C_5 (%)	D.L.	D.L.
Fraction of aromatics (%)	100	100

Reaction temperature: 873 K, TOS = 90 min, W/F= 0.44 [kg-catalyst h mol^{-1}].

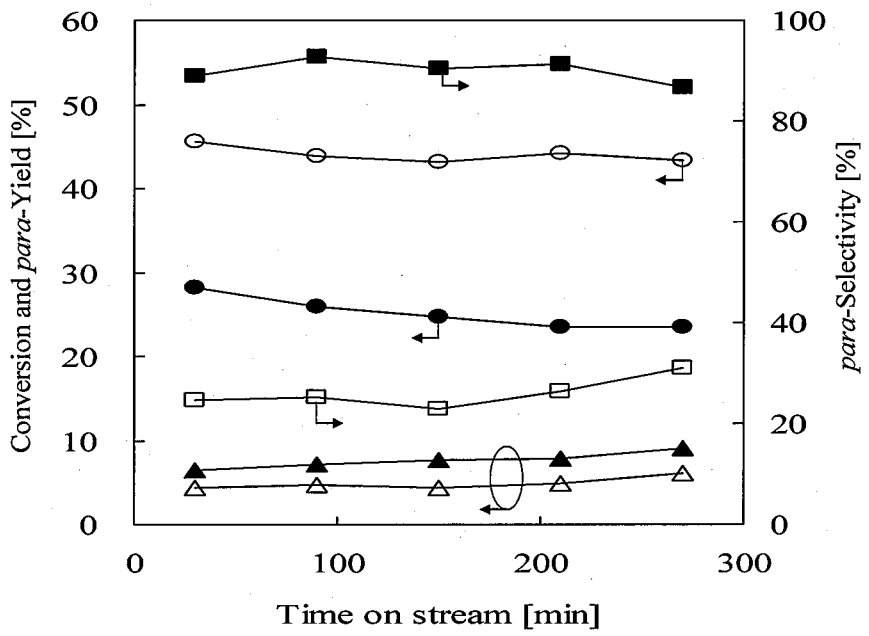

Fig. 5.1 Toluene disproportionation over catalysts: open symbol: H-ZSM-5(50); filled symbol: silicalite-1/H-ZSM-5(50) at 873 K, W/F=0.44 [kg-cat h mol^{-1}]; circle: Toluene conversion; square: *para*-Selectivity; triangle: *para*-Yield.

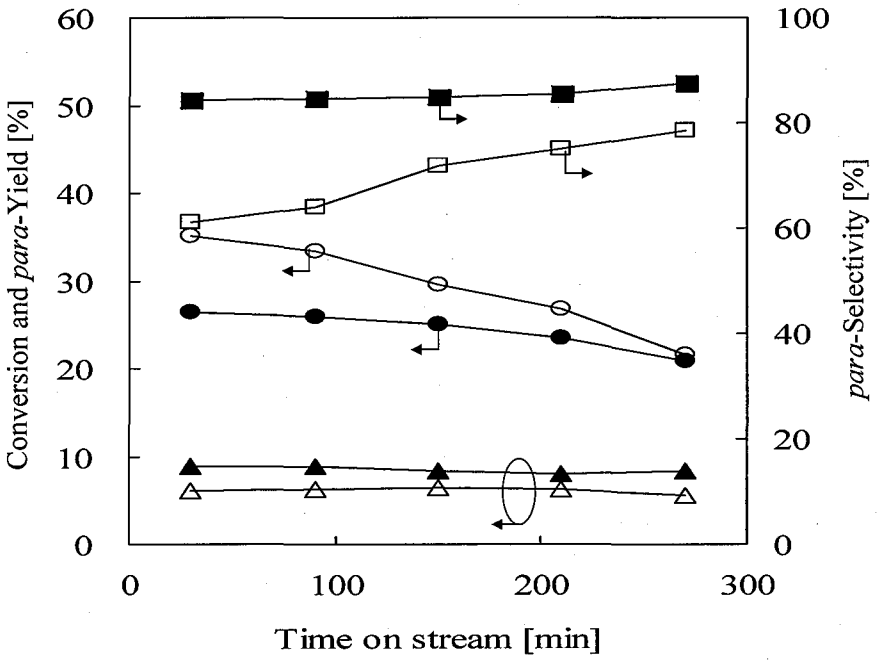

Fig. 5.2 Toluene disproportionation over catalysts: open symbol: H-ZSM-5(70); filled symbol: silicalite-1/H-ZSM-5(70) at 873 K, W/F=0.44 [kg-cat h mol^{-1}]; circle: Toluene conversion; square: *para*-Selectivity; triangle: *para*-Yield.

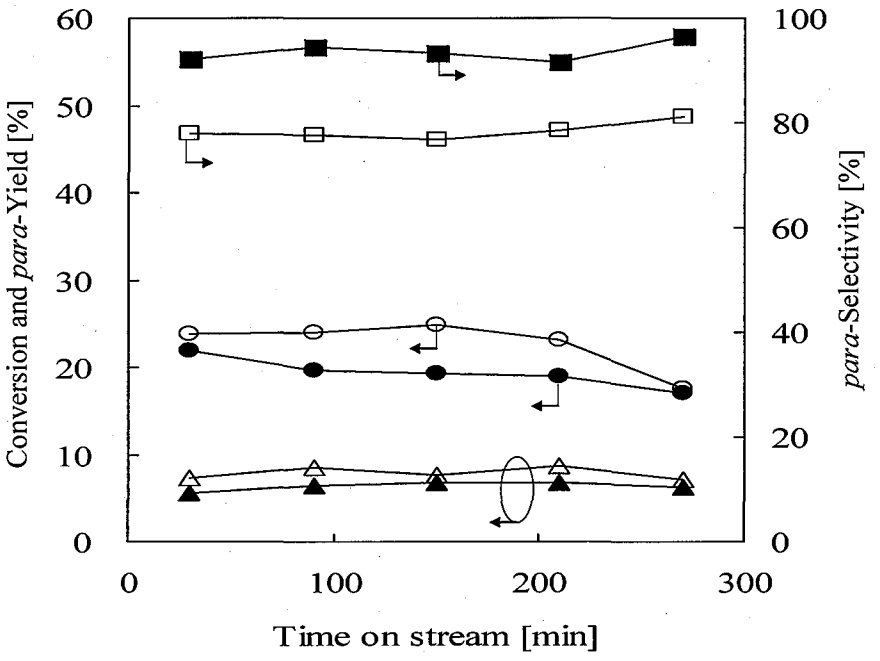

Fig. 5.3 Toluene disproportionation over catalysts: open symbol: H-ZSM-5(100); filled symbol: silicalite-1/H-ZSM-5(100) at 873 K, W/F=0.44 [kg-cat h mol^{-1}]; circle: Toluene conversion; square: *para*-Selectivity; triangle: *para*-Yield.

Time courses of toluene conversion, *para*-selectivity and *para*-yield over the uncoated and coated catalysts with Si/Al ratios of 50, 70 and 100 were shown in Figs. 5.1-5.3. Generally, H-ZSM-5 and silicalite-1/H-ZSM-5 catalysts in the toluene disproportionation showed better catalytic stability than that in alkylation of toluene with methanol, which would be due to the absence of olefins produced from methanol as a coke precursor [5,6]. The higher toluene conversion and lower *para*-selectivity were shown over the samples with low Si/Al ratios. The decrease of conversions after the coating over all samples is due to the extension of diffusion length by silicalite-1 crystals [3]. The catalytic stability of the coated catalysts was obviously enhanced at high Si/Al ratios, which would be explained by the coking restriction on the surface of H-ZSM-5 by silicalite layer. The *para*-selectivities of all composite catalysts were about 90% regardless of Si/Al ratios. The *para*-yield was increased over the coated samples with Si/Al ratios of 50 and 70 after coating. However, *para*-yield decreased over the sample with a Si/Al ratio of 100 because of a lower toluene conversion.

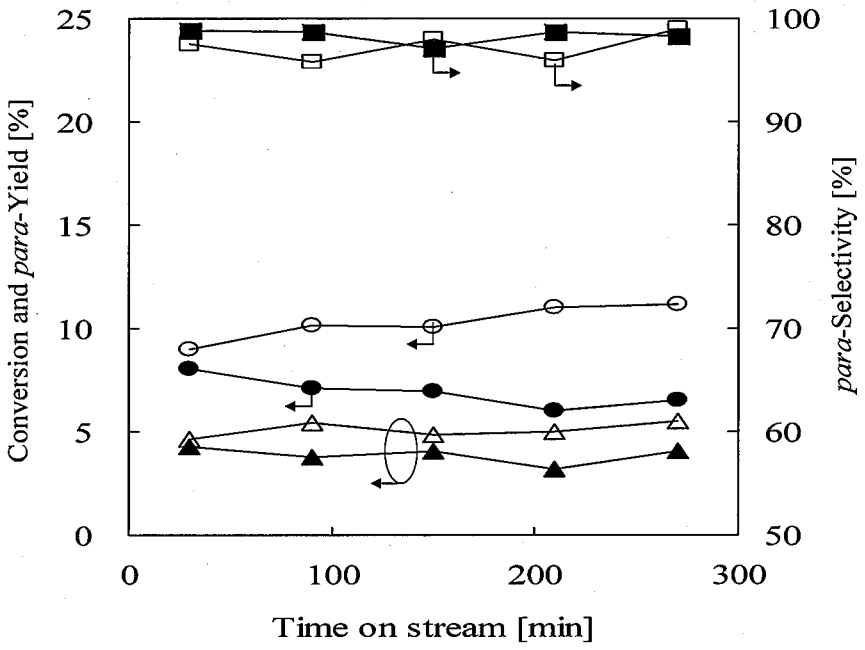

Fig. 5.4 Toluene disproportionation over silicalite-1/H-ZSM-5(70) catalyst at different temperatures; filled symbol: at 673 K; open symbol: at 773 K; W/F=0.44 [kg-cat h mol^{-1}]; circle: Toluene conversion; square: *para*-Selectivity; triangle: *para*-Yield.

Fig. 5.4 shows the toluene conversion, *para*-selectivity and *para*-yield over silicalite-1/H-ZSM-5(70) at 673 K and 773 K. The lower reaction temperature provided a higher *para*-selectivity and a lower *para*-yield, which would be caused by decreases of reaction rate and

product diffusivity at low temperature. The toluene conversion was significantly increased up to 15% at 773 K.

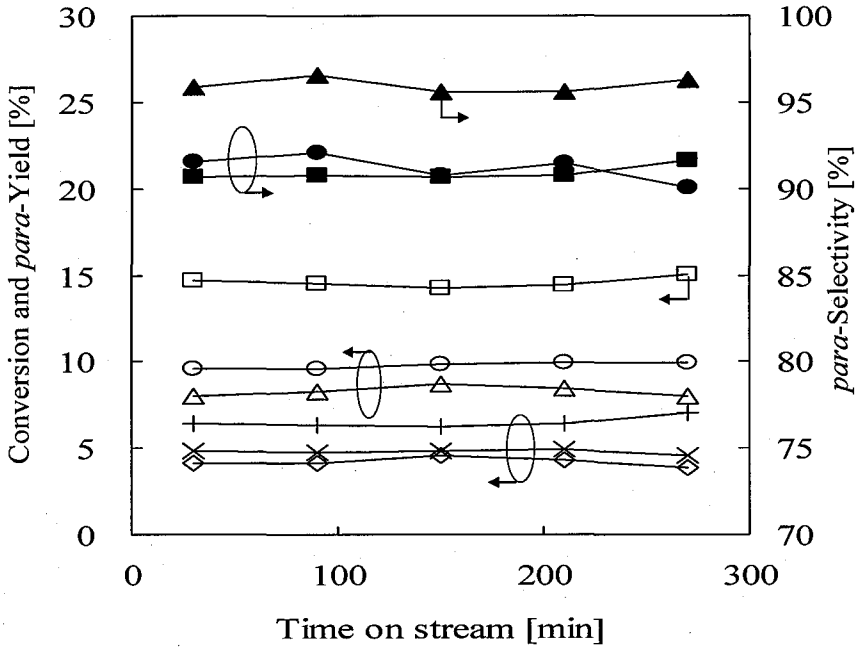

Fig. 5.5 Toluene disproportionation over silicalite-1/H-ZSM-5 with different Si/Al ratios of 50; 70; 100 carried out with the feed of hydrogen of 15 ml/min at 873 K; W/F=0.44 [kg-cat h mol^{-1}]; Toluene conversion: □: 50; O: 70; Δ: 100; *para*-Selectivity: ■:50; ●:70; ▲: 100; *para*-Yield: +: 50; ×: 70; ◊:100).

In the designs for the industrial units of disproportionation and alkylation, (for example ExxolMobil Chemical's technologies-PxMax), the feed of reactants is combined with hydrogen-rich recycle gas at a fixed ratio. Hydrogen is preheated and passed through the catalyst bed reactor to enhance the proficiency of catalysts [4].

The change in *para*-selectivity with a combined hydrogen flow was observed. The selectivity was increased up to 97% in the toluene disproportionation. However, there is a general trend of decreasing toluene conversion by feeding hydrogen regardless of the Si/Al ratio. The decreasing activity of the silicalite-1/H-ZSM-5 catalysts has been reported so far [7,8], and it could be caused by a lower residence time of toluene in the reactor. The highest *para*-selectivity was about 97% over silicalite-1/H-ZSM-5(100) in the presence of Hydrogen. The silicalite-1/H-ZSM-5(50) was more active for the toluene disproportionation than silicalite-1/H-ZSM-5(100) possibly because amount of acid sites is larger for the H-ZSM5 with a low Si/Al ratio.

It was found that the toluene conversions were very stable irrespective of Si/Al ratios. This

result indicates that hydrogen contributed to the removal of coke components by hydrogen cracking reaction. Fig. 5.6 shows the images of silicalite-1/H-ZSM-5(70) before and after the reactions. The color of the used catalyst was still in white after 5h of reaction with the presence of hydrogen in the feed of toluene (Fig. 5.6b). The darker color must be caused by the coke deposition on the surface of the composite particles (Fig. 5.6c).

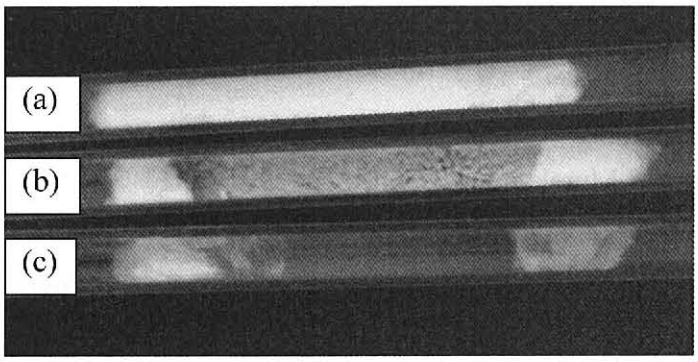

Fig. 5.6 A picture of silicalite-1/H-ZSM-5(70) catalysts used for disproportionation reaction at 873 K, W/F= 0.44 [kg-catalyst h mol^{-1}]; (a): before reaction test; (b): TOS = 5h with hydrogen in the feed; (c) TOS = 5h without hydrogen in the feed.

5.4 Conclusions

Toluene disproportination over core-shell silicalite zeolite composite catalysts is one of candidates for the selective formation of *para*-xylene. High fraction of *p*-xylene in the final product with a small amount of by-products was observed while the selectivity to *para*-xylene was still kept at high level.

In addition, the catalyst lifetime would be improved through the disproportionation of toluene over the composite catalyst. The yield of *para*-xylene was enhanced at high temperatures (873 K) and at high *W/F* conditions. The obtained *para*-selectivity (85%) and yield of *para*-xylene (9%) were much higher than the reported values in the toluene disproportionation. But, the *para*-selectivity decreased from 98% to 85% when temperature rose from 663 to 873K over the composite catalyst. This result can be explained by an increase of diffusivity of xylene isomers especially *m*–xylene and *o*-xylene at high temperature.

The selectivities and yields of *para*-xylene over the sample with a high Si/Al ratio of 100 were contrast in the presence of hydrogen. The findings in this study would be expected to make suggestions for large scale operations for *para*-xylene production in practical application.

References

[1] S. Svelle, F. Joensen, J. Nerlov, U. Olsbye, K-P. Lillerud, S. Kolboe, M. Bjørgen, J. Am. Chem. Soc., 128 (46) (2006) 14770

[2] M. Seiler, U. Schenk, M. Hunger, Catal. Lett. 62 (1999) 139

[3] Z. Zhu, Q. Chen, Z. Xie, W. Yang, C. Li, Micropor. Mesopor. Mater. 88 (2006) 16

[4]http://www.exxonmobilchemical.com/Public_Products/TechLicensing/Worldwide/Technologies/Tech_Technologies_Aro_PxMax.asp

[5] D. Fraenkel, Ind. Eng. Chem. Res. 29 (1990) 1814

[6] T. Hibino, M. Niwa, Y. Murakami, J. Catal. 128 (1991) 551

[7] Y.S. Bhat, A.B. Halgeri, T.S.R. Prasada Rao, Ind. Eng. Chem. Res. 28 (1989) 890

[8] J.L. Sotelo, M.A. Ugina, D.P. Serrano, Ind. Eng. Chem. Res. 28 (1989) 890.

Chapter 6

Synthesis of Nanoscale H-ZSM-5 Crystals by Incorporating Al Species Dissolved from FAU Zeolite and αAl_2O_3

This chapter describes a novel synthesis method of HZSM-5 nanocrystals by using low silica zeolite and alumina as aluminum sources. The Al species dissolved from the low silica zeolite (FAU) and alumina (αAl_2O_3) were incorporated into the MFI structure during a formation of zeolite crystals. The synthesized ZSM-5 nanocrystals by using FAU zeolite were 500 nm in size and showed very high catalytic activity in alkylation of toluene and isomerization of *m*-xylene. The surface morphology and crystalline structure of nanosized HZSM-5 were characterized by XRD, EDX, FE-SEM and TEM analyses.

6.1 Introduction

Typically, zeolites are industrially manufactured with micron-sized crystals or aggregates of nanocrystals that have been widely used in applications such as catalysis, ion exchange, and separation [1,2]. Recently the synthesis and application of nanosized zeolites have been gaining interests [3-8].

The crystal size of zeolites has a great effect on catalytic activity and selectivity. In Chapter 3, H-ZSM-5 with a small crystal size (5 μm) showed a high activity in alkylation of toluene. By decreasing a diffusion resistance and increasing an external surface area, the overall reaction rate was increased. Nanosized crystals of zeolites are expected to show a very high activity. However, it has been hard to synthesize ZSM-5 nanocrystals (less than 1 μm) by the conventional hydrothermal synthesis.

In this study, the preparation of nanosized HZSM-5 crystals by using a very unique synthesis method has been concentrated. Spherical FAU-type zeolite pellets or alumina particles (αAl_2O_3) with a diameter of about 2 mm were used as aluminum sources. The nanosized ZSM-5 crystals were coated with a silicalite-1 layer. The catalytic activities in the alkylation of toluene and isomerization of *m*-xylene over the nanosized zeolites were compared with those over conventional ZSM-5 catalysts.

6.2 Experimental Section

6.2.1 Preparation of HZSM-5

The precursor sol without Al species was consisted of tetrapropylammonium hydroxide (TPAOH), tetraethyl orthosilicate (TEOS), ethanol (all reagents were purchased from Wako Pure Chemical Industries, Ltd.) and deionized water with molar ratios of 0.5 TPAOH: 0.2 TEOS: 8 EtOH: 120 H_2O. The synthesis solution was mixed for 30 min at 303 K. After mixing, about 15 grams of the precursor sol were poured into a Teflon-lined autoclave together with different amount of 0.35 gram of FAU spheres with a diameter of 1.4-2.36 mm (ZEOLUM F9, Tosoh). Hydrothermal synthesis was carried out at 453 K for 24 h in forced convection Oven with rotation rate of 2 rpm. The products were rinsed and gathered by centrifugation washed by water and dried. Spherical FAU particles were removed after coating. The products were then calcined at 873 K for 5 h to receive H-ZSM-5.

As another study, αAl_2O_3 spheres with a diameter of 1-2 mm (KHO-12, Sumika alchem Co. Ltd.) were used instead of the FAU-type zeolite. For a reference study, HZSM-5 was prepared by a

conventional hydrothermal synthesis using a precursor solution containing aluminum source of $Al(NO_3)_3$. The crystallization was similar to the case of using FAU type as described above.

The samples synthesized using the 0.35 g of spherical FAU and Al_2O_3 particles are designated as ZSM-5(F), ZSM-5(A), and the sample using $Al(NO_3)_3$ is named as ZSM-5(N), respectively.

6.2.2 Preparation of Silicalite-1/HZSM-5

Nanosized ZSM-5(F) crystals were immersed in the silicalite-1 coating solution. The crystallization was carried out under hydrothermal conditions at 453 K for 24 h in a stainless steel vessel with agitation condition. The precursor solution consisted of TEOS, tetraprophylammonium hydroxide (TPAOH), ethanol (EtOH) and deionized water with the molar ratios of 0.5TPAOH: $120H_2O$: 8EtOH: $2SiO_2$. The coating was repeated twice. The products were rinsed repeatedly by deionized water and dried at 363K overnight, then calcined in air at 873K for 5 h with a heating rate of 1K min^{-1}. The product then was gathered by centrifugation and rinsed repeatedly by deionized water. After dried at 363K overnight, the products were calcined in air at 873K for 5 h.

6.2.3 Characterization

The products were characterized by X-ray diffraction (XRD) recorded on a Rigaku Miniflex using Cu-Kα radiation. The composition of samples was characterized by EDX (Energy Dispersive X-ray spectrometry) (Hitachi S2250) analysis. The surface and morphology of samples were observed by the field emission scanning electron microscopy (FE-SEM) on a Hitachi S-5000L microscope at an acceleration voltage of 21 kV, and the transmission electron microscope (TEM) on FEI Tecnai 20 at 120 kV and 200 kV. The catalytic performances in the alkylation of toluene with methanol and the isomerization of *m*-xylene were performed over the prepared catalysts. The reactions were performed using a fixed bed reactor at 673K. The alkylation was carried out at the space time, *W/F,* of 0.11 [kg-catalyst h mol^{-1}] and the molar ratio of methanol/toluene was 1.0. The isomerization was performed at *W/F* of 0.37 [kg-catalyst h mol^{-1}]. The products of alkylation were analyzed by a gas chromatograph GC-2014 (Shimadzu Co.) equipped with a flame ionization detector (FID) using a Xylene Master column PRC 7791 (50 m, 0.32 mm). The reaction data were collected after 60 min of the operation time.

6.3 Results and Discussion

6.3.1 Morphology and Crystalline Characterizations

Fig. 6.1 shows the XRD patterns of catalytic samples The XRD patterns for all the indicated samples. HZSM-5 products showed that the formed crystals had an MFI structure.

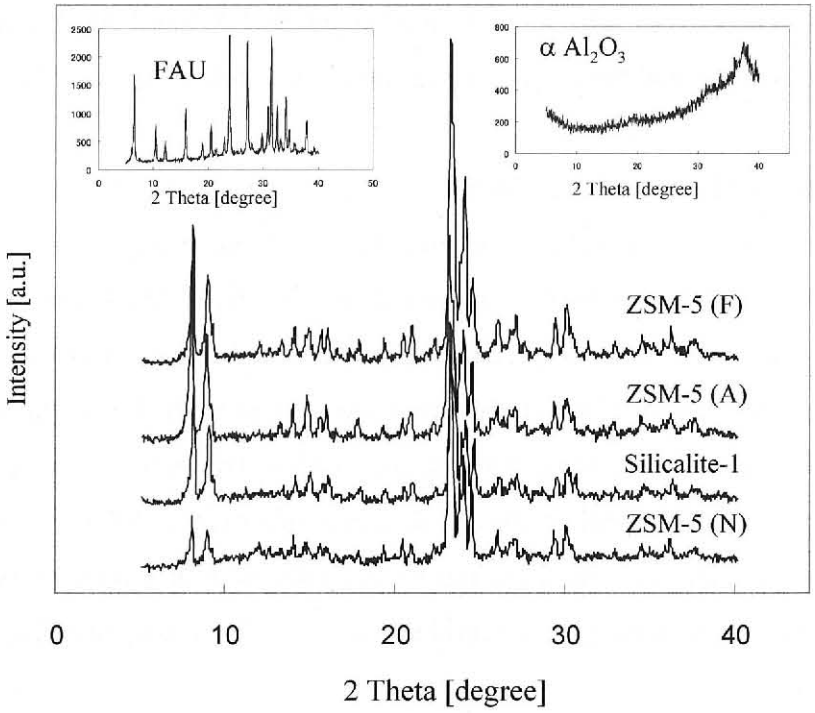

Fig. 6.1 XRD patterns of samples synthesized from different aluminum sources

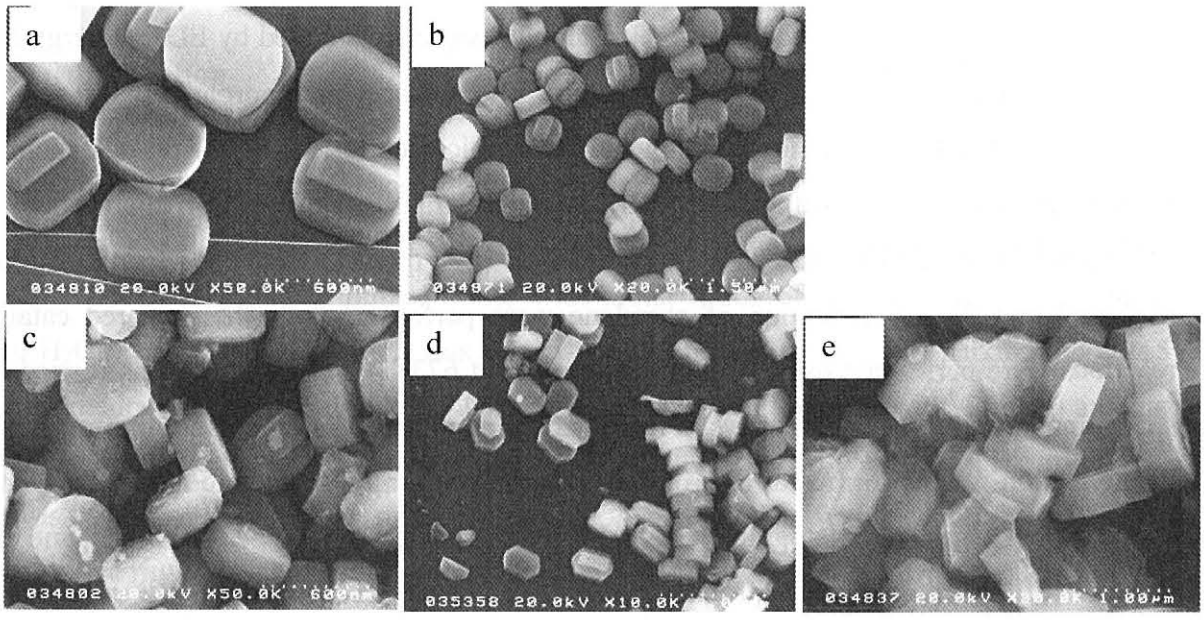

Fig. 6.2 FE-SEM images of (a): silicalite-1; (b): ZSM-5(F); (c): ZSM-5(A); (d): ZSM-5 (N); (e): Silicalite-1/ZSM-5(F).

The crystal morphologies of synthesized samples were shown in Fig. 6.2. The sample synthesized without FAU or αAl_2O_3 is silicalite-1. For observation, the crystal sizes of samples prepared from FAU or αAl_2O_3 are not so much different. The addition of different aluminum sources in this method did not affect on the crystal size. Crystal size was very uniform with a size of about 500 nm, while crystal size of ZSM-5(N) was about 1.2 μm. These results suggest that the crystal growth rate accelerated in the presence of $Al(NO_3)_3$ in the precursor solution.

After the coating, an overgrowth of a silicalite layer on ZSM-5(F) was clearly observed (Fig. 4(e). The crystal size of silicalite-1/ZSM-5(F) composite catalyst was much increased to nearly 1.0 μm.

The surface of ZSM-5(F), ZSM-5(A), ZSM-5(N) and silicalite-1 were observed by the FE-SEM at high magnification. The FE-SEM images in Fig. 6.3 show that the surface of the ZSM-5(F) and ZSM-5(A) crystals was not flat, while the silicalite-1 crystal and ZSM-5(N) have a smooth surface. The dissolved Al species might be fragments of the FAU framework in a subnanometer scale for ZSM-5(F) and fragment of alumina for ZSM-5(A). These fragments must have partially inhibited a crystallization of ZSM-5 and created a large number of defects formed on the external surface, which resulted in a rough surface of ZSM-5 (F) and ZSM-5(A) crystals. The crystalline structure of nanoscale ZSM-5 (F) and ZSM-5(A) were observed by TEM (Fig. 6.4). No discontinuity of the lattice figure was observed, indicated that all dissolved Al species from aluminum sources were incorporated to ZSM-5 structure. From the EDX analysis, the Si/Al ratios of the ZSM-5 were 171, 101, and 262 for ZSM-5(F), ZSM-5(A) and ZSM-5 (N), respectively. The Si/Al ratio of ZSM-5(A) is lower than that of ZSM-5(F); the fact implies that the Al species derived from the Al_2O_3 particles was much readily introduced into the MFI framework compared to that from the FAU crystals.

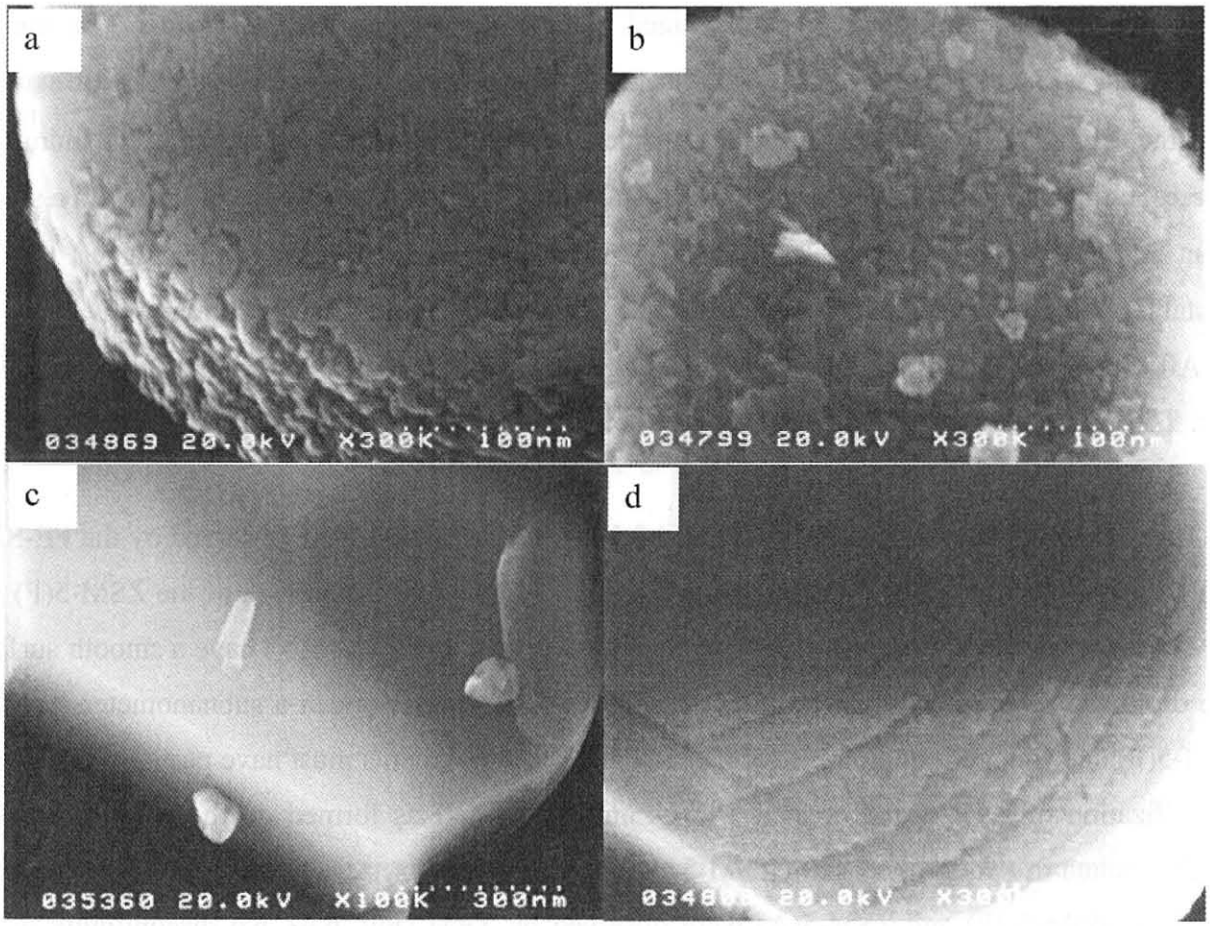

Fig. 6.3 Crystal surface of (a): ZSM-5(F); (b): ZSM-5(A); (c): ZSM-5(N); (d): Silicalite-1

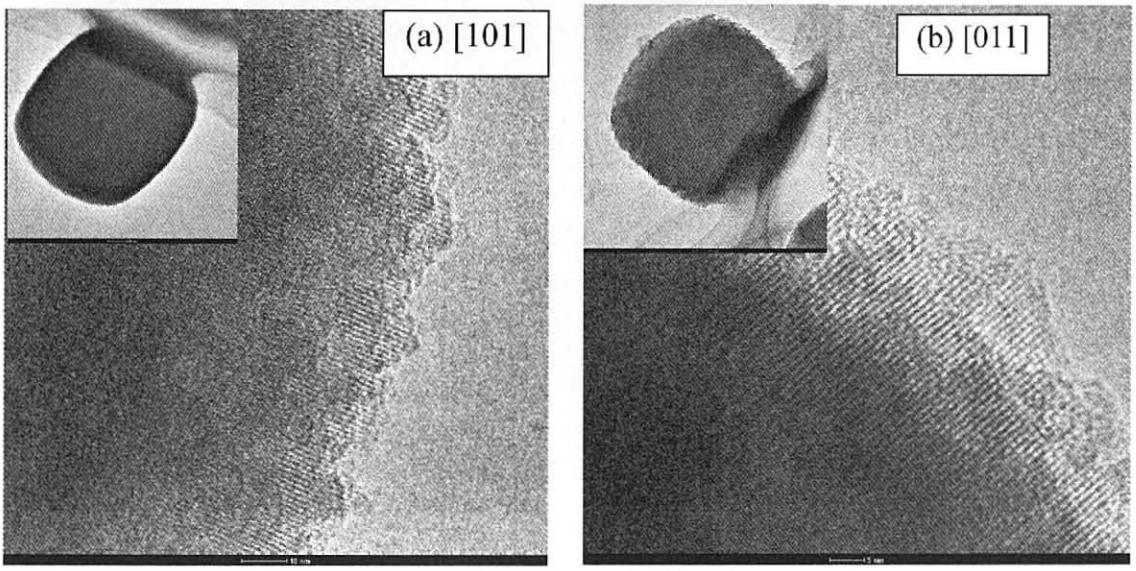

Fig. 6.4 TEM images of (a): ZSM-5(F); (b): ZSM-5(A)

6.3.2 Catalytic Characterization

The catalytic activities of alkylation of toluene over ZSM-5(F), ZSM-5(A) and ZSM-5(N) were summarized in Table 6.1. The conversion of toluene on ZSM-5(F) was 81%, much higher than that of the other catalysts even though the particle size is not so different. The high catalytic activity of ZSM-5(F) catalyst implies that the acid sites derived from the fragment of the FAU framework function as highly active sites compared to that of other catalysts.

The *para*-selectivities over both ZSM-5(F) and ZSM-5(A) samples were similar to that in the thermodynamic equilibrium (*p*-: *m*-: *o*-= 23: 53: 24), suggesting that the reaction on the external surface of ZSM-5 crystals might be dominant due to their large external surface area. Moreover, the short diffusion path length of nanocrystals resulted in the low selectivity of *p*-xylene. The lower toluene conversion and higher *para*-selectivity over ZSM-5(N) would be explained by the bigger crystal size and higher Si/Al ratio.

The yields of bulky products such as ethyltoluenes and trimethylbenzenes were significantly larger than that over ZSM-5(A) and ZSM-5(N). The fraction of these bulky materials over ZSM-5(F) was more than 50 % in the total products, which explains for the presence of a large number of external strong acid sites of ZSM-5(F).

Table 6.1 Toluene alkylation with methanol (TOS = 60 min)

	ZSM-5(F)	ZSM-5(A)	ZSM-5(N)	Silicalite/HZSM-5(F)
Crystal size [μm]	0.4	0.5	1.2	1.0
Si/Al (EDX)	171	101	262	-
Conversion of toluene [%]	81	51	54	61.3
Product yield [%]				
benzene	D.L.	D.L.	D.L.	D.L
ethylbenzene	0.4	D.L.	0.2	2.39
xylenes	35.5	34.9	42.0	30.4
ethyltoluenes	39.0	16.0	8.7	23.8
trimethylbenzenes	6.5	D.L.	3.2	D.L
Fraction of xylenes [%]				
p-xylene	23.8	23.1	76.8	54.2
m-xylene	49.1	53.0	13.7	32.0
o-xylene	27.1	23.9	9.6	13.9

D.L: Below detection limit

The *para*-selectivity of ZSM-5(F) was much increased after the coating with silicalite-1 (about 58%) However, the *para*-selectivity was much lower than that shown in previous chapters. This might be caused by an incorporation of aluminum species from the core ZSM-5(F) nanocrystals.

Aluminum in the nanocrystals is easily dissolved to the solution during the coating process, which causes the reconstruction of external acid sites on the silicalite-1/ZSM-5(F) composite. The inhibition of acid-site reconstruction over silicalite-1/ZSM-5(F) should be studied in the future.

The results of isomerization of *m*-xylene were listed in Table 6.2. Generally, *m*-xylene hardly permeates through the micropores of ZSM-5 because of its bigger size. Thus, the reaction takes place mainly on the external surface of the ZSM-5 crystals. Similarly to the results of the alkylation, the conversion of *m*-xylene over the ZSM-5(F) catalyst was 46%, much higher than that over the other ZSM-5 catalysts.

Table 6.2 *m*-Xylene isomerization reaction result (TOS = 60 min)

	ZSM-5 (F)	ZSM-5 (A)	ZSM-5 (N)
Conversion of *m-xylene* [%]	46	25	14
Product yield [%]			
benzene	D.L.	D.L.	D.L.
toluene	5.5	1.5	5.6
ethylbenzene	D.L.	D.L.	D.L.
o, *p*-xylenes	34.0	21.7	7.7
ethyltoluenes	D.L.	D.L.	D.L.
trimethylbenzenes	5.8	1.9	0.2

D.L: below detection limit.

6. 4 Conclusions

A very unique synthesis method has been found to form ZSM-5 nanocrystals by incorporating Al species dissolved from an FAU type zeolite. The novel catalyst prepared by this method showed an excellent catalytic activity.

However, it is hard to deactivate the external surface activity of nanoscale ZSM-5 catalytic particles by the silicalite-1 coating possibly because aluminum released from ZSM-5 is incorporated to the external surface during the coating process.

References

[1] M. Yamamura, K. Chaki, T. Wakatsuki, H. Okado, K. Fujimoto, Zeolites 14 (1994) 643

[2] S.C. Larsen, J. Phys. Chem. C. 111 (2007) 18464

[3] S. Zheng, H.R. Heydenrych, A. Jentys, J.A. Lercher, J. Phys. Chem. B 106 (2002) 9552

[4] S. Svelle, F. Joensen, J. Nerlov, U. Olsbye, K.-P. Lillerud, S. Kolboe, M. Bjorgen, J. Am. Chem. Soc. 128 (2006) 14770

[5] J.-H. Kim, T. Kunieda, M. Niwa, J. Catal. 173 (1998) 433

[6] K. Wang, X. Wang, Micropor. Mesopor. Mater. 112 (2008) 187

[7] C. Ding, X. Wang, X. Guo, S. Zhang, Catal. Commun.9 (2007) 487

[8] M. Sugimoto, H. Katsuno, K. Takatsu, N. Kawata, Zeolites 7 (1987) 503.

Chapter 7

Control of Acidic Strength of H-ZSM-5 Catalyst for Light Olefin Production: High Propylene Selectivity in the Methanol-to-Olefin Reaction over H-ZSM-5 Catalyst Treated with Phosphoric Acid

H-ZSM-5 zeolite was treated with phosphorous acid by impregnating H-ZSM-5 with phosphoric acid aqueous solutions with various concentrations. Phosphorous acid-modified H-ZSM-5 (P-HZSM-5) was used as a catalyst for a methanol-to-olefin reaction. The P-HZSM-5 catalyst showed very high propylene selectivity up to 57 % with a methanol conversion of 100%. Furthermore, catalyst stability was significantly improved for the P-HZSM-5 catalysts. Ammonia TPD spectra shows that strong acid sites of H-ZSM-5 disappeared after the phosphoric acid treatment. Consequently, the formation of aromatics and coke was inhibited, resulting in increases of light-olefin selectivity and catalyst stability.

7.1 Introduction

The demand of light olefins has been rising year by year because they are important starting materials for many chemical processes, especially propylene. Light olefins are very versatile building block and are the feedstock for a wide range of important monomers, polymers, intermediates and chemicals. Normally, the primary production of light olefins is through either steam cracking or recovery from refinery processes. Nowadays, the raw material of methanol can be easily obtained from a huge natural gas resource, so the methanol-to-olefin (MTO) reaction has been gaining interest recently.

Many researchers have concentrated on converting methanol to hydrocarbons such as methanol to gasoline (MTG), methanol to hydrocarbons (MTH) and MTO using zeolite catalysts such as ZSM-5 [1-7], zeolite Beta [8,9], and SAPO-34 [10-16]. A large number of proposed reaction mechanisms are available to explain the conversion of methanol to hydrocarbons. The most discussed mechanisms were the consecutive reaction mechanism [17] and "hydrocarbon pool mechanism" [18]. ^{13}C MAS NMR spectroscopy turned out to be a powerful tool with respect to the identification of the intermediates formed, and a number of investigations have been conducted mainly for ZSM-5 and SAPO-34 catalysts [19-23]. Recently, Haw et al. [24] have concluded that methanol and DME react on cyclic organic species contained in the cages or channels of the inorganic host.

Silicoaluminophosphate SAPO-34 (pore size ca. 0.43 nm) has been considered as an excellent catalyst for the selective production of light olefins (ethene and propylene) in MTO reaction. However, this catalyst was rapidly deactivated by the coke accumulation in the internal narrow channels of SAPO-34 crystals [25,26]. On the other hand, ZSM-5 catalyst with the medium pore size (ca. 0.55 nm) is one of the candidates to enhance the catalytic lifetime in the MTO reaction. However, the strong acid sites of the catalyst result in a large fraction of by-products through oligomerization reactions [27], especially aromatic compounds. To enhance the catalytic performances of ZSM-5 catalyst with respect to the selectivity to light olefins, several techniques have been suggested [28-31]. Recently, Xue et al. [32] and Jiang et al. [33] have proposed phosphorous-modified HZSM-5 catalysts for cracking butene and C_4 –alkanes to produce light olefins.

In this study, phosphoric acid-treated H-ZSM-5 catalysts have been first used for the MTO reaction. The objective of this study is to control acid strength distribution of H-ZSM-5 to improve product selectivity. The stability of H-ZSM-5 catalyst for the production of propylene in the MTO

reactions was studied. The effect of the treatment with phosphoric acid on the light-olefin selectivity and catalyst stability was discussed.

7.2 Experimental

7.2.1 Catalyst Preparation and Characterization

H-ZSM-5 (Tosoh Corporation Co., Ltd., crystal size = ca. 3 μm, SiO_2/Al_2O_3 = 310 (EDX analysis)) was used as a catalyst. H-ZSM-5 was impregnated with phosphoric acid (H_3PO_4) aqueous solutions with various concentrations. The solvents were completely evaporated by heating. Thus, all H_3PO_4 molecules in the solutions were loaded on H-ZSM-5. The mass ratios of phosphorous (P) in the solutions to H-ZSM-5 were 0.01, 0.02, 0.03, 0.045 and 0.055. Hereafter, the H-ZSM-5 samples modified with H_3PO_4 (P-HZSM-5) were designated as: 1P-Z, 2P-Z, 3P-Z, 4.5P-Z and 5.5P-Z, respectively. The P-HZSM-5 catalysts were dried again at 383 K for 5 h and then calcined in air at 873 K for 5 h with a heating rate of 1 K min^{-1}. After calcination, the samples of 1P-Z, 2P-Z, 3P-Z, 4.5P-Z and 5.5P-Z were washed with deionized water to remove excess H_3PO_4 on the catalysts. Here, the P-HZSM-5 samples were immerged in deionized water for 3 h at room temperature with stirring, then dried at 383 K and calcined again at 873 K for 5 h. After the washing, the samples were renamed as: W1P-Z, W2P-Z, W3P-Z, W4.5P-Z and W5.5P-Z.

The products were characterized by X-ray diffraction (XRD) recorded on a Rigaku Miniflex using Cu-Kα radiation. The chemical compositions of the samples were analyzed by Energy Dispersive X-ray Spectrometer (EDX).

The acidic strength of the samples was analyzed by temperature-programmed desorption of ammonia (NH_3-TPD) using Autosorb-1-Chemi (Quantachrome Instruments) in the temperature range from 373 to 973 K. Here, 0.2 g sample was pretreated in helium at 773 K for 1 h, cooled to 373 K for 1 h. After NH_3 was adsorbed on the samples for 2 h, temperature-programmed desorption was started at a rate of 10 K/min from 373 to 973 K. The signal was acquired by Quantachrome TPRWin v2.0.

7.2.2 Catalytic Test

MTO reactions over HZSM-5 and phosphorous modified catalysts were performed using a fixed bed reactor made of quartz glass (i.d. 4 mm) with a continuous flow system under atmospheric pressure. The temperature and space-time, *W/F* (mass of the catalyst [kg] divided by the feed rate of methanol [mol/h]) were systematically changed for comparison. The reaction products were

analyzed by a GC-14B (Shimadzu Co.) gas chromatograph equipped with a flame ionization detector (FID) using an SM-6 column (6 m, 3 mm) and a gas chromatograph GC-2014 (Shimadzu Co.) equipped with a flame ionization detector (FID) using a Xylene Master column PRC 7791 (50 m, 0.32 mm).

7.3 Results and Discussion

7.3.1 Catalyst Characterizations

Fig. 7.1 shows the XRD patterns of the H-ZSM-5 and P-HZSM-5 catalysts. The MFI structure of H-ZSM-5 was retained after the treatment with H_3PO_4. The XRD patterns of P-HZSM-5 did not contain a broad peak for an amorphous phase. However, the peak intensity of the XRD patterns decreased after the H_3PO_4 treatment. This might be caused by partial blockage of HZSM-5 pores by excess H_3PO_4 molecules because the XRD peak intensity of P-HZSM-5 decreased with increasing contents of H_3PO_4 and recovered after removal of the excess H_3PO_4 by washing.

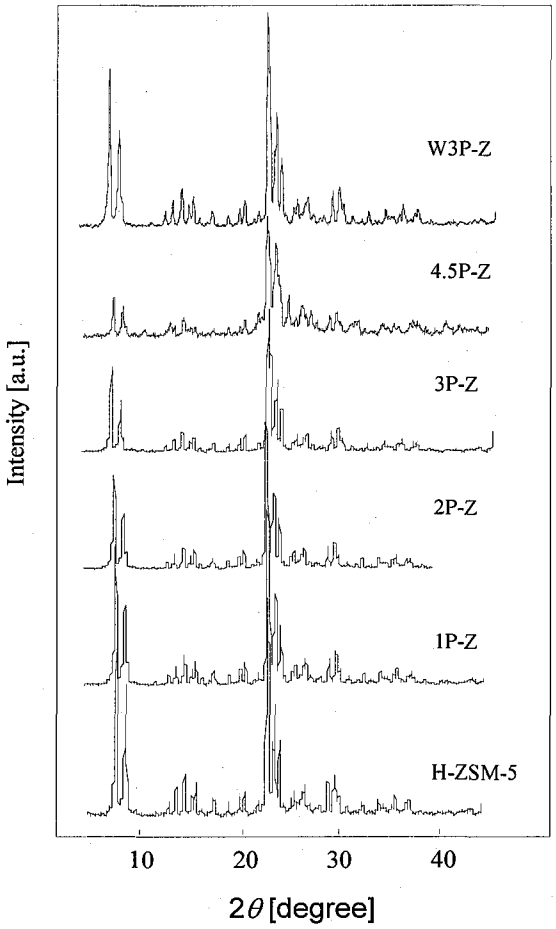

Fig. 7.1 XRD pattern of H-ZSM-5 and P-HZSM-5.

The molar ratios of P/Si and Si/Al in H-ZSM-5 and P-HZSM-5 were measured by EDX analysis and are shown in Fig. 7.2. The molar ratio of P/Si was largely decreased after washing. The H_3PO_4 molecules deposited on the external surface and on the entrances of the pores of H-ZSM-5 would be easily removed. The P/Si molar ratio was directly proportional to the H_3PO_4 concentrations in the aqueous solutions. The remaining phosphorous after the washing must be strongly incorporated and interacted with the pore surface of H-ZSM-5 zeolite.

The Si/Al ratios were increased after washing. The Si/Al molar ratios increased with increasing the concentration of H_3PO_4 in the solution, which might be caused by a partial dealumination over H-ZSM-5 by the H_3PO_4 treatment. For the 5.5P-Z samples, more than half of Al was dissolved from the framework of H-ZSM-5. The models for H_3PO_4 deposited on the external surface and inside the pore before and after calcination were indicated by Kalbasi et al. [34]. The interaction of phosphorous with the Brönsted acid sites of H-ZSM-5 prepared by impregnation with H_3PO_4 and calcinations were proposed by some researchers [35-37]. Recently, Xue et al. [32] showed the schematic mechanism for the phosphorous interaction with H-ZSM-5. They stated that two zeolitic hydroxyls condensed with one phosphate molecule after calcination in air leading the decrease in the number of OH groups on P modification. This result has been convincingly supported by D_2/OH measurements.

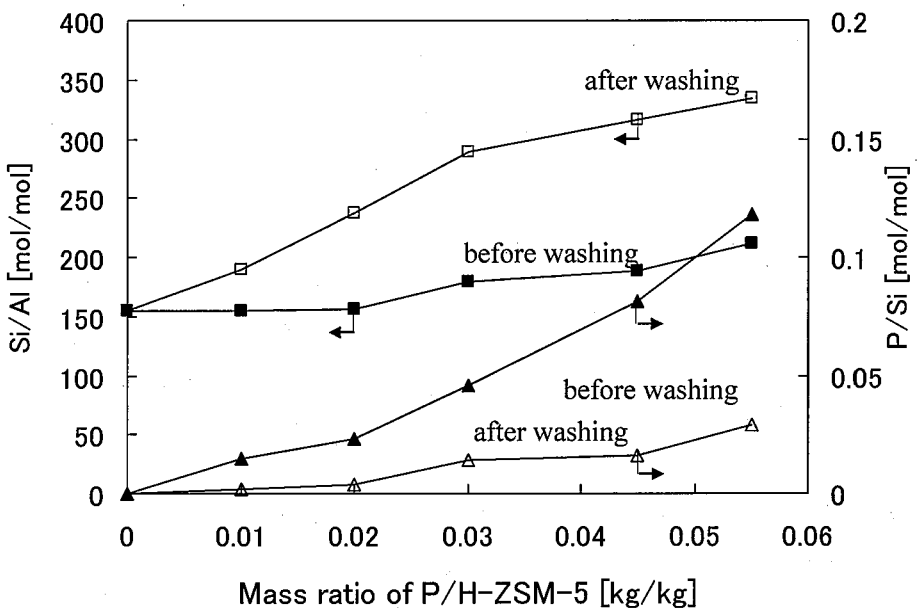

Fig. 7.2 Molar ratio of P/Si and Si/Al measured by EDX analysis

Fig. 7.3 shows NH_3-TPD profiles of H-ZSM-5 and P-HZSM-5. There are two desorption peaks for H-ZSM-5, one distributed in the range of 373-473 K and the other distributed from 523 to 723 K, corresponding to the weak acid sites and strong acid sites, respectively. The peak intensity for the strong acid sites decreased with increasing H_3PO_4 content while the desorption peak for weak acid sites was not changed so much. After washing by deionized water, the peak for strong acid sites slightly reappeared.

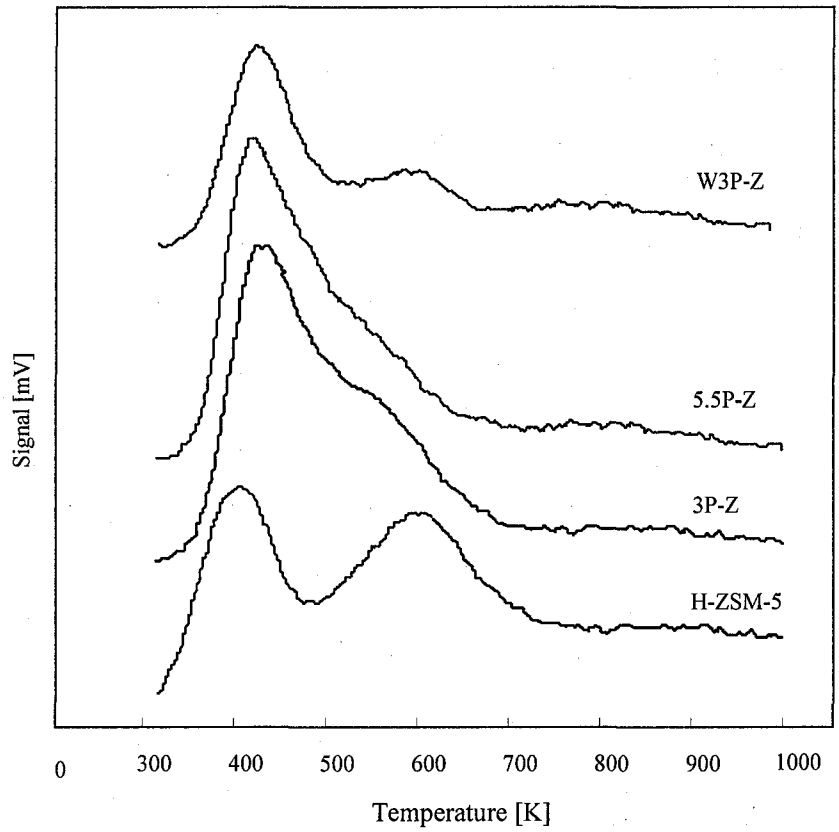

Fig. 7.3 NH_3-TPD profiles of the H-ZSM-5 and P-HZSM-5 catalysts.

7.3.2. MTO Reaction over H-ZSM-5 and P-HZSM-5

The conversion of methanol (MeOH) and selectivity over various catalysts were listed in Table 7.1. Here, the product selectivities were calculated based on the total amount of the products, including aromatic compounds. With increasing H_3PO_4 content, the selectivities to ethene and aromatics were decreased and the propylene selectivity was increased instead. The highest propylene selectivity obtained in this study was about 57% which are very high compared to the reported values.

Bjørgen et al. [38] have reported that ethene was formed predominantly via aromatics such as xylenes and/or trimethylbenzenes. The hydrogen transfer reactions take place on strong acid sites. Apparently, the formation of aromatics and ethene was inhibited by the decrease of the amount of the strong acid sites after the H_3PO_4 treatment.

Table 7.1. Methanol conversion and product selectivity over HZSM-5 and P-HZSM-5 catalysts.

Catalyst	Conversion (%)	Selectivity (%)								
		C_1	$C_2^=$	C_3	$C_3^=$	C_4	$C_4^=$	$C_{5}\sim$	DME	Aromatics
H-ZSM-5	100	1.45	22.5	3.12	39.04	3.71	13.41	5.77	0	11.0
1P-Z	100	1.69	19.91	2.42	44.07	3.30	16.43	7.88	0	4.31
2P-Z	100	1.86	17.35	1.28	48.35	2.10	17.99	8.15	0	2.94
3P-Z	100	1.90	8.89	0.73	54.88	1.58	17.10	13.88	0	1.26
4.5P-Z	86.78	4.82	6.76	0.42	52.63	0.69	18.3	14.7	0.62	1.05
5.5P-Z	71.07	1.27	2.27	0.42	0.54	0.42	0.32	0.25	94.51	0
W1P-Z	100	2.06	21.98	3.78	37.25	5.23	14.69	7.59	0	7.41
W2P-Z	100	2.56	22.57	3.31	40.74	4.28	15.13	6.99	0	4.41
W3P-Z	100	1.47	19.86	2.37	45.73	2.82	16.66	8.09	0	2.99
W4.5P-Z	100	1.22	9.59	0.58	56.96	0.95	18.84	10.72	0	1.14
W5.5P-Z	97.4	2.59	11.37	0.43	52.91	0.93	16.16	14.42	0	1.09

W/F=0.065 [kg.h.mol^{-1}]; at 723K; TOS = 30 min

The selectivity to propylene reached 54.88 % over 3P-Z catalyst. But, by increasing H_3PO_4 content further, the methanol conversion over 5.5P-Z decreased to 71.07 % and light olefin selectivity was about 3 %. Instead, dimethylether (DME) was a main product. After the removal of excess H_3PO_4 by washing, the selectivity to ethene and aromatics as well as propylene was increased again due to a partial recovery of strong acid sites. However, the acidic strength of the strong acid sites of washed catalysts was still lower than that of the untreated H-ZSM-5 due to the removal of partial dealumination.

Fig.s 7.4-7.9 show changes in MeOH conversion and selectivities with reaction time. Here, the selectivities to hydrocarbons were calculated from the product amounts excluding aromatic compounds. The selectivity to propylene over the 3P-Z catalyst was slightly decreased after several hours with the presence of DME. The selectivity to DME was slightly increased after 200 min of operation time, indicating that the catalytic deactivation by coke formation occurred over the

catalyst with high phosphorous contents. After the deactivation, DME was mainly produced. DME is formed by methanol dehydration which is the first step of MTO reactions. The strong acid sites must be covered with excess H_3PO_4 molecules which inhibit a reaction of DME into other hydrocarbons. The MeOH conversion and propylene selectivity over the P-HZSM-5 catalysts was much improved after washing. The catalyst performance of W4.5P-Z and W5.5P-Z was very stable with very high propylene selectivities because acid strength of the strong acid sites of H-ZSM-5 after dealumination is lower than that of untreated H-ZSM-5.

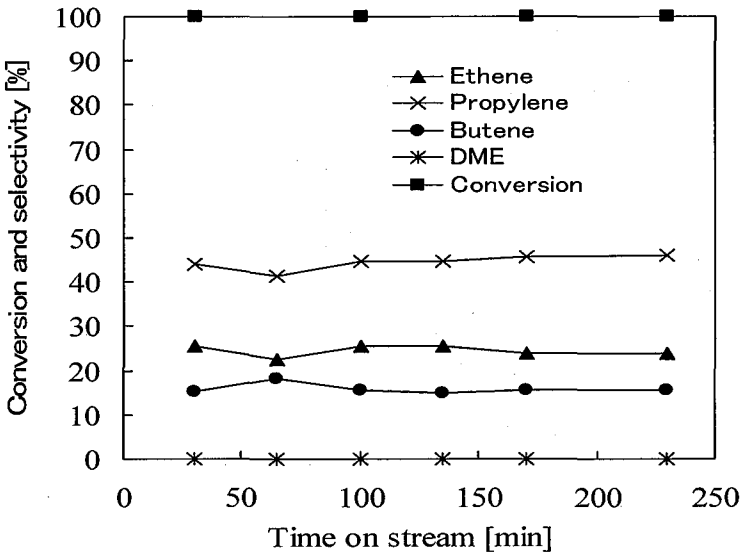

Fig. 7.4 Conversion and product selectivities over H-ZSM-5 at 723K, *W/F* of 0.065 [kg h mol^{-1}].

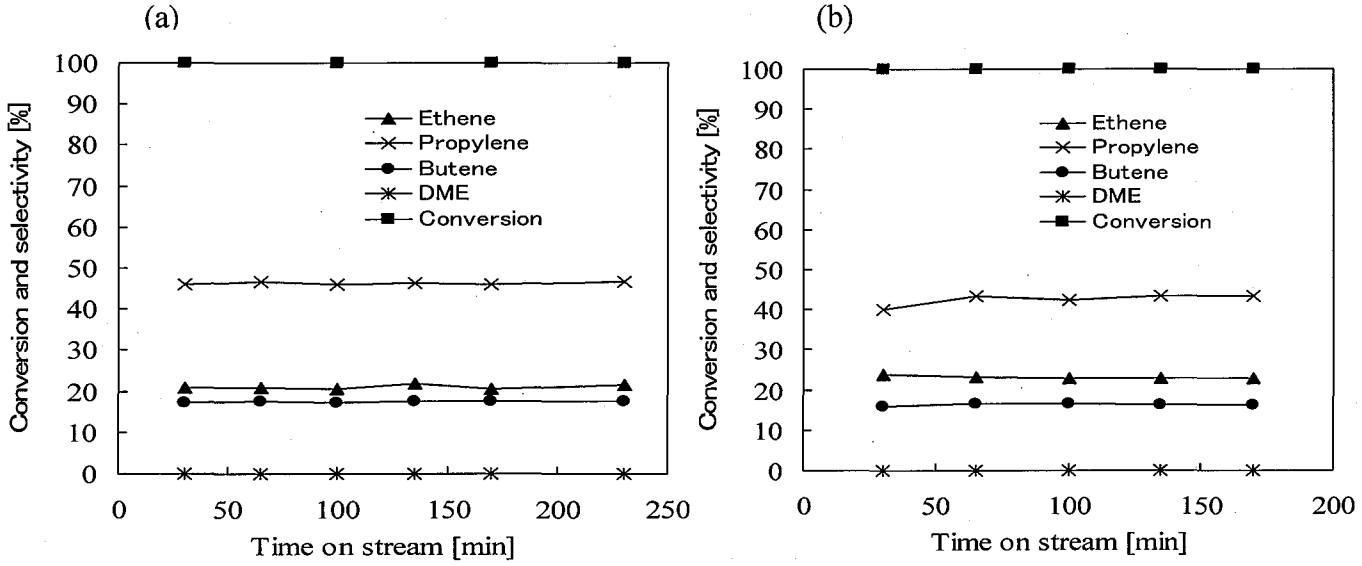

Fig. 7.5 Conversion and product selectivities over (a): 1P-Z; (b): W1P-Z at 723K, *W/F* of 0.065 [kg h mol $^{-1}$].

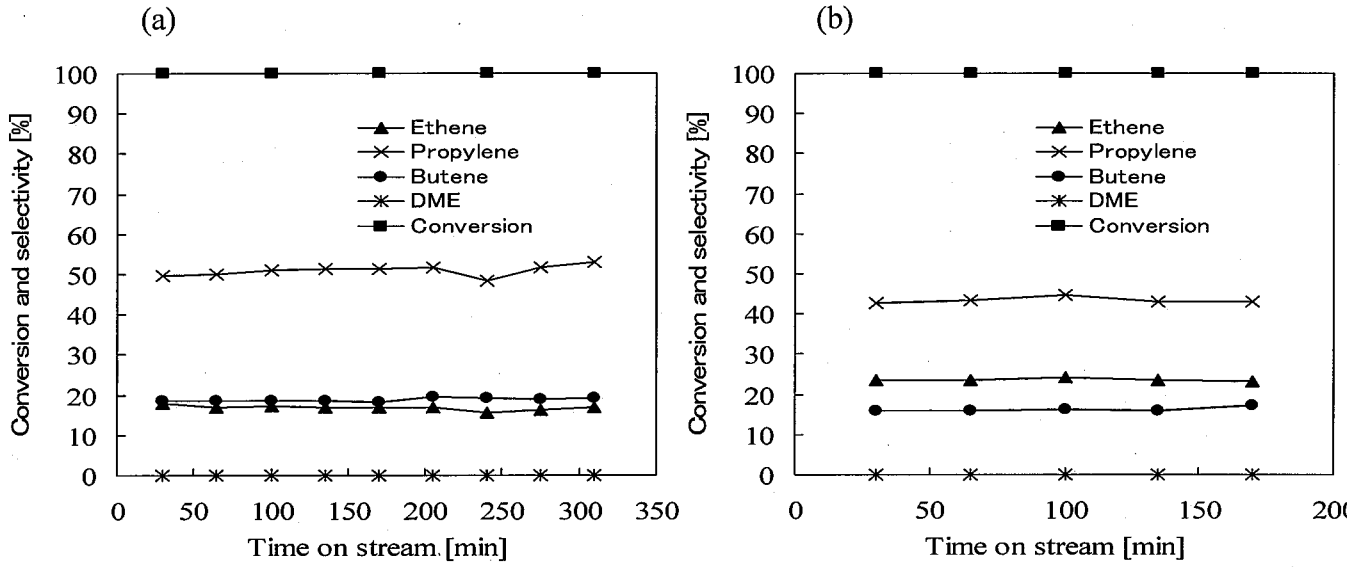

Fig. 7.6 Conversion and product selectivities over (a) 2P-Z; (b): W2P-Z at 723K, *W/F* of 0.065 [kg h mol^{-1}].

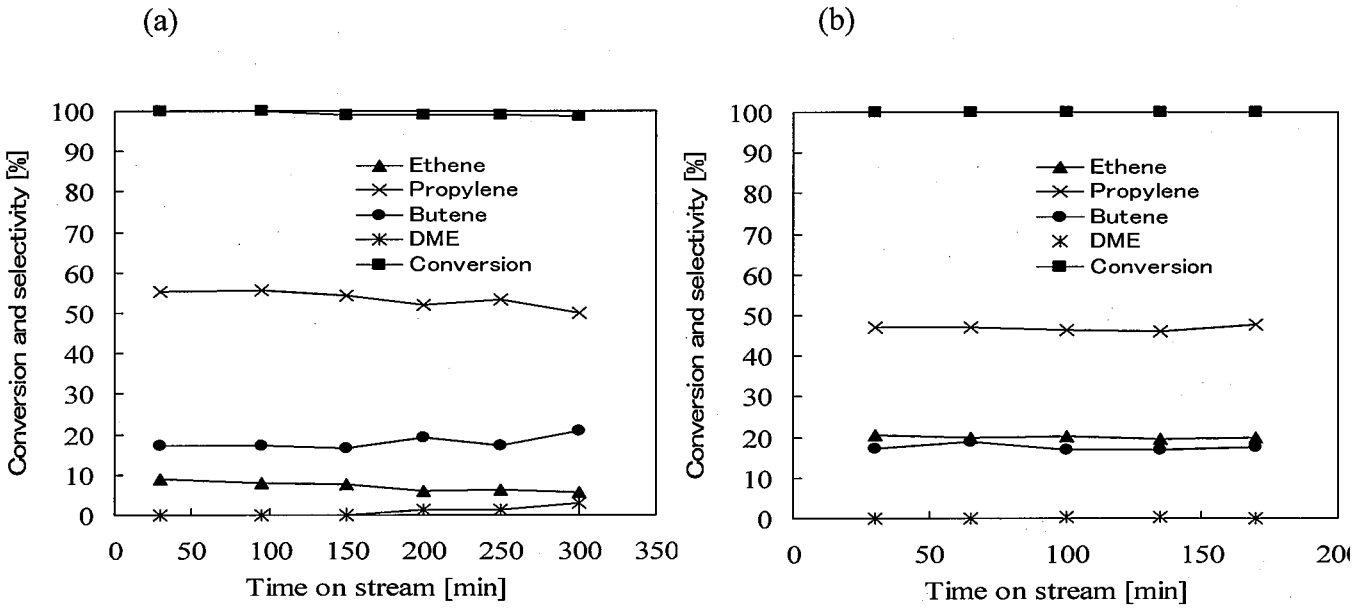

Fig. 7.7 Conversion and product selectivities over (a) 3P-Z; (b): W3P-Z at 723K, *W/F* of 0.065 [kg h mol^{-1}].

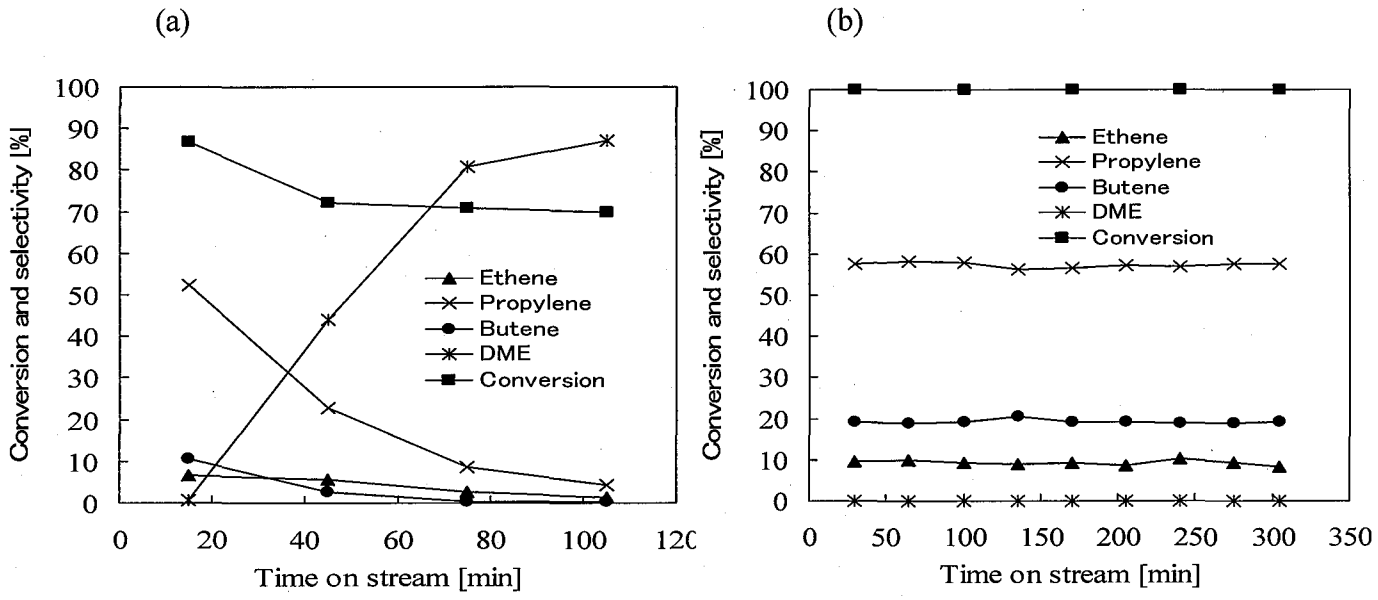

Fig. 7.8 Conversion and product selectivities over (a): 4.5P-Z; (b): W4.5P-Z at 723K, *W/F* of 0.065 [kg h mol $^{-1}$].

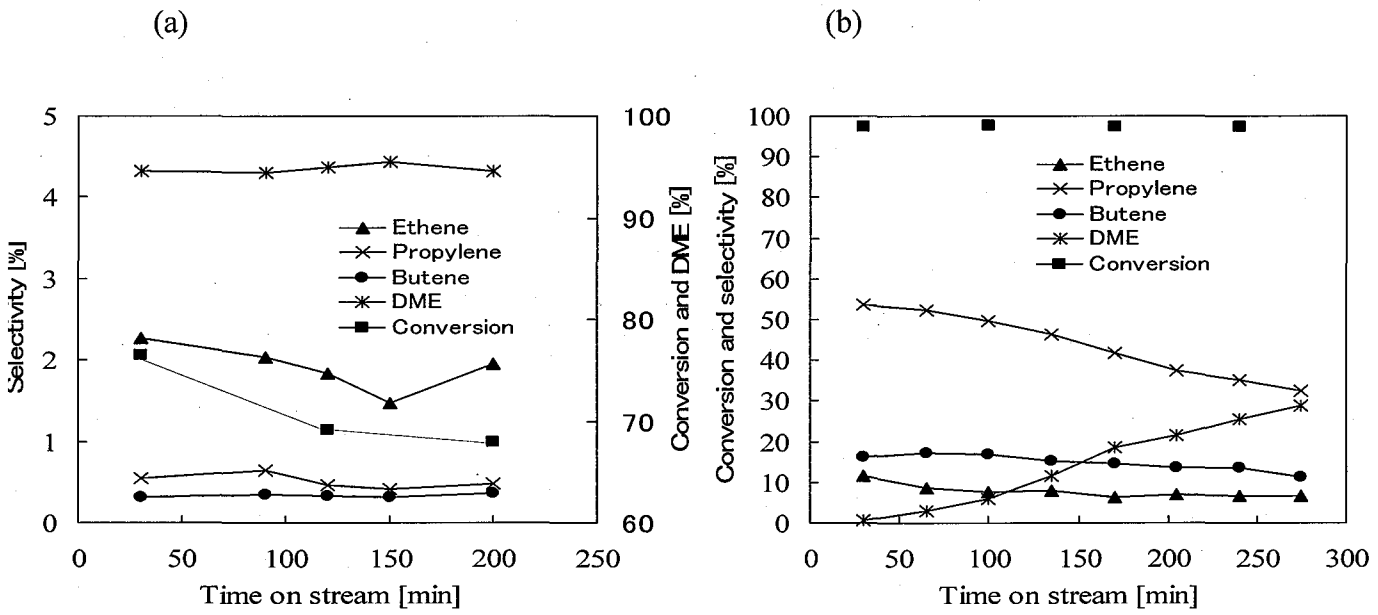

Fig. 7.9 Conversion and product selectivities over (a): 5.5P-Z; (b): W5.5P-Z at 723K, *W/F* of 0.065 [kg h mol $^{-1}$].

The catalytic deactivation was obviously observed over the 4.5P-Z and 5.5P-Z catalysts (Fig. 7.8 and 7.9). The main product was DME which is formed by methanol dehydration as the first step of MTO reaction. The acid sites must be covered with excess H_3PO_4 molecules, which inhibits a reaction of DME into other hydrocarbons. The MeOH conversion and propylene selectivity of the P-HZSM-5 catalysts was much improved after washing. The catalyst performance of W4.5P-Z was very stable with very high propylene selectivity.

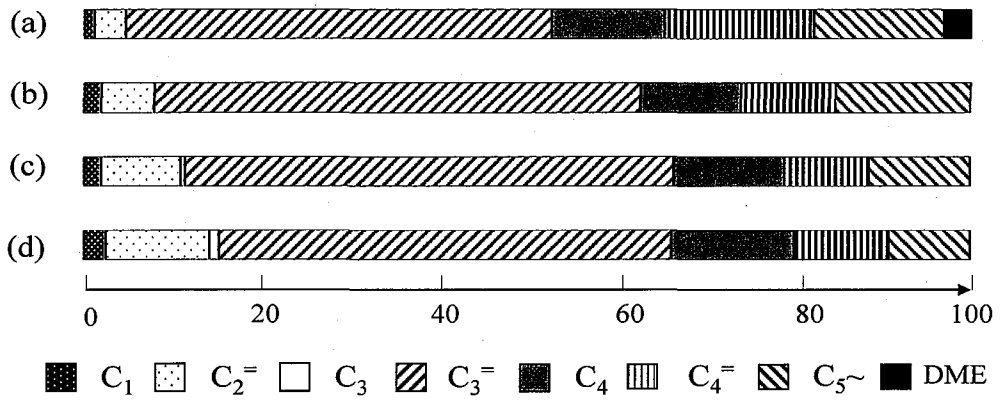

Fig. 7.10 Product selectivities over 3P-Z catalyst at 723K, *W/F*: (a) 0.02; (b) 0.03; (c) 0.07; (d) 0.20 [kg h mol^{-1}]. TOS = 30 min.

The effect of space velocity (*W/F*) on the product selectivities was shown in Fig. 7.10. The reactions were performed over the 3P-Z catalyst at 723K. The data were collected after reaction for 30 min. Here, the selectivities to hydrocarbon were calculated based on the amount of products excluding aromatic compounds. The conversion of MeOH was 100% for each space time. However, a small fraction of DME was found at a low space time of 0.024 kg h mol^{-1}, indicating that the contact time was not enough to convert all DME to olefins. The highest selectivities to propylene were obtained at the space time from 0.033 to 0.065 kg h mol^{-1}.

The influence of reaction temperature on MeOH conversion and selectivity was shown in Fig. 7.11. The reactions were carried out at the space time of 0.065 kg h mol^{-1} over the 3P-HZ catalyst. The MeOH conversion was nearly 80% at 573K, while the main product was DME with minority of other hydrocarbons. On the other hand, MTO reaction over untreated HZSM-5 showed nearly 100% of MeOH conversion with a small amount of DME at 573K. These results indicate that the strength of acidity was weakened by the H_3PO_4 treatment, suggesting that higher temperature is required for MTO reactions over the P-HZSM-5 catalysts. The highest selectivity to propylene was obtained at 723K although the selectivity to aromatics was not significantly increased at different temperature.

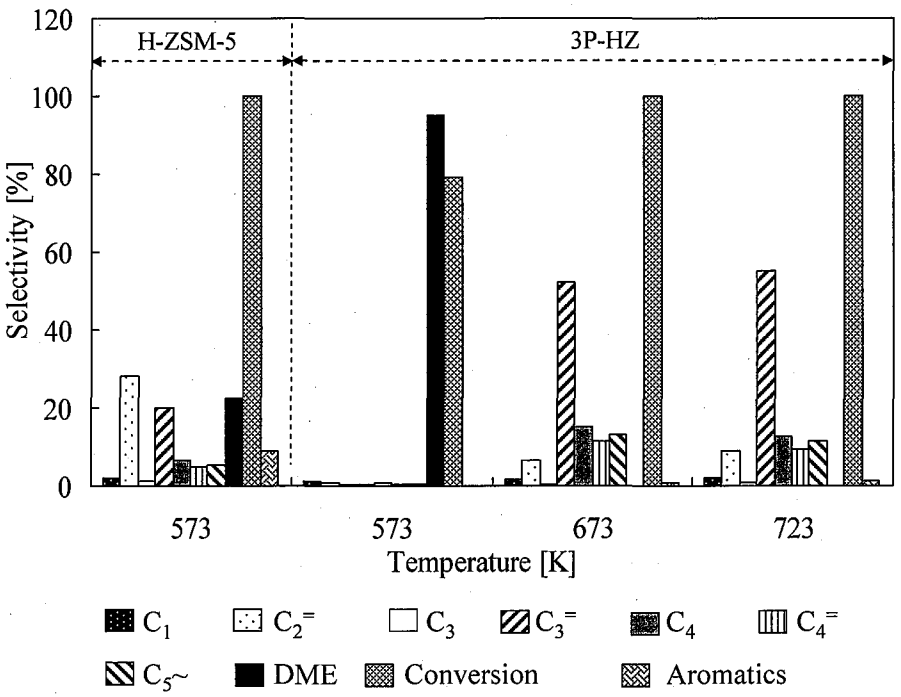

Fig. 7.11 Effect of temperature on the methanol conversion and product selectivities over H-ZSM-5 and 3P-Z catalysts in MTO reaction at *W/F* of 0.065 [kg h mol^{-1}]. TOS = 30 min.

7.4 Conclusions

H-ZSM-5 catalyst was treated with H_3PO_4 solutions with various concentrations. The selectivities to olefin over P-ZSM-5 in the MTO reactions were significantly improved by the H_3PO_4 treatments. With increasing the phosphorous content in P-HZSM-5, the selectivity to ethene and aromatics noticeably decreased due to weakening acid strength of the strong acid sites of H-ZSM-5 by dealumination. The highest selectivity to propylene over modified P-HZSM-5 reached up to 57% with a small amount of by-products of aromatics. The removal of excess H_3PO_4 after washing resulted in a partial recovery of strong acid sites. The catalyst performance of washed P-HZSM-5 was very stable with very high propylene selectivities.

The significant increase in propylene selectivity over P-HZSM-5 catalysts would make suggestions for practical application in the present petroleum chemistry.

References

[1] W.O. Haag, R.M. Lago, P.G. Rodewald, J. Mol. Catal. 17 (1982) 161

[2] B. Valle, A. Alonso, A. Atutxa, A.G. Gayubo, J. Bilbao, Catal. Today. 106 (2005) 5239

[3] T. Tago, K. Iwakai, K. Morita, K. Tanaka, T. Masuda, Catal. Today. 105 (2005) 662

[4] J.F. Haw, J.B. Nicholas, W. Song, F. Deng, Z. Wang, T. Xu, C.S. Heneghan, J. Am. Chem. Soc. 122 (2000) 4763

[5] A.G. Gayubo, A.T. Aguayo, M. Olazar, R. Vivanco, J. Bilbao, Chem. Eng. Sci. 58 (2003) 5239

[6] B. Valle, A. Alonso, A. Atutxa, A.G. Gayubo, J. Bilbao, Catal. Today. 106 (2005) 118

[7] S.A. Tabak, S. Yurchak, Catal. Today. 6 (1990) 307

[8] M Bjørgen, U. Olsbye, D. Petersen, S. Kolboe, J. Catal. 221 (2004) 1

[9] A. Sassi, M.A. Wildman, J.F. Haw, J. Phys. Chem. B 106 (2002) 8768

[10] Y. Wei, D. Zhang, Y. He, L. Xu, Y. Yang, B.L. Su, Z. Liu, Catal. Lett. 114 (2007) 30

[11] J.Q. Chen, A. Bozzano, B. Glover, T. Fuglerud, S. Kvisle, Catal. Today. 106 (2005) 103

[12] J.W. Park, J.Y. Lee, K.S. Kim, S.B. Hong, G. Seo, Appl. Catal. A 339 (2008) 36

[13] J. Liang, H. Li, S. Zhao, W. Guo, R. Wang and M. Ying, Appl. Catal. 64 (1990) 31

[14] Y. Xu, C.P. Grey, J.M. Thomas, A.K. Cheetham, Catal. Lett. 4 (1990) 251

[15] G.F. Froment, W.J.H. Dehertog, A.J. Marchi, Catal. (London) 9 (1992) 1

[16] B. Vora, J.Q. Chen, A. Bozzano, B. Glover, P. Barger, Catal. Today. 141 (2009) 77

[17] I.M. Dahl, S. Kolboe, J. Catal. 149 (1994) 458

[18] I.M. Dahl, S. Kolboe, Catal. Lett. 20 (1993) 329

[19] E.J. Munson, N.D. Lazo, M.E. Moellenhoff, J.F. Haw, J. Am.Chem. Soc. 113 (1991) 2783

[20] F. Salehirad, M.W. Anderson, J. Catal. 164 (1996) 301

[21] M.W. Anderson, B. Sulikowski, P.J. Barrie, J. Klinonowski, J. Phys. Chem. 94 (1990) 2730

[22] G. Mirth, J.A. Lercher, M.W. Anderson, J. Klinowski, J. Chem. Soc. Faraday Trans. I 86 (1990) 3039

[23] V. Bosacek, J. Phys. Chem. 97 (1993) 10732

[24] J.F. Haw, W. Song, D.M. Marcus, J.B. Nicholas, Acc. Chem. Res. 36 (2003) 317

[25] D. Chen, K. Moljord, T. Fluglerud, A. Holmen, Micropor. Mesopor. Mater. 29 (1999) 191

[26] H. van Heyden, S. Mintova, T. Bein, Chem. Mater. 20 (2008) 2956

[27] M. Bjørgen, S. Svelle, F. Joensen, J. Nerlov, S. Kolboe, F. Bonino, L. Palumbo, S. Bordiga, U. Olsbye, J. Catal 249 (2007) 195

[28] C. Mei, P. Wen, Z. Liu, H. Liu, Y. Wang, W. Yang, Z. Xie, W. Hua, Z. Gao, J. Catal. 258 (2008) 243

[29] M. Bjørgen, F. Joensen, M.S. Holm, U. Olsbye, K-P. Lillerud, S. Svelle, Appl. Catal. A 345 (2008) 43

[30] M. Kaarsholm, F. Joensen, J. Nerlov, R. Cenni, J. Chaouki, G.S. Patience, Chem. Eng. Scien. 62 (2007) 5527

[31] J. Li, Y. Qi, L. Xu, G. Liu, S. Meng, B. Li, M. Li, Z. Liu, Catal. Commun. 9 (2008) 2515

[32] N. Xue, X. Chen, L. Nie, X. Guo, W. Ding, Y. Chen, M. Gu, Z. Xie, J Catal. 248 (2007) 20

[33] G. Jiang, L. Zhang, Z. Zhao, X. Zhou, A. Duan, C. Xu, J. Gao, Appl Catal. 340 (2008) 176

[34] R.J. Kalbasi, M. Ghiaci, A.R. Massah, Appl. Catal. A 353 (2009) 1

[35] T. Blasco, A. Corma, M.J. Triguero, J. Catal. 237 (2006) 267

[36] W.W. Keading, S.A. Butter, J. Catal. 61 (1980) 155

[37] J.A. Lercher, G. Rumplmayr, Appl. Catal. 25 (1986) 215

[38] M. Bjørgen, S. Svelle, F. Joensen, J. Nerlov, S. Kolboe, F. Bonino, L. Palumbo, S. Bordiga, U. Olsbye, J. Catal. 249 (2007) 195.

Chapter 8

Summary and Suggestions for Future Work

8.1 Summarization

8.1.1 The Production of *p*-Xylene over Silicalite-1/H-ZSM-5 Catalyst

In this study, new types of silicalite-1/H-ZSM-5 composite catalysts were developed based on controlling external acid sites and the crystalline morphology by changing the synthesis compositions. The synthesized catalysts were then used for the production of *p*-xylene through the alkylation, disproportionation and isomerization reactions at different reaction conditions. The results were summarized from Chapters 2-5:

In **Chapter 2**, H-ZSM-5 crystals with different Si/Al molar ratios of 30, 50 and 70 were synthesized then coated with silicalite-1 layers by hydrothermal synthesis. The coatings were repeated twice. The silicalite layers formed consisted of oriented polycrystallites of a few μm thicknesses which grew on the surface of the substrate H-ZSM-5 in the early stage of synthesis. The presence of Al in the core H-ZSM-5 affected the formation of the polycrystalline layer. The silicalite/H-ZSM-5 catalysts showed excellent *para*-selectivity, >99.9 % under all the reaction conditions in the alkylation of toluene with methanol. The toluene conversion over the silicalite/H-ZSM-5 catalyst was almost constant, indicating that the silicalite coating inhibited coke formation on the external surface of H-ZSM-5. The high selectivity to *p*-xylene and high stability can be explained by the removal of acid sites on the external surface of H-ZSM-5.

In chapter 3, H-ZSM-5 catalysts with different crystal sizes with the same Si/Al ratio of 70 were synthesized under hydrothermal conditions. The crystal sizes were controlled by changing the synthesis conditions. Polycrystalline silicalite layers were formed on H-ZSM-5 with different crystal sizes of 5–30 μm by repeated coating times. The catalysts were then used for the alkylation of toluene with methanol to produce *p*-xylene. The interlayer between silicalite-1 layer and the core HZSM-5 was observed at different synthesis time by FE-SEM and TEM observations. The silicalite-1/H-ZSM-5 composite with a crystal size of 5 μm showed high *p*-xylene selectivity (nearly 100%), and the toluene conversion over the silicalite-1/H-ZSM-5 composite (5 μm) was

high and stable with reaction time. Para-selectivity slightly decreased with increasing crystal size and the catalyst with a large crystal size rapidly deactivated, indicating that the large crystals could not be fully covered with a silicalite layer. The acid site on the external surface for the large crystal must contribute to the deactivation. High catalytic activity and selectivity of silicalite-1/H-ZSM-5 composites must be caused by the direct pore-to-pore connection between H-ZSM-5 and silicalite-1. An oriented crystal growth of the silicalite-1 crystals along the surface of the H-ZSM-5 crystals was found at the early stage of the hydrothermal synthesis.

In **Chapter 4**, the morphology control of the silicalite/HZSM-5 composite catalysts was studied. Considering that the deposited polycrystals after the second synthesis were randomly oriented and were not densely packed in the previous work. Thus, repeated coating processes were required for obtaining highly selective catalysts. The morphology of the silicalite/HZSM-5 composite crystals was studied by changing the molar ratios of silica source and structure directing agent (SDA) in the coating solutions. The alkylation of toluene with methanol was performed using the composite catalysts with different morphologies.

The results showed that the *para*-selectivity of the composite catalysts was significantly affected by the synthesis conditions. The catalysts prepared at lower concentration of silica source and SDA in the coating solutions showed higher *para*-selectivity. Excellent *para*-selectivity of 99.6% with nearly 40% of toluene conversion could be obtained over the single crystal-like composite crystals prepared by only one coating process. Revised synthesis conditions also inhibited a homogeneous nucleation of silicalite in the solution. The mass gain of the single crystals was much reduced, and very thin silicalite layer was formed on the HZSM-5 surface.

In **Chapter 5**, toluene disproportionation over core-shell silicalite zeolite composite catalysts is one of candidates for the selective production of *p*-xylene. High fraction of *p*-xylene in the final product with a small amount of by-products was observed while the selectivity to *para*-xylene was still kept at high level.

In addition, the catalyst lifetime would be improved through the disproportionation of toluene over the composite catalyst compared to that in the alkylation reaction due to the absence of olefins produced from methanol as a coke precursor. The yield of *p*-xylene was enhanced at high temperatures (873 K) and at high *W/F* conditions. The obtained *para*-selectivity (85%) and yield of *para*-xylene (9%) were much higher than the reported values in the toluene disproportionation. But, the *para*-selectivity decreased from 98% to 85% when temperature rose from 663 to 873K

over the composite catalyst. This result can be explained by an increase of diffusivity of xylene isomers especially *m*–xylene and *o*-xylene at high temperature. To enhance further *para*-selectivity and catalyst lifetime in the toluene disproportionation, hydrogen should be introduced to the feed, but the toluene conversion decreased due to the lower residence time of toluene in the reactor.

8.1.2 Synthesis of Nanoscale H-ZSM-5 Crystals

In **Chapter 6**, a unique synthesis method to synthesis uniform HZSM-5 nanocrystals (<500nm) by incorporating Al species dissolved from FAU type zeolite and αAl_2O_3 was found. The catalyst expressed very high catalytic activity in the alkylation of toluene with methanol and *m*-xylene isomerization. The external surface deactivation of nano particles by silicalite-1 was also studied in the alkylation reaction. The reaction data suggested that it is hard to deactivate completely the external acid sites of H-ZSM-5 nanocrystals by silicalite-1. Highly-active H-ZSM-5 nanocrystals are expected to apply and modify for the practical application.

8.1.3 Light Olefin Production

In **Chapter 7**, the control of acid-strength distribution for H-ZSM-5 catalyst with various phosphorous acid contents was studied for the selective production of light olefin in MTO reaction. The modified P-HZSM-5 catalyst showed very high propylene selectivity up to 57 % with a methanol conversion of 100%. The inhibition of ethene and by-products such as aromatic compounds was caused by weakening acidic strength with phosphorous incorporation. In addition, the reaction variables for the MTO reaction were optimized. The removal of excess H_3PO_4 after washing resulted in a partial recovery of strong acid sites, which demonstrates the interactions between phosphorous acid and HZSM-5 zeolite.

8.2 Suggestions for Future Work

The silicalite-1 coating on ZSM-5 crystals is one of the good candidates for the production of *para*-xylene with high selectivity and conversion. However, the reaction data were just obtained after a few hours in the laboratory scale. Thus, a long-term stability tests for the catalysts should

also be required. From the view point practical application, it is necessary to enhance the toluene conversion at low temperature over the composite catalyst, especially in the toluene disproportionation. In order to increase the catalytic activity of the composite catalyst, the diffusivity of reactants and reaction products should be increased through the zeolite pore channels, so the micro/mesoporous silicalite-1/H-ZSM-5 composite catalyst is one of candidates to solve those problems [1].

Silicalite-1 coating on bi-functional catalysts would provide a unique catalytic property such as loading on ZSM-5 with some different kinds of rare metal [2,3]. From this way, the production of *p*-xylene, light olefins and other valuable aromatics would be obtained from the conversion of cheaper materials such as paraffins olefins and alcohols, for examples.

The combination of different structure of zeolites with silicalite-1, such as silicalite-1/MOR, silicalite-1/β-zeolite, silicalite-1/MCM-22 for the production of *p*-xylene would also be suggested [4-7].

References

[1] P. Prokesova, N. Zilkova, S. Mintova, T. Bein, J. Cejka, Appl. Catal. A 281 (2005) 85

[2] T. Komatsu, H. Ikenaga, J. Catal. 241 (2006) 426

[3] L.G. A. van de Water, J.C. van der Waal, J.C. Jansen, T. Maschmeyer, J. Catal. 223 (2004) 170

[4] Y. Bouizi, L. Rouleau, V.P. Valtchev, Micropor. Mesopor. Mater. 91 (2006) 70

[5] D. Kong, J. Zheng, X. Yuan, Y. Wang, D. Fang, Micropor. Mesopor. Mater. 11 (2009) 91

[6] Y. Bouizi, I. Diaz, L. Rouleau, V.P. Valtchev, Adv. Func. Mater. 15 (2005) 1955

[7] P.N. Joshi, P.S. Niphadkar, P.A. Desai, R. Patil, V.V. Bokade, J. Natural Gas Chemistry. 16 (2007) 37.

List of Publications

Papers

[1] Dung Van Vu, Manabu Miyamoto, Norikazu Nishiyama, Yasuyuki Egashira, Korekazu Ueyama "Selective formation of *para*-xylene over H-ZSM-5 coated with polycrystalline silicalite crystals", Journal of Catalysis, 243 (2006) 389-394

[2] Dung Van Vu, M. Miyamoto, Norikazu Nishiyama, Satoshi Ichikawa, Yasuyuki Egashira, Korekazu Ueyama

"Catalytic activities and structures of silicalite-1/HZSM-5 zeolite composites", Microporous and Mesoporous Materials, 115 (2008) 106-112

[3] Dung Van Vu, Manabu Miyamoto, Norikazu Nishiyama, Yasuyuki Egashira, Korekazu Ueyama "Morphology control of silicalite/HZSM-5 composite catalysts for the formation of *para*-xylene", Catalysis letters, 127 (2009) 233-238

[4] Dung Van Vu, Norikazu Nishiyama, Yasuyuki Egashira, Korekazu Ueyama; "High propylene selectivity in the methanol-to-olefin reaction over H-ZSM-5 catalyst treated with phosphoric acid", submitted.

Related paper

[1] Norikazu Nishiyama, Masumi Kawaguchi, Yuichiro Hirota, Dung Van Vu, Yasuyuki Egashira, Korekazu Ueyama; "Size Control of SAPO-34 Crystals and Their Catalyst Lifetime in the Methanol-to-Olefin Reaction" Applied Catalysis A. 362 (2009) 193-199.

International Conferences

[1] Dung Van Vu, Norikazu Nishiyama, Manabu Miyamoto, Yasuyuki Egashira, Korekazu Ueyama, "The Formation of *para*-Xylene over Single and Poly-Crystalline Silicalite/HZSM-5 Composite Catalysts", The international symposium on Zeolite and Microporous Crystals 2009 (ZMPC2009), Tokyo, Japan, 2009.

[2] Dung Van Vu, Manabu Miyamoto, Norikazu Nishiyama, Yasuyuki Egashira, Korekazu Ueyama, "Core-shell zeolite composite catalysts for production of *p*-xylene", Proceedings of Recent Research Report (RRR)-The 4th International FEZA (Federation of European Zeolite Associations), Paris, France, 2008.

[3] Dung Van Vu, Norikazu Nishiyama, Manabu Miyamoto, Yasuyuki Egashira, Korekazu Ueyama, "Synthesis of nano-sized HZSM-5 and silicalite-1/HZSM-5 catalysts", Proceeding of the 1st International Global COE Symposium on Bio-Environmental Chemistry (GCOEBEC-1), Osaka, Japan, 2008.

[4] Norikazu Nishiyama, Dung Van Vu, Manabu Miyamoto, Yasuyuki Egashira, Korekazu Ueyama, "Catalyst particles coated with a silicalite layer for reactant-selective and product-selective reactions" The 1st SCEJ (Kansai-Branch)/SSCCI Joint International Conference on Chemical Engineering, Osaka, Japan, 2007.

[5] Dung Van Vu, Manabu Miyamoto, Norikazu Nishiyama, Yasuyuki Egashira, Korekazu Ueyama, "Catalytic Activities of Silicalite-1/HZSM-5 Zeolite Composites in Alkylation and MTO Reactions" Proceedings of the 4th International Zeolite Membrane Meeting (IZMM4), Zaragoza, Spain, 2007.

[6] Dung Van Vu, Manabu Miyamoto, Norikazu Nishiyama, Yasuyuki Egashira, Korekazu Ueyama, "A silicalite Film Coating on ZSM-5 Catalysts for Selective Production of *p*-Xylene", Proceedings of the 3rd Vietnamese-Japanese Students' Scientific Exchange Meeting (VJSE), Kobe, Japan, 2006.

[7] Manabu Miyamoto, Dung Van Vu, Norikazu Nishiyama, Yasuyuki Egashira, Korekazu Ueyama, "Selective Formation of *para*-Xylene over Silicalite/H-ZSM-5 Zeolite Composites", Proceedings of the 9th International Conference of Inorganic Membranes (ICIM9), Lillehammer, Norway, 2006.

Domestic conferences

[1] Dung Van Vu, Norikazu Nishiyama, Yasuyuki Egashira, Korekazu Ueyama, "Core-shell zeolite composite catalyst for the selective formation of *p*-xylene", the meeting of the petroleum society of Japan, Tokyo, 2009.

[2] Dung Van Vu, Manabu Miyamoto, Norikazu Nishiyama, Yasuyuki Egashira, Korekazu Ueyama, "Selective *p*-Xylene Formation on H-ZSM-5 Silicalite Core-Shell Zeolite Composites", Proceedings of the 100th Catalysis Society of Japan Meeting (CatSJ), Hokkaido, Japan, 2007.

Acknowledgments

Firstly, I would like to acknowledge my supervisors, Professor Dr. Korekazu Ueyama, Associate Professor Dr. Norikaru Nishiyama, Associate Professor Dr. Yasuyuki Egashira (Division of Chemical Engineering, Graduate School of Engineering Science, Osaka University) for all the guidance and contribution to my research work.

Professor Dr. Korekazu Ueyama is also deeply acknowledged for giving me opportunity to study in his laboratory, and he is a person who is always beside me on the way of finding the financial support for my life in Japan.

Associate Professor Dr. Norikazu Nishiyama is gratefully acknowledged for his directed instructions in this work through weekly discussions. His critical comments and suggestions make my research work go properly. I am also indebted to his kindness and understanding not only in scientific field but also in personal matters.

Associate Professor Dr. Yasuyuki Egashira is acknowledged for his comments and questions during the seminars, from which I can propose ideas logically.

Secondly, I gratefully acknowledge Professor Dr. Koichiro Jitsukawa, Professor Dr. Takayuki Hirai and Professor Dr. Masahito Taya for their critical comments and helpful suggestions on this dissertation. I also would like to thank Mr. Masao Kawashima (GHAS, Division of Chemical Engineering, Osaka University) for FE-SEM measurements. I also thank Dr. Satoshi Ichikawa (Organization for the Promotion of Research on Nanoscience and Nanotechnology, Osaka University) for TEM measurements. Acknowledgements are also given to the Global Centers of Excellence (GCOE) Program "Global Education and Research Center for Bio-Environmental Chemistry" of Osaka University.

Thirdly, thanks are given to my co-workers, Dr. Manabu Miyamoto, Ms. Masumi Kawaguchi, Mr. Satoshi Tohyama and Mr. Yuichiro Hirota for their cooperation. Special thanks to Dr. Takashi Maruo, Dr. Yuko Nishiyama (current last name is Maruo), Dr. Yong-Rong Dong for all their helps and valuable advices. It is pleasure to thank Ms. Jin Jin, Ms. Megumi Yamada (current last name is Azumi), Mr. Masahiro Yamaguchi, Mr. Tohru Katayama, Mr. Masaru Nakao, Mr. Hiroshi Nishizawa, Mr. Fidelis Stefanus Hubertson Simanjuntak, Mr. Naoyuki Ueno, Mr. Kenji Murata, Mr. Kyouhei Makita, Mr. Masaki Taniyama and Ms. Miyoko Ono, Mr. Ishikado Akinori for their kindness, nice talks and pleasant time. Thanks are also given to other present and former colleagues in Ueyama Laboratory whose names can not be listed here because of space reason.

Fourthly, I would like to express special thanks for the financial support of the Vietnamese Overseas Scholarship Program and Toyonaka Rotary Club (TRC) Organization.

Finally, I would like to thank father Vu Van Dao, my mother Luu Thi Minh, my wife Nguyen Thi Thu Huyen, my son Vu Nhat Quang and all other members in my family for their love, patience and encouragement.

Vu Van Dung

Osaka, Japan
September 2009